

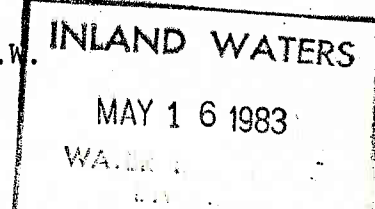


K. U. WEYER:

SALT DISSOLUTION, KARST GEOLOGY, GLACIAL
EVENTS AND GROUNDWATER FLOW IN THE PINE
POINT REGION, N.W.T.

VOL. 2: FIGURES

National Hydrology Research Institute
Ground Water Division
101 - 4616 Valiant Drive N.W.
Calgary, Alberta
T3A 0X9



Draft, March 1983,
subject to final revision.

Vol. 1: Text
Vol. 2: Figures
Vol. 3: Tables and
Appendices.

List of Figures

Chapter 1

Figure 1-1 Regional hydraulic-head distribution, Western Canada Sedimentary Basin, slice + 1000 to -1250 ft. (Datum: M.S.L.). Caribou Mountains stand out as a major regional recharge area (modified after Hitchon, 1969a, Fig. 5).

Chapter 2

Figure 2-1 Approximate flow pattern in uniformly permeable material between the sources distributed over the air-water interface and the valley sinks (figure and caption from Hubbert, 1940, Fig. 45).

Figure 2-2 Schematic sketch of the head changes along an assumed flow line from a recharge area (hill) to a discharge area (valley). Flowing conditions occur at ④, although no artesian aquifer is present (from Weyer, 1978, Fig. 6).

Figure 2-3 Schematic cross-section showing a confined aquifer of limited extent. Recharge is through an aquitard.

Figure 2-4 General case of an artesian aquifer without outcrop. The topography is reflected in the head distribution in the

aquifer. Flow in the aquifer is from highlands to lowlands.

Figure 2-5 Schematic cross-section showing confined aquifer extending under a lake. Recharge through aquitard.

Figure 2-6 Conventional model of artesian systems. Recharge at outcrop of artesian aquifer only. 1: artesian aquifer, 2: confining layer, A: piezometric level (head) of aquifer below topographic surface, B: piezometric level of aquifer above topographic surface - artesian (flowing) borehole.

Figure 2-7 Stratigraphy of the Red Earth region and schematic relationship of topography and piezometric surfaces in the Devonian aquifers D_I and D_{II} . Stratigraphy modified after Tóth (1978, Fig. 3).

Chapter 3

Figure 3-1 Geographical and topographical features south of Great Slave Lake. BL = Buffalo Lake; BR = Buffalo River; FS = Fort Smith; FR = Fort Resolution; HC = Hanbury Creek; HP = High Point; HR = Hay River (river and town); JR = Jackfish River; KL = Kakisa Lake; KR = Kakisa River; LBR = Little Buffalo River; MR = Mackenzie River; NR = Nyarling River; PP = Pine Point; PR = Peace River; SB = Sulphur Bay; SLR = Slave River; SP = Sulphur Point; SR = Salt River; TL = Tathlina Lake; YK = Yellowknife.

Figure 3-2 A. Mineral and hydrocarbon exploration holes adjacent to Great Slave Lake.

B. Location of boreholes included in geologic evaluation by computer.

- Figure 3-3** Oil wells evaluated for the study. For cross-section 1 to 3, see Fig. 4-3. BM = Birch Mountains; CH = Cameron Hills; CM = Caribou Mountains; EL = Escarpment Lake No. 1, No. 2 and No. 3; F = Hay River Test No. 1, No. 2, No. 3, No. 5b, No. 6, No. 8 (compare Fig. 4-2); WBNP = Wood Buffalo National Park; WP = Windy Point No. 1. Triangles = oil wells; full circles = discharge gaging stations; diamond = karst spring and borehole 104.
- Figure 3-4** Map of surficial geology of the area investigated (after Alberta Research Council, 1970; Douglas, 1974; Douglas and Norris, 1974). Qal = Quaternary; uD = Upper Devonian; mD = Middle Devonian; pC = Precambrian; HL = 'hinge line'; MDF = McDonald Fault; PF = Prebble Fault; PP = Pine Point.
- Figure 3-5** Thickness of glacial till in the Pine Point area (ft). Arrows indicate probable reflections of karstic and structural features of the Devonian bedrock.
- Figure 3-6** Stratigraphic correlation of Devonian Formations, Western Canada Sedimentary Basin (from Meijer-Drees and Davies, 1976).
- Figure 3-7** North-South cross-section, Horn Plateau, Great Slave Lake, Caribou Mountains, Peace River, foot of Birch Mountains (after Meijer-Drees and Davies, 1976). For position of cross-section and boreholes, see Fig. 3-19 (cross-section A).
- Figure 3-8** Phanerozoic stratigraphy and significant events in the Pine Point area (from Krebs, 1982, Fig. 11).

Figure 3-9 Geologic nomenclature adopted for the evaluation of borehole data by this report (modified after Skall, 1975).

Figure 3-10 Schematic north-south cross-section through Middle Devonian, Pine Point property, N.W.T., showing some of the major orebodies (from west to east: A-70, Z-63-N, K-57, O-42, M-40, W-17, X-15, N-204). Letters in circles are facies-types identified by Skall (1975). From Macqueen and Powell (1983) after Skall (1975) and Kyle (1981).

Figure 3-11 N-S and NE-SW fault zones in the Precambrian based on interpretation of large-scale geomagnetic maps (after Douglas, 1970, aeromagnetic map).

Figure 3-12 Average orientation of vertical joint sets in host rocks of Pine Point open pits J-44, N-31, N-32, N-38A, N-42, O-32, O-42, P-29 and P-32 (after Kessler et al., 1972, Fig. 3).

Figure 3-13 Elevation of top of E-shale, based on the evaluation of available exploration boreholes. Fault A in Fig. 3-13B is vertical displacement fault found by Abadene Oil.

Figure 3-14 Elevation of top of Amco shale (ft), based on the evaluation of available exploration boreholes.

Figure 3-15 Elevation of surface of Devonian rocks (ft), according to evaluation of available borehole logs.

Figure 3-16 Isopach map of Presqu'ile Formation (modified after Vasquez, 1968, map 3).

- Figure 3-17** Occurrence of top of presqu'ilization in the Slave Point Formation (B), Watt Mountain Formation (C) and Pine Point Group (D); A is composite of B, C and D (triangle = SPF; circle = WM; cross = PPG). Presqu'ile in PPG extends south towards Wood Buffalo National Park.
- Figure 3-18** Occurrence of green waxy Watt Mountain shale in fractures, vugs and cavities under the Watt Mountain Formation (A) and in Presqu'ile dolomite (B).
- Figure 3-19** Occurrence of Lotsberg salt in the Upper Mackenzie River area (after Meijer-Drees and Davis, 1976). For cross-section A see Fig. 3-7; for cross-section B see Fig. 3-25.
- Figure 3-20** Occurrence of Cold Lake Salt in the Upper Mackenzie River area and Northern Alberta (after Meijer-Drees and Davies, 1976).
- Figure 3-21** Facies map of the Muskeg Formation and equivalent strata (from Meijer-Drees and Davies, 1976).
- Figure 3-22** Salt dissolution, East-central Alberta (after Hamilton, 1971).
- Figure 3-23** Dissolution of Cold Lake Salt NW of Great Slave Lake and associated collapse and brecciation (after N.C. Meijer-Drees, personal communication, 1982).
- Figure 3-24** Salt solution breccia from 540 ft depth in oil well Iskut Silver Little Buffalo K-22. Photo: B. C. Rutley, ISPG.

- Figure 3-25** Stratigraphic cross-section B-B', Great Slave Lake (Cominco G-4) to Wood Buffalo National Park (Iskut Little Buffalo K-22) (modified after Rice, 1967, Fig. 4).
- Figure 3-26** Deformation of post-Cold Lake strata due to dissolution of Cold Lake salt (after Meijer-Drees and Davies, 1976).
- Figure 3-27** Solubility of gypsum in aqueous solutions in dependence of NaCl concentrations and temperature. A: from van Everdingen (1970, Fig. 1; example only, not to be used for actual determinations), B: after Shternina (1960).
- Figure 3-28** Diagrams of Mg^{2+} , Ca^{2+} and HCO_3^- concentrations versus Cl^- concentrations of 593 water samples collected south of Great Slave Lake, 1978-1980.
- Figure 3-29** A. Occurrence of igneous rocks, gneiss and carbonate pebbles in unconsolidated layers directly above the Paleozoic rock.
B. Occurrence of igneous rocks in sinkholes and within orebody A-55.
- Figure 3-30** Various sequences of basal thermal regime and associated erosional processes encountered beneath the Laurentide Ice Sheet at its maximum (from Sugden, 1977, Fig. 12).
- Figure 3-31** Morphology of the Laurentide Ice Sheet at its maximum (from Sugden, 1977, Fig. 2).
- Figure 3-32** Zones of contrasting basal thermal regime beneath the Laurentide Ice Sheet at its maximum (from Sugden, 1977, Fig. 11).
- Figure 3-33** Maximum western extent of glacial Great Slave Lake (after Craig, 1965, Fig. 2).

- Figure 3-34** Elevated beach lines of glacial and postglacial Great Slave Lake in the Buffalo River area (after McGregor, 1949, Fig. 1; isohyps from topographical map Buffalo Lake NTS 85B, Scale 1:250 000).
- Figure 3-35** Distribution of "normal" karst features in the Pine Point Barrier according to Rhodes (1982, Plate 8).
- Figure 3-36** Regional occurrence of unconsolidated internal sediments as extracted from available borehole logs. A = sand; B = mud in cavities, fractures or vugs (other than green waxy mud); C= black mud; D = green waxy mud below Watt Mountain Formation; E = erratics.
- Figure 3-37** Schematic diagram showing position of anomalous unconsolidated collapse orebodies within the Pine Point Barrier (after Rhodes, 1982, Plate 9).
- Figure 3-38** Major geological features and outline of orebody on 4th and 14th bench (after Alldrick, 1982, Figs. 2 and 3). Cross-section is shown in Fig. 3-39.
- Figure 3-39** Geologic cross-section through the A-55 orebody. Location of cross-section is shown on Figure 3-38 (after Alldrick, 1982, Fig. 4).
- Figure 3-40** Temporary rebound of water level in well hole 7, A-55 pump test, December 1979 (from Weyer 1981b; source of data: Pine Point Mines Ltd.).
- Figure 3-41** Longitudinal NE-SW corss-section through the tabular orebody L-37 showing Pleistocene sinkhole and spatially associated sulphide precipitation (after Webb, 1982).

Figure 3-42 Hypothetical groundwater flow system at the time of initiation of the Howe Lake structure (modified after Christiansen et al., 1982, Fig. 14).

Figure 3-43 Occurrence of formations in boreholes evaluated. A = overburden with reported depth; B = Hay River Formation; C = Slave Point Formation; D = Watt Mountain Formation; E = Pine Point Group; F = Lower Keg River Formation; G = Chinchaga Formation; H = Mirage Point Formation; I = Precambrian (open square = not certain).

Figure 3-44 Occurrence of open and infilled cavity systems in Devonian Formation of the Pine Point area, based on the evaluation of available borehole logs and drilling records. A = all formations; B = Hay River Formation (open squares = erratics in Hay River shale); C = Slave Point Formation; D = Watt Mountain Formation; PPG = Pine Point Group; LA = Lower Keg River Formation; CH = Chinchaga Formation.

Figure 3-45 Overall occurrence of collapse structures, breccia and sinkholes, according to the evaluation of available borehole logs. A = composite; B = collapse structures; C = breccia; D = sinkholes (more than 100 sinkholes were not listed due to time restrictions imposed by management).

Figure 3-46 Occurrence of brecciation in individual formations according to the evaluation of available borehole logs. A = all formations; B = Hay River Formation; C = Slave Point Formation; D = Watt Mountain Formation; E = Pine Point Group; F = Lower Key River Formation; G = Chinchaga Formation.

- Figure 3-47** Occurrence of vugs according to the evaluation of available borehole logs. A = all formations; B = Slave Point Formation; C = Watt Mountain Formation; D = Pine Point Group; E = Lower Keg River Formation; F = Chinchaga Formation.
- Figure 3-48** Occurrence of spongy (A), very vuggy (B) and pin point porosity (C) structures as well as completely filled vugs (D), according to evaluation of available borehole logs.
- Figure 3-49** Occurrence of broken and badly broken rocks, according to evaluation of available borehole logs. A = all formations; B = Hay River Formation; C = Slave Point Formation; D = Watt Mountain Formation; E = Pine Point Group; F = Lower Keg River Formation; G = Chinchaga Formation.
- Figure 3-50** Locations of orebodies (squares) and mineral showings (crosses; > 1% metal contents) according to evaluation of available borehole logs and other sources available to us.
- Figure 3-51** Occurrence of sphalerite and galena according to evaluation of borehole logs. A = all formations (triangle = sphalerite; square = galena; cross = both); B = overburden; C = Hay River Formation; D = Slave Point Formation; E = Watt Mountain Formation; F = Pine Point Group; G = Lower Keg River Formation.
- Figure 3-52** Occurrence of elemental sulphur (A-F) and massive amounts of H_2S (G) according to evaluation of available borehole logs. A = all formations; B = Hay River

Formation; C = Slave Point Formation; D = Watt Mountain Formation; E = Pine Point Group; F = Lower Keg River Formation; G = occurrence of massive amounts of H₂S.

Figure 3-53 Occurrences of hydrocarbons according to evaluation of available borehole logs. A = bitumen and tar; B = oil; C = bitumen and oil stain; D = methane (CH₄).

Figure 3-54 Occurrence of oil in individual formations of the Pine Point area according to evaluation of available borehole logs. A = all formations; B = Hay River Formation; C = Slave Point Formation; D = Watt Mountain Formation; E = Pine Point Group; F = Lower Keg River Formation.

Figure 3-55 Occurrence of bitumen and tar in individual formations of the Pine Point area according to evaluation of available borehole logs. A = all formations; B = Hay River Formation; C = Slave Point Formation; D = Watt Mountain Formation; E = Pine Point Group; F = Lower Keg River Formation.

Chapter 4

Figure 4-1

- A. Occurrence of artesian conditions in boreholes on Great Slave Lake and in adjacent discharge areas south of the lake, as reported in the available borehole files.
- B. Cessation of flow from artesian boreholes and karst springs (stars for both) since commencement of dewatering at Pine Point Mines.

- Figure 4-2** Detailed location and surface elevation (in feet) of oil wells Hay River Test 1, 2, 3, 5B, 6 and 8. Location of wells from a map by Frobisher Exploration Company (1946); elevation data from D. Adams (1982, personal communication).
- Figure 4-3** North-south cross-section from oil well Windy Point No. 1 to Alexandra Falls B-07 showing the occurrence of artesian flow conditions below the Chinchaga evaporites (modified after K. Williams, 1982, personal communication). Compare Fig. 3-3 for position of cross-section.
- Figure 4-4** Results of discharge measurements in m^3/s taken along the Buffalo River, Hanbury Creek, Little Buffalo River, Nyarling River and Salt River (modified after Weyer et al., 1979, Fig. 4).
- Figure 4-5** Buffalo River: stretches without bridging ice cover, November 30, 1975 (modified after Weyer, 1975, Fig. 1).
- Figure 4-6** Reef facies underlying Watt Mountain Formation near Buffalo River (modified after Wiley, 1970, Fig. 5).
- Figure 4-7** Natural sulphur spring discharging at left bank of Buffalo River, downstream of highway bridge (from Weyer, 1978b, Fig. 5).
- Figure 4-8** Belts of regional discharge areas of sulphurous and saline/sulphurous groundwater along Little Buffalo River and Salt River. Mapped from a Landsat 1 image (August 27, 1973; E-1400-181600-6; bands 5, 6 and 7; chemistry determined by selected ground control).

stripes, isotopic balances were calculated from measured $\delta^{34}\text{S}$ values and concentrations of sulphate and sulphide ions. In areas without stripes, measured $\delta^{34}\text{S}$ values for sulphates only were used, since sulphide data were lacking.

Figure 4-17 Scatter diagrams of $\delta^{34}\text{S}$ in SO_4^{2-} versus sulphate concentrations in natural waters south of Great Slave Lake. The numbers 26 and 50 signify 26 or 50 data points not plotted in the area of the number.

- A. Using measured distribution of $\delta^{34}\text{S}$ in dissolved sulphate.
- B. Using corrected $\delta^{34}\text{S}$ values, after the isotopic balance and the initial SO_4^{2-} content had been calculated using H_2S values.

Figure 4-18 Population of ^2H isotopes in water samples and comparison of Cl^- concentration (A) and topographic elevation (B).

Figure 4-19 Occurrence of lighter ^2H values ($<-165\text{\textperthousand}$; group 2) in surface waters and discharging groundwaters. Similar groundwater discharge pattern are indicated as in Figs. 4-8, 4-11, 4-12 and 4-13.

Figure 4-20 Effect of groundwater discharge on chemistry of river waters south of Great Slave Lake, compared with flow volume.

Figure 4-21 $\delta^{34}\text{S}$ (SO_4^{2-}) for river waters south of Great Slave Lake. Nyarling River, Little Buffalo River and Salt River are dominated by discharge of deep groundwater.

Figure 4-22 Vugs in cores from oil well CDR Wood Buffalo C-74.

- A: depth 893.6 ft, Upper Keg River Formation
- B: depth 930.1 ft, Upper Keg River Formation
- C: depth 959.8 ft, Upper Keg River Formation
- D: depth 971.6 ft, Lower Keg River Formation.

Figure 4-23 Appearance and porosity of vuggy cores from oil well CDR Wood Buffalo C-74.

Figure 4-24 Occurrence of karst features, internal sediments, vugs and fractures in the Muskeg Formation. A = boreholes penetrating Muskeg Formation; B = collapse and brecciation; C = mud, green mud and sand; D = vugs; E = fractured (open square = open fracture, Fig. 4-25); F = gypsum in vugs and on fractures.

Figure 4-25 Open fractures in anhydrite, CDR Wood Buffalo L-42, 389.7 ft depth.

Figure 4-26 Dissolution of anhydrite and conversion of anhydrite to gypsum on horizontal fractures in core from oil well CDR Wood Buffalo L-42; depth about 390 ft. in Muskeg Formation.

Figure 4-27 Dissolution of anhydrite and conversion of anhydrite to gypsum on horizontal fracture in core from oil well CDR Wood Buffalo L-42.

Figure 4-28 Core from oil well CDR Wood Buffalo L-42; two blebs of gypsum positioned on hairline fractures; depth 534 ft in Muskeg Formation.

Figure 4-29 Core from oil well CDR Wood Buffalo L-42: oblique hairline fractures with a rim of salt crystals, depth 534 ft in Muskeg Formation.

Figure 4-30 Core from oil well CDR Wood Buffalo L-42: Growthrings in gypsum bleb associated with hydrogeologically active hairline fracture; depth 534 ft in Muskeg Formation; scale in mm.

Chapter 5

Figure 5-1 Location of discharge observation sites (arrowheads), pits with hydrochemical sampling program (dots) and other pits (triangles) referred to in the report.

Figure 5-2 Groundwater ridge or mound at the orebody R-190 of Westmin Resources. Elevation of waterlevels prior to pumping (modified after Golder Associates, 1980, Fig. 4).

Figure 5-3 1980 distribution of Cl^- concentrations at open pit A-70. Dots = wells sampled.

Figure 5-4 1980 distribution of SO_4^{2-} concentrations at open pit A-70. Dots = wells sampled.

Figure 5-5 3-D plot of 1980 Cl^- concentrations at open pit A-70. Area covered and data used are the same as in Fig. 5-3. Marks on horizontal axes are 100m apart.

Figure 5-6 3-D plot of 1980 SO_4^{2-} concentrations at open pit A-70. Area covered and data used are the same as in Fig. 5-4. Marks on horizontal axes are 100m apart.

- Figure 5-7** Measured Zn + Fe contents of pumped water at open pit K-57 (after Santos, 1975, Plates 3 and 6).
- Figure 5-8** 1977 distribution of SO_4^{2-} concentrations at open pit R-61. Dots = wells sampled.
- Figure 5-9** 3-D plot of 1977 Cl^- concentrations at open pit R-61. Marks on horizontal axes are 100m apart.
- Figure 5-10** Position of orebody W-17 and collapse structures in relation to outline of open pit (modified after Santos 1975, Plate 12; collapse structures mapped by K.M. Newman).
- Figure 5-11** Measured Zn + Fe concentrations in pumped water at open pit W-17 in July 1974 (modified after Santos 1975, Plate 9).
- Figure 5-12** Open pit W-17: Distribution of Cl^- concentrations, 1977.
- Figure 5-13** Open pit W-17: 3-D plot of Cl^- concentrations, 1977. Area covered and data used are same as in Fig. 5-12. Marks on horizontal axes are 100m apart.
- Figure 5-14** Plan and cross-section of open pit W-17, showing geologic cross-section, depth of pumping well and salt-concentrations (square: saline water).
- Figure 5-15** Open pit W-17: distribution of sulphate concentrations. A: 1977; B: 1978.

- Figure 5-16** Open pit W-17: 3-D plot of SO_4^{2-} -concentrations. A: 1977; B: 1978. Area covered and data used are the same as in Figs. 5-15A and 5-15B. Marks on horizontal axes are 100m apart.
- Figure 5-17** Open pit A-55: Distribution of Cl^- concentrations, 1980.
- Figure 5-18** Open pit A-55: 3-D plot of Cl^- concentrations, 1980.
- Figure 5-19** Open pit A-55: Distribution of SO_4^{2-} -concentrations, 1980
- Figure 5-20** Open pit A-55: 3-D plot of SO_4^{2-} -concentrations, 1980.
- Figure 5-21** Sketch of microbiological sampling points, open pit S-65.
:
- Figure 5-22** Outlay of pump test at open pit K-77.
- Figure 5-23** Schoeller diagram showing the range of chemical (major ions) changes recorded between October 4 and October 21, 1980 during the K-77 pump test (from Weyer and Horwood, 1981, Fig. 7).
- Figure 5-24** Composite diagram showing changes over time in chemical parameters and the *Thiobacillus* population during the pump test K-77 (from Weyer and Horwood, 1981, Fig. 23).

- Figure 5-25** Changes of Thiobacillus population during K-77 pump test (from Weyer and Horwood, 1981, Fig. 22).
- Figure 5-26** Schematic diagram of discharge measurement sites at open pit S-65 (from Weyer and Horwood, 1980a, Fig. 2).
- Figure 5-27** Pumping history at Pine Point Mines 1971 - 1980 (source of data: Pine Point Mines Ltd.).
- Figure 5-28** A. Borehole 104, May 1978; sulphurous deposits are indications for previous artesian flow.
B. Spring near borehole 104, May 1978; sulphurous deposits and lack of vegetation are indications for previous discharge.
- Figure 5-29** Photograph of flow at Angus Tower Spring, October 1977 (from Weyer 1978b, Fig. 6).
- Figure 5-30** Photograph of flow at Halfway Spring, October 1977 (from Weyer 1978b, Fig. 7).
- Figure 5-31** Spring pool and dry creek, Angus Tower Spring, summer 1980.
- Figure 5-32** Spring pool at Angus Tower Spring seen from creek outlet, summer 1980. Water level in pool receding.
- Figure 5-33** Gaging station at Angus Tower Spring, summer 1980; no flow.
- Figure 5-34** Angus Tower Spring seen from creek outlet, summer 1981. Vegetation has covered the creek bed.

- Figure 5-35** Gaging station at Angus Tower Spring, summer 1981; grassy and bushy vegetation covers part of creek bed. View similar to Fig. 5-33.
- Figure 5-36** Angus Tower Spring, summer 1981; appearance of creek shown in Fig. 5-29.
- Figure 5-37** Creek outlet at Angus Tower Spring, August 1982. Person in center stands at water level of pond. Compare to Figs. 5-32 and 5-34.
- Figure 5-38** Gaging station at Angus Tower Spring, August 1982. Compare with Figs. 5-33 and 5-35.
- Figure 5-39** Comparison of hydrologic data at karst springs and pumping history for 1978 (source of pumping data: Pine Point Mines).
- Figure 5-40** Comparison of hydrologic data at karst springs and pumping history for 1979 (source of pumping data: Pine Point Mines).
- Figure 5-41** Chloride concentrations in waters discharging at springs and flowing boreholes, 1977, 1978 and 1980.
- Figure 5-42** Comparison of Cl^- and SO_4^{2-} concentrations in the surface water at the mouth of Little Buffalo River and pumping stress at W-17 open pit.

Chapter 6

Figure 6-1 Known Pb-Zn occurrences and deposits on the Canadian Shield east of Pine Point, N.W.T. (data from D. Sangster, GSC, 1982).

Chapter 7

Figure 7-1 Coal districts in Hungary subject to water inrushes from karstic layers (after Milde, 1963).

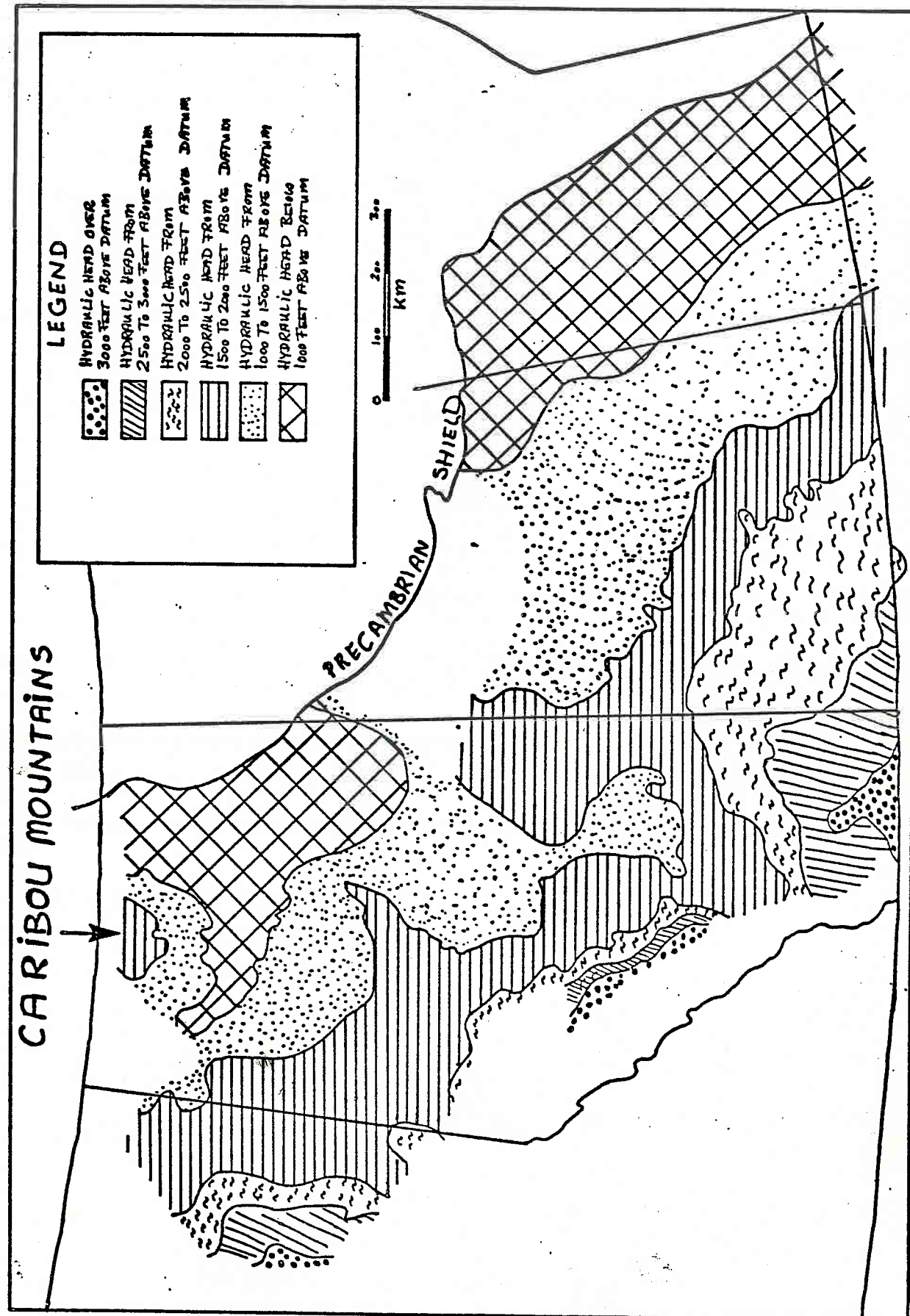
Figure 7-2 Schematic cross-section of karst aquifer systems in the Hungarian Central Mountains (after Ajtay et al., 1962).

Figure 7-3 Schematic positioning of sand injection well into karstic solution channel (after Ajtay et al., 1962).

Figure 7-4 Hydraulic mining of sands and schematic arrangement of feeder system for sand injection well (after Ajtay et al., 1962).

Figure 7-5 Effect of sand-gravel injection on the permeability k , the hydraulic gradient h and the groundwater flow Q in a karstic solution channel.

FIG. 1-1



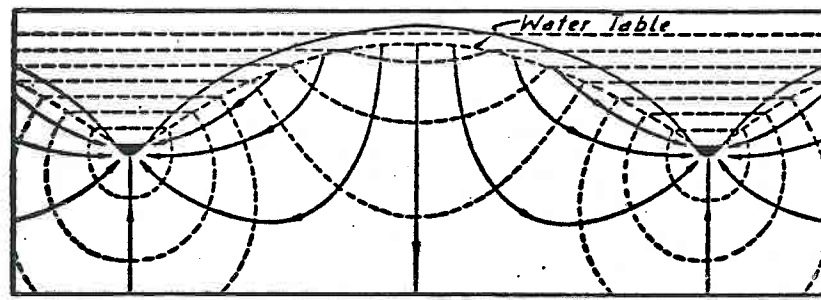


FIG. 2-1

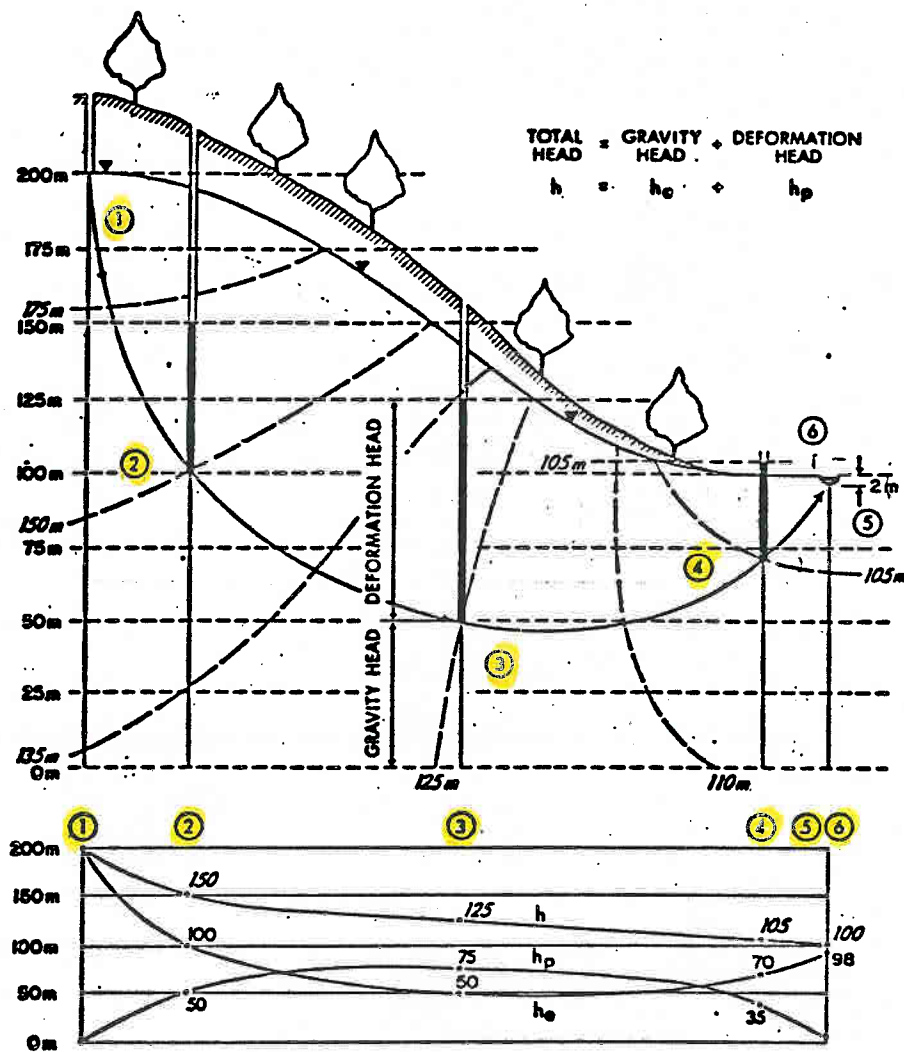


FIG. 2-2

FIG. 2-3

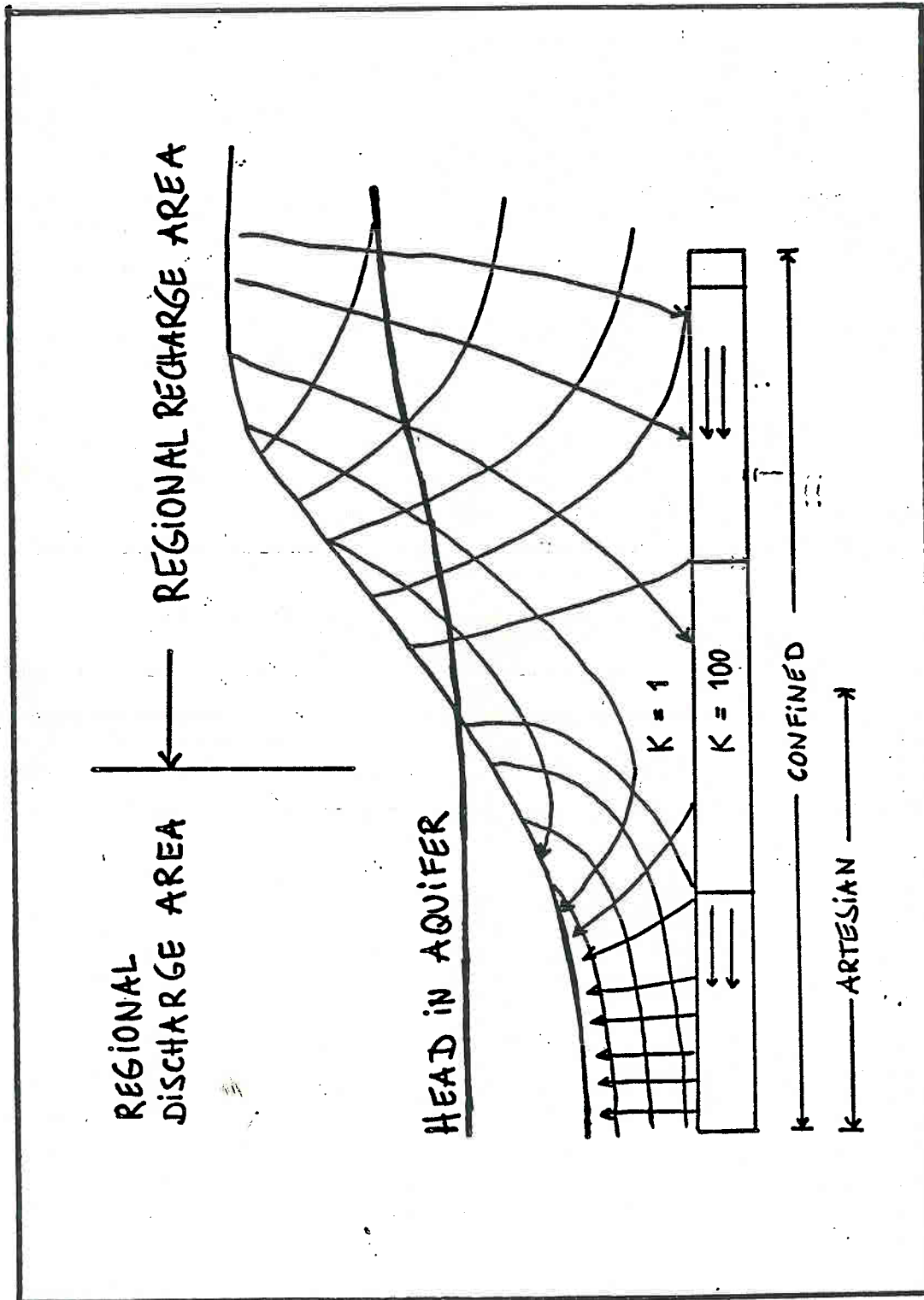


FIG. 2-4

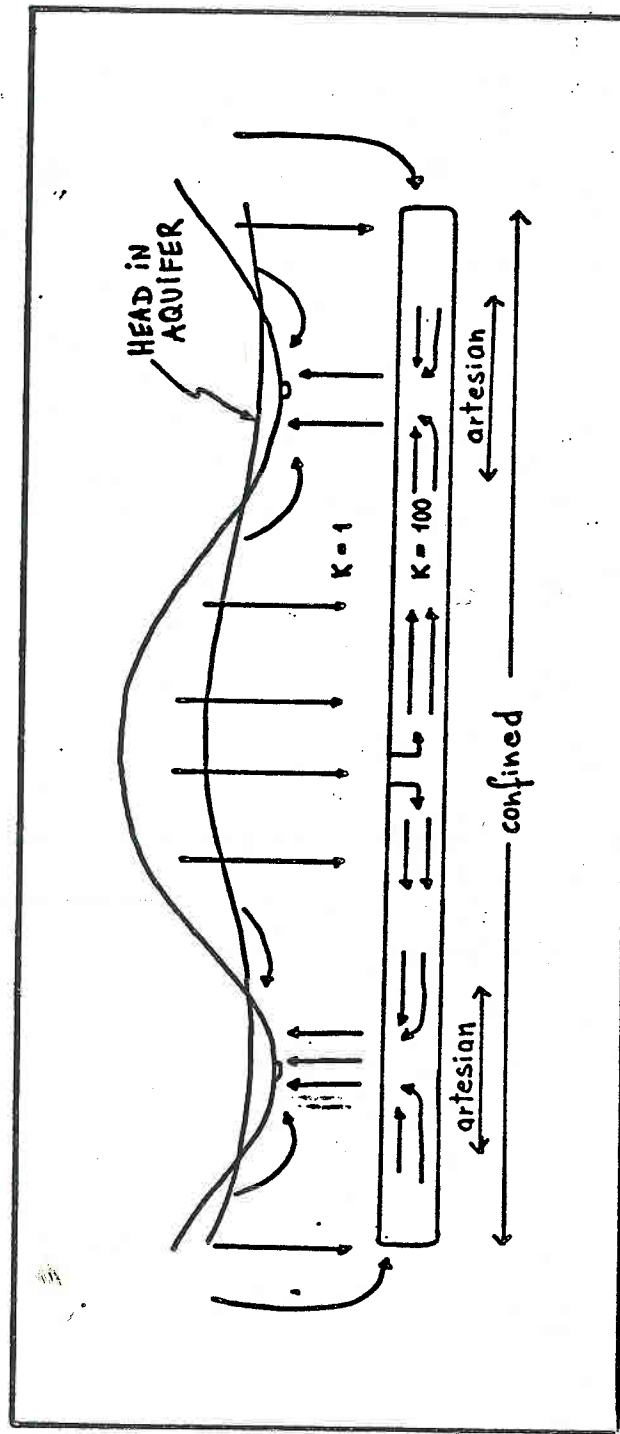


FIG. 2-5

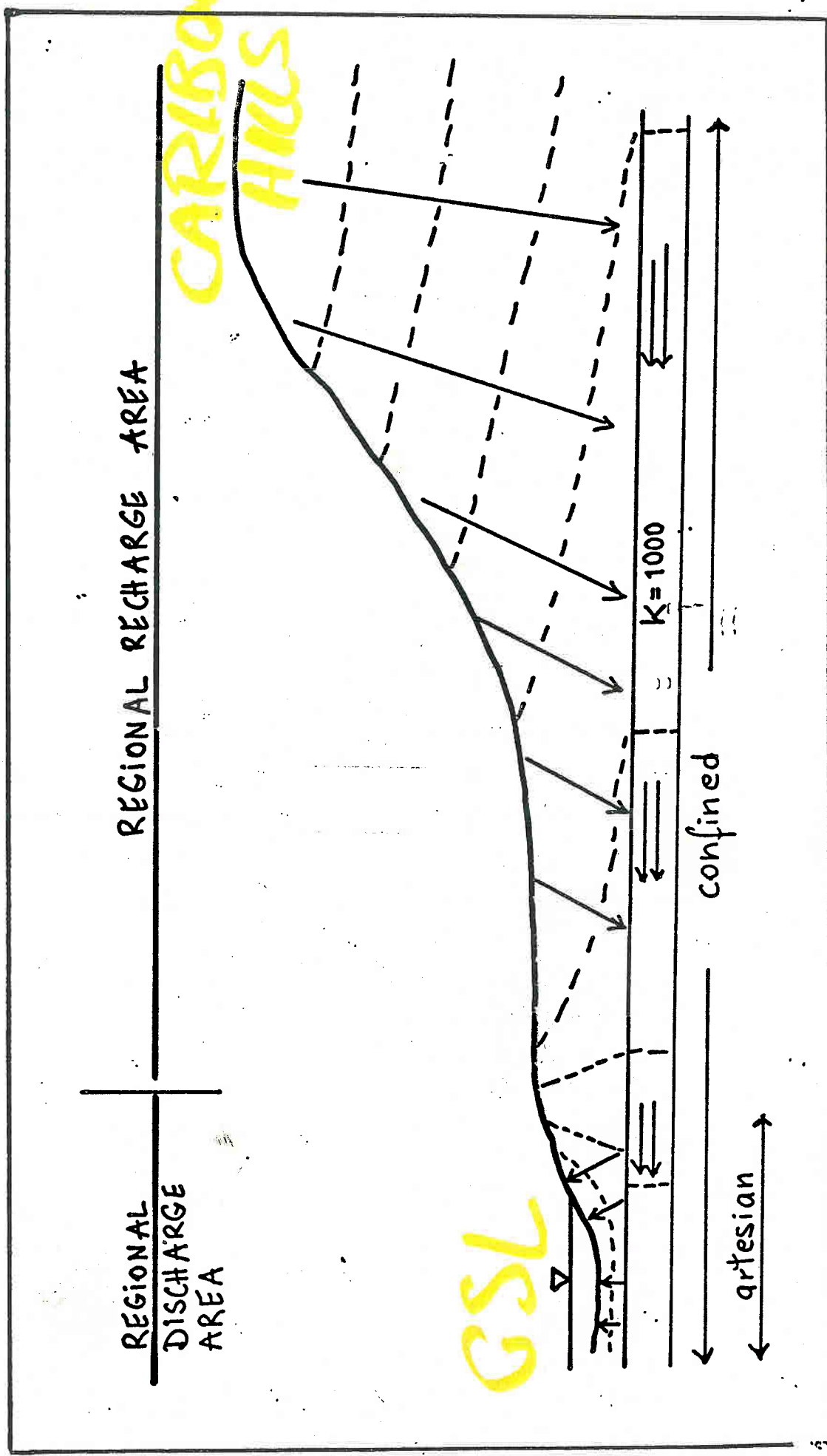
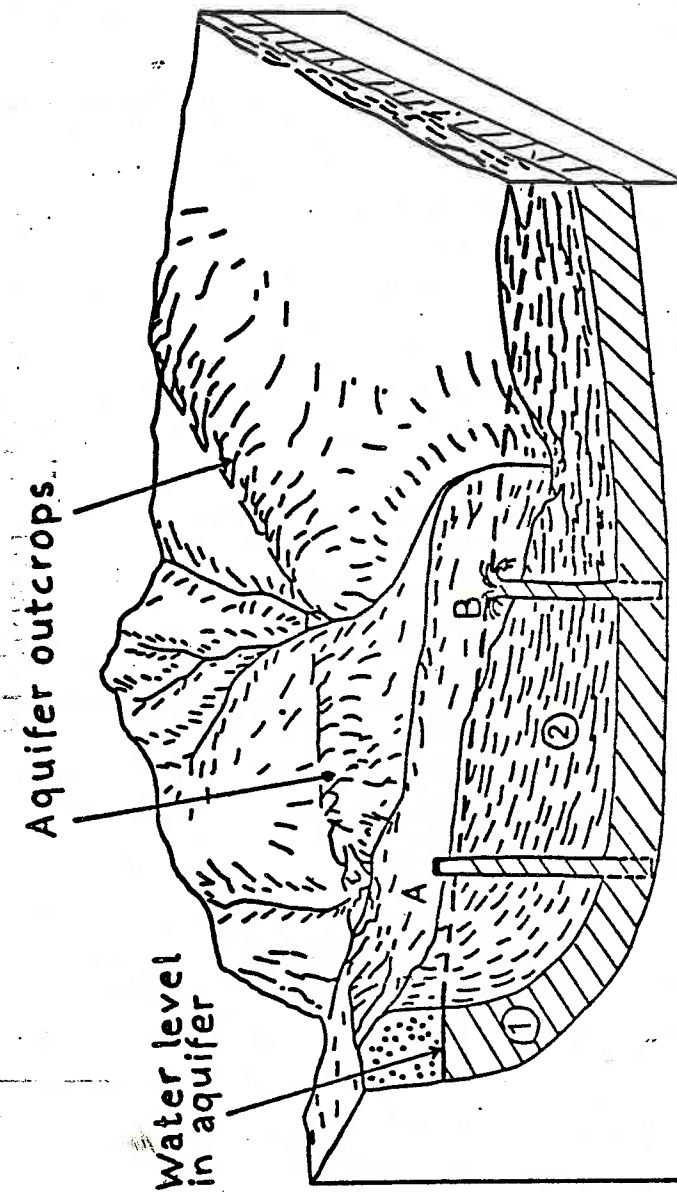


FIG. 2-6



ERA	FORMATIONS ¹⁾	TOPOGRAPHY
Cenozoic	Holocene, Pleistocene: Q _I	
Mesozoic	Cretaceous: K _I , K _A , K _{II} , K _B , K _{III}	
Paleozoic	Permian: P _I	
	Mississippian: M _A , M _I , M _B	
	D _{III} Wabamun Calmar Nisku	
	D _B Ireton Beaverhill Lake	
Devonian	D _{II} Slave Point Watt Mountain	
	D _A Muskeg Prairie Evaporites	
	D _I Keg River Chinchaga Ernestina Lake granite wash	
Precambrian		

1) Roman subscript denotes aquifer; letter subscript denotes aquitard; numbering and lettering from deeper layers upwards.

FIG. 2-7

GEOGRAPHICAL
AND
TOPOGRAPHICAL
FEATURES SOUTH
OF
GREAT SLAVE LAKE

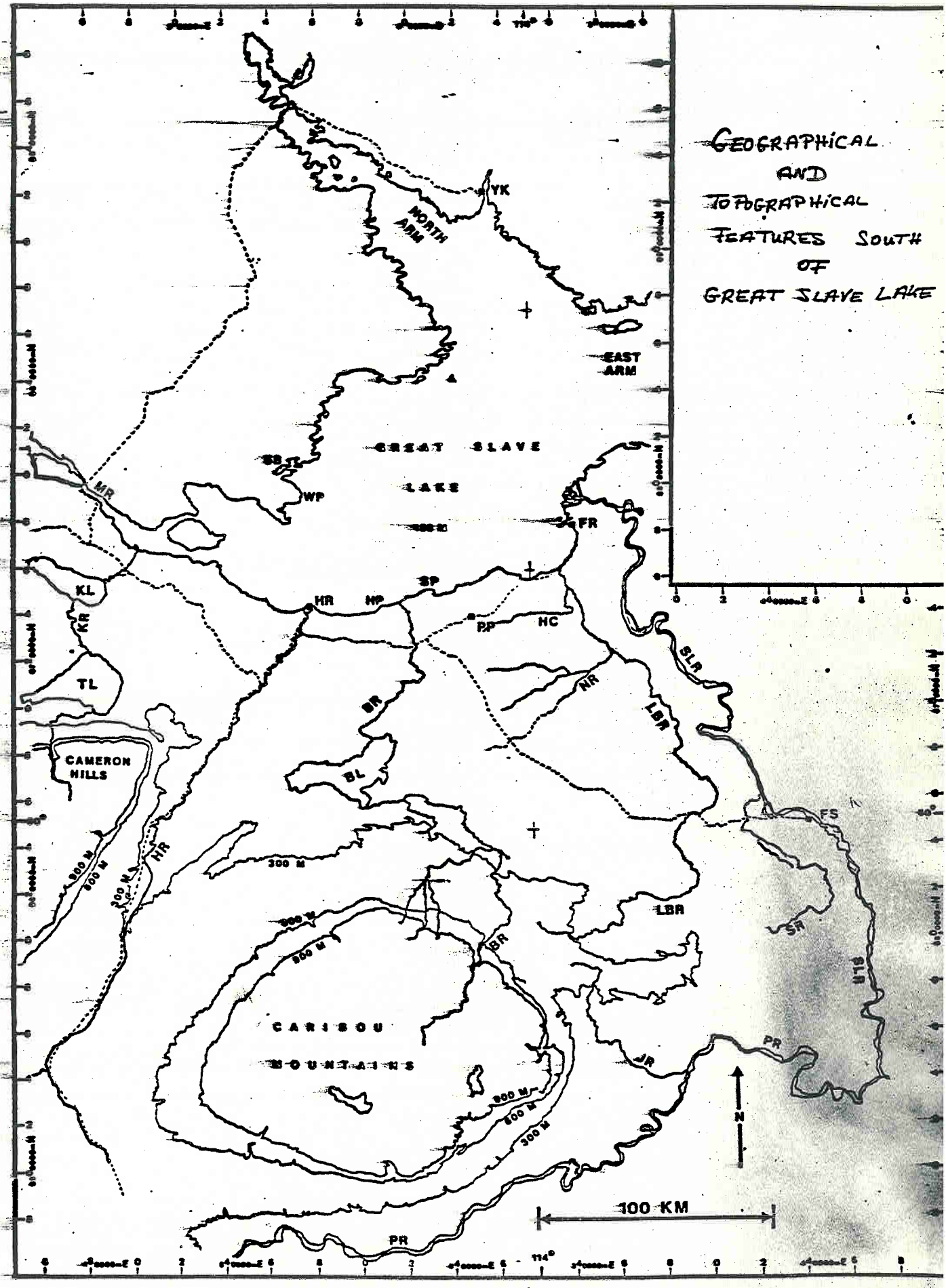
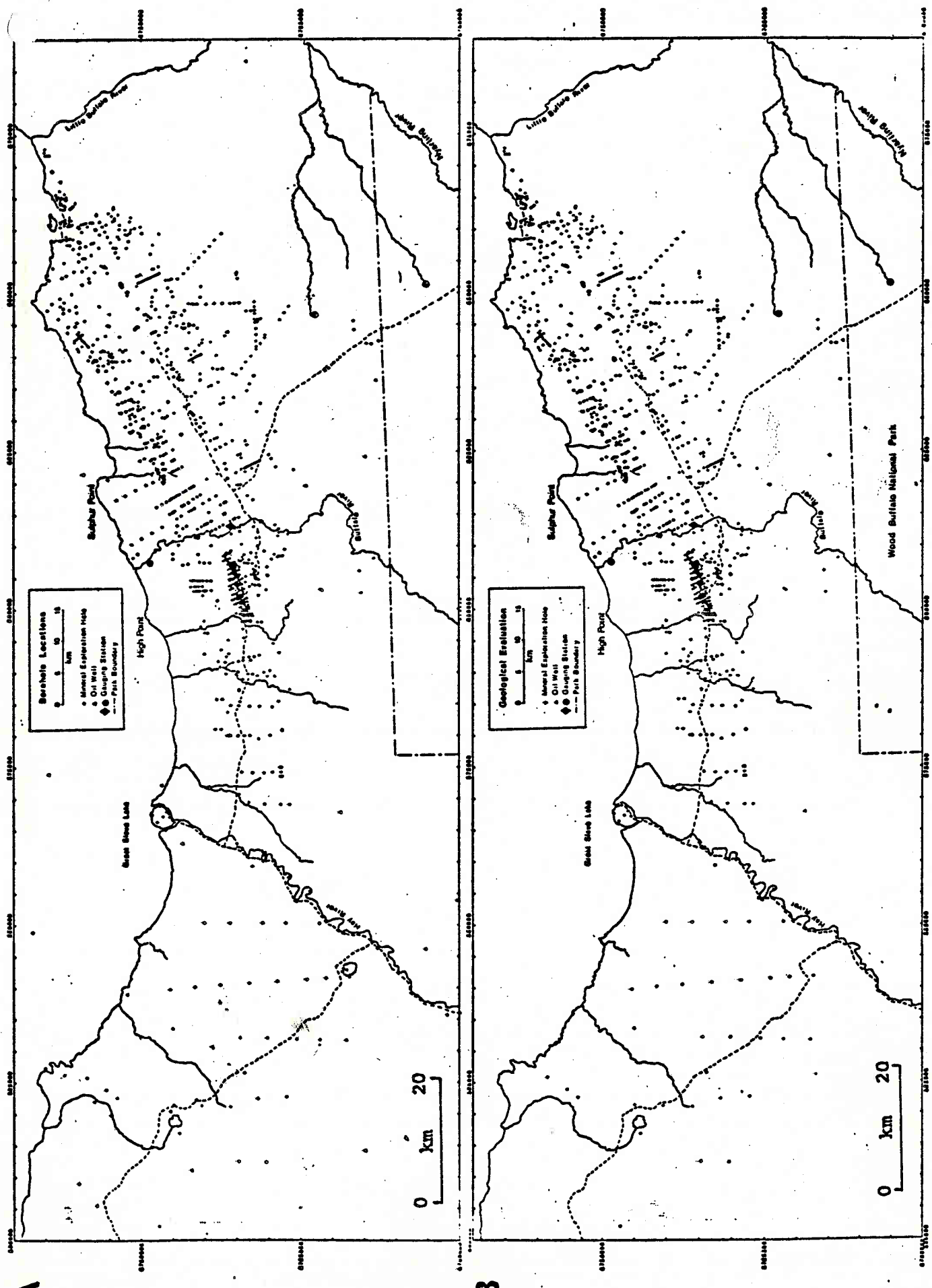


FIG. 3-2



A

B

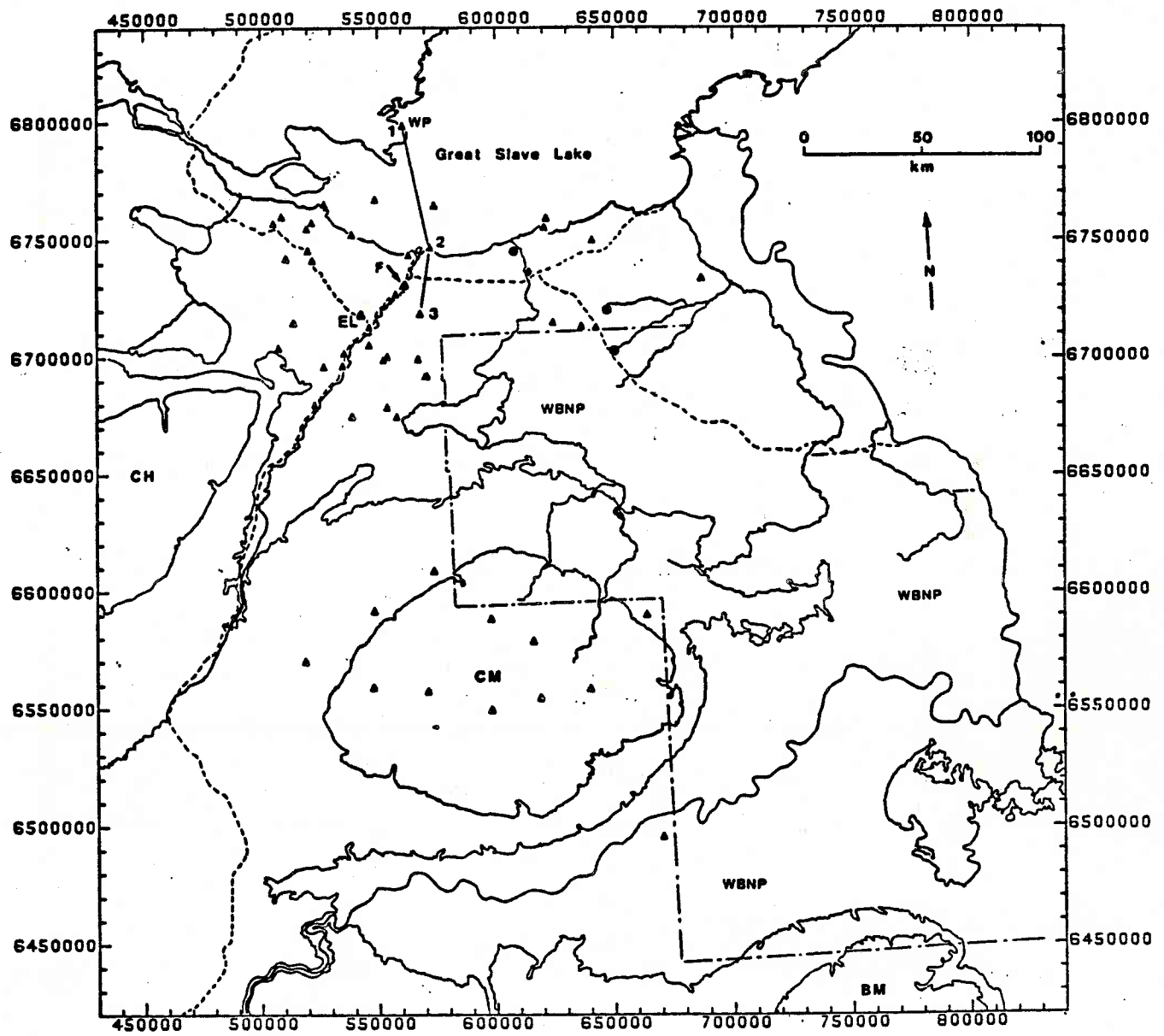


FIG. 3-3

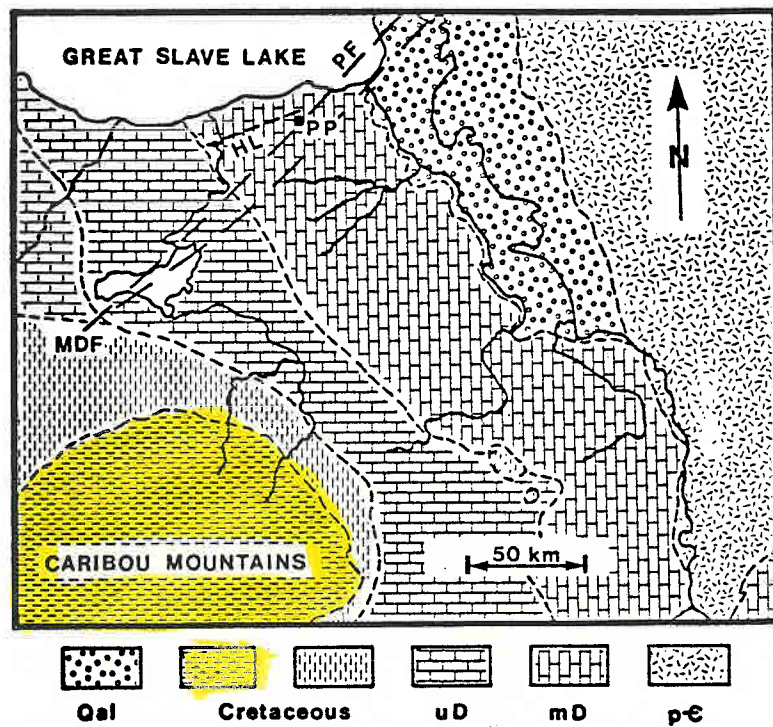


FIG. 3-4

FIG. 3-5

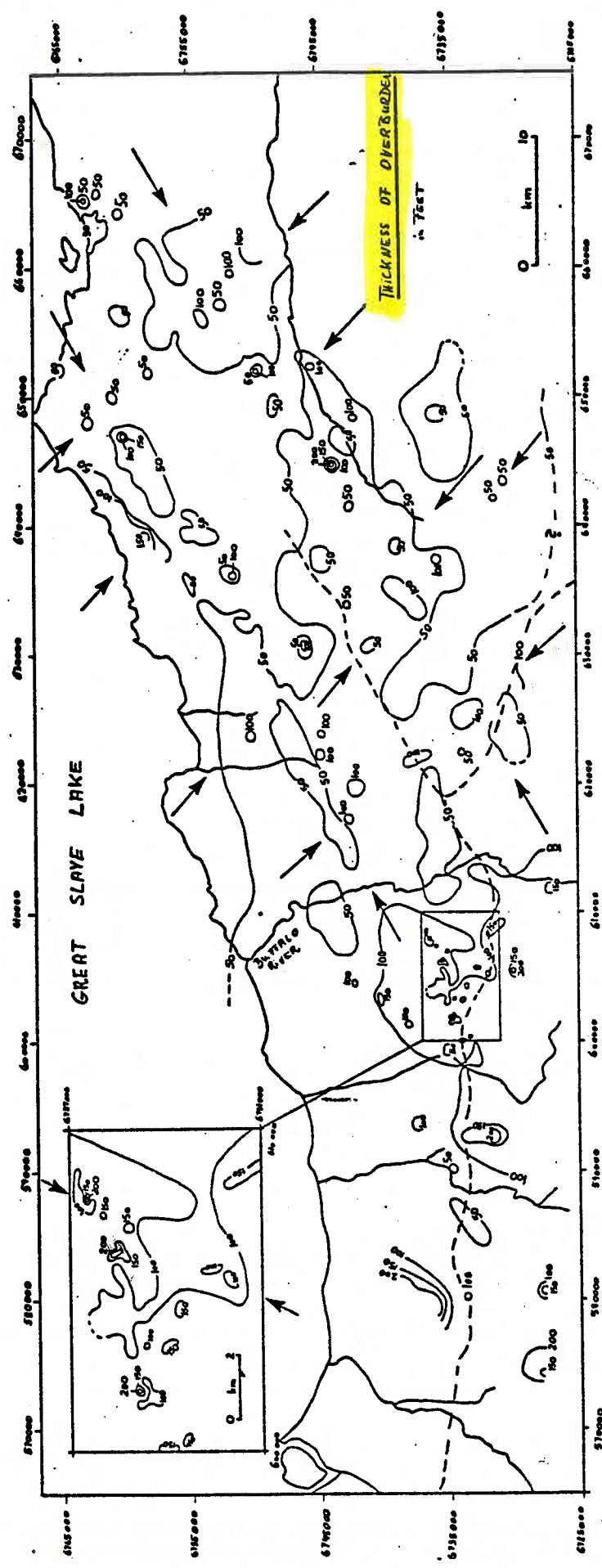
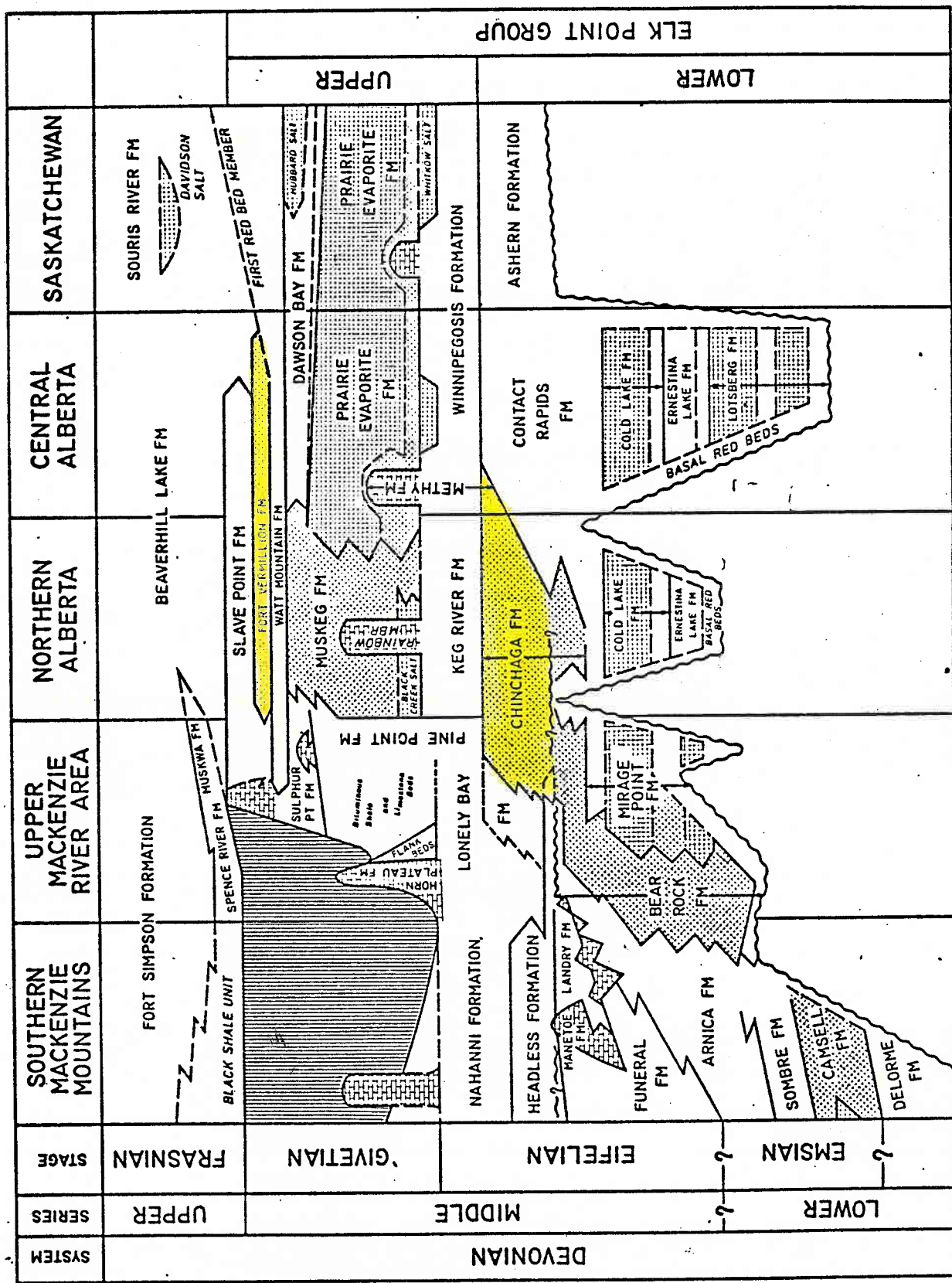
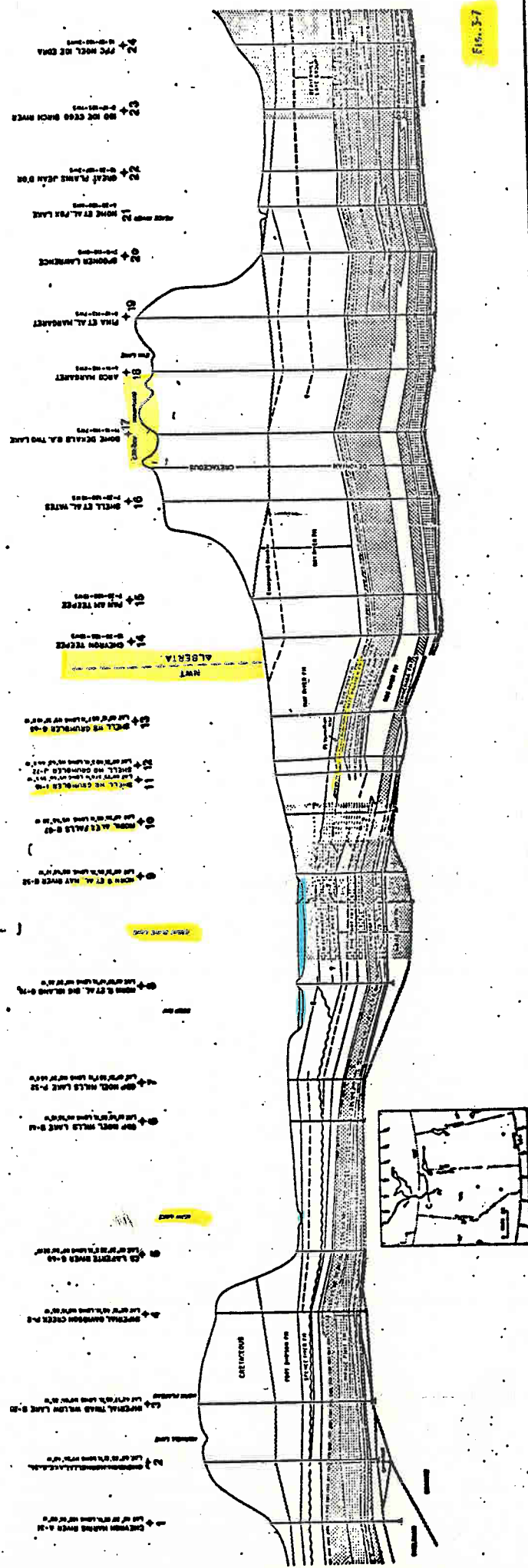


FIG. 3-6





	<i>Stratigraphic units in the Pine Point area</i>	<i>Significant events</i>
<i>Quaternary</i>	<i>Pleistocene gravel</i>	<i>30 m</i>
<i>Tertiary</i>		<i>erosion</i>
<i>Cretaceous</i>	<i>100</i> <i>young Cretaceous?</i> <i>Fort St. John</i>	<i>magmatism?</i> <i>600 - 1000 m</i>
	<i>135</i>	
<i>Jurassic</i>	<i>195</i>	<i>non-deposition and/or erosion</i>
<i>Triassic</i>	<i>225</i>	
<i>Permian</i>	<i>280</i> <i>..Pennsylvanian-Permian emergence"</i>	
<i>Pennsylvanian</i>	<i>320</i>	<i>tilting, erosion, peneplanation</i>
<i>Mississippian</i>	<i>345</i>	
<i>Upper Devonian</i>	<i>358</i> <i>Late Givetian- Mississippian sequence</i>	<i>1200 - 1500 m</i>
<i>Middle Devonian</i>	<i>370</i> <i>Pine Point Keg River Chinchaga</i>	<i>Watt Mountain Fm</i> <i>M.J.U. Givetian emergen</i> <i>Pine Point barrier reef</i> <i>310-350 m</i> <i>unconformity</i>
<i>Lower Devonian</i>		<i>emergence</i>
<i>Silurian</i>	<i>440</i>	
<i>Ordovician</i>	<i>500</i> <i>Mirage Point Old Fort Island</i>	<i>100-340 m</i> <i>unconformity</i>
<i>Cambrian</i>	<i>570</i>	<i>emergence</i>
<i>Precambrian</i>	<i>Precambrian basement</i>	<i>Mc Donald fault system</i>

FIG. 3-8

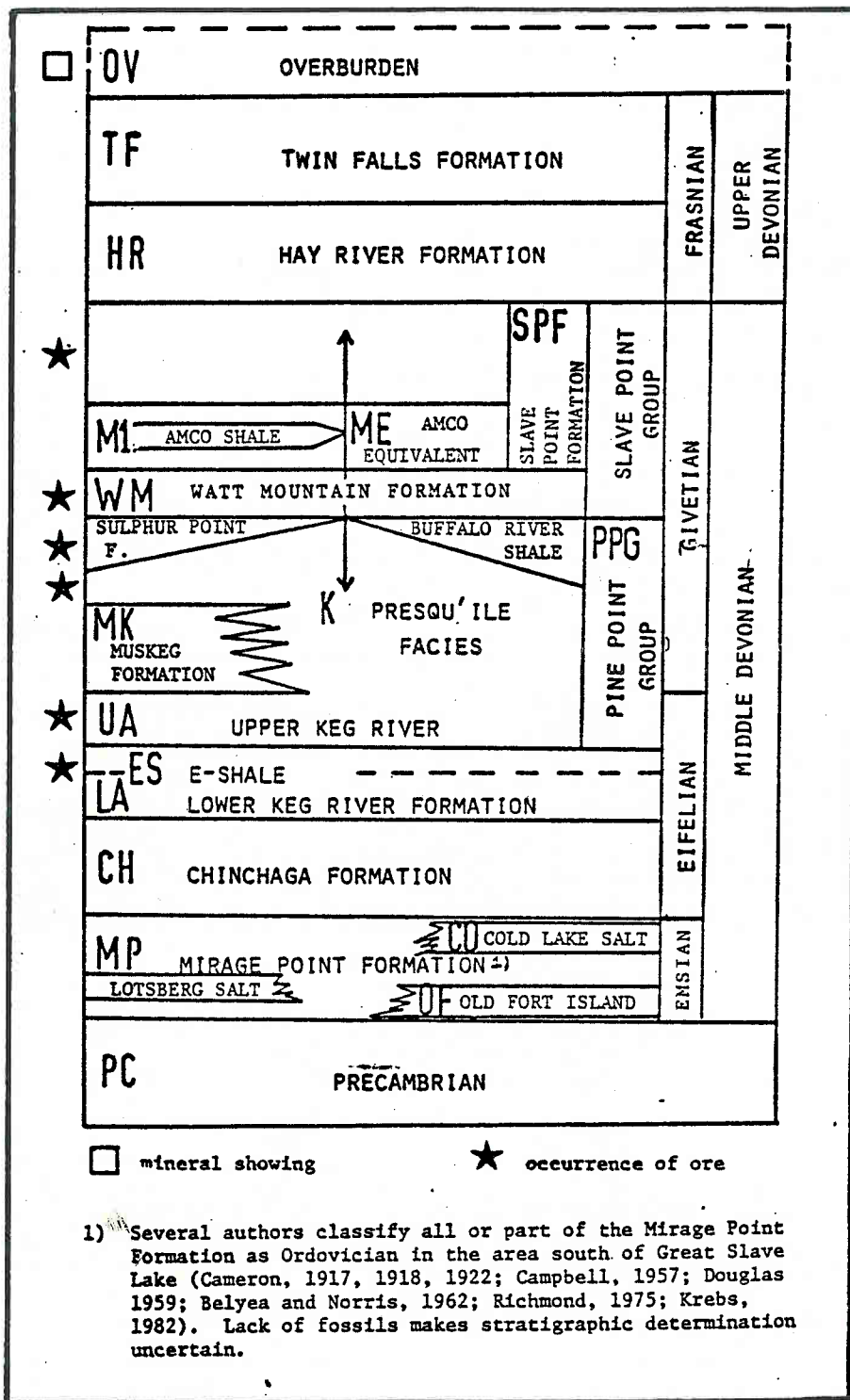
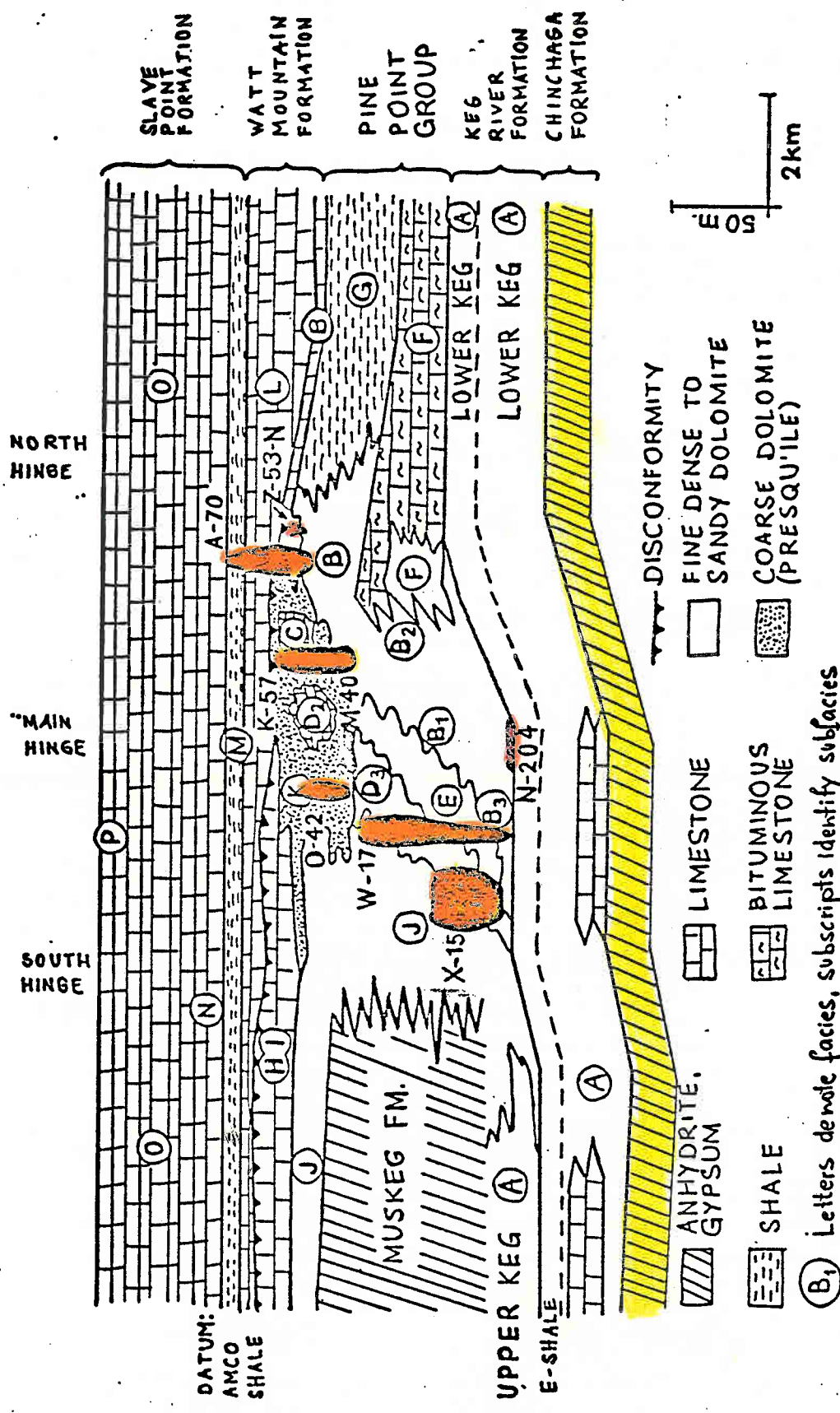


FIG. 3-9

FIG. 3-10



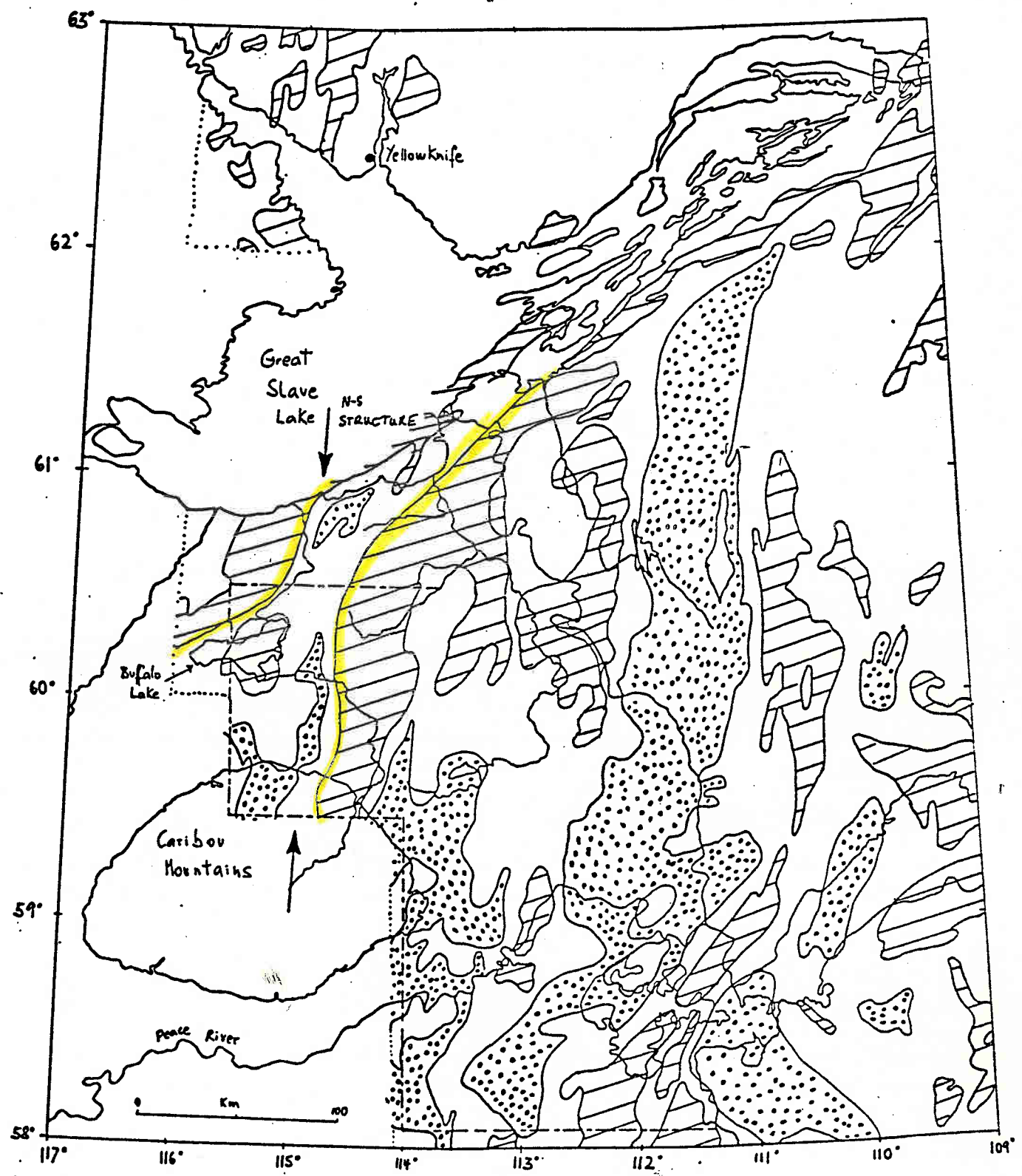


FIG. 3-11

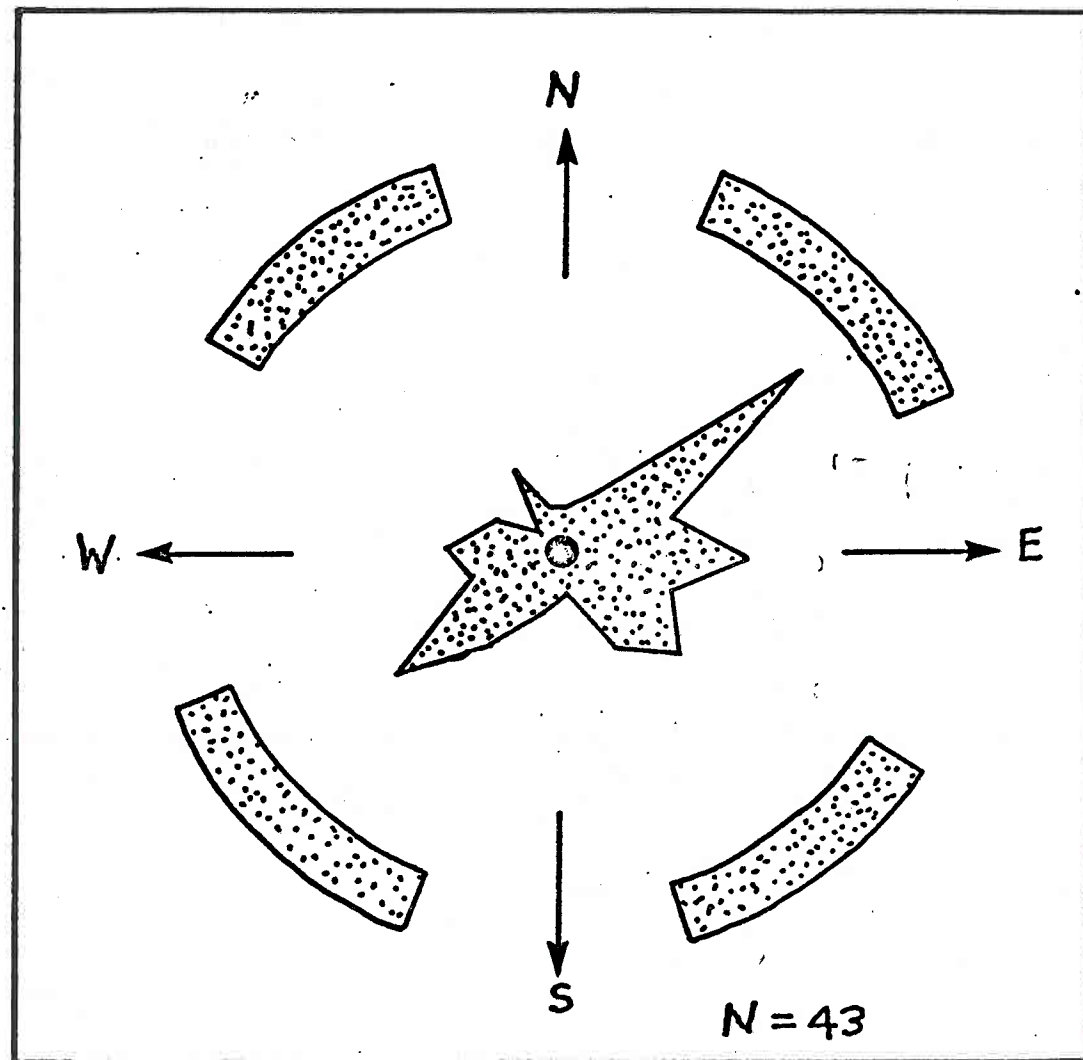


FIG. 3-12

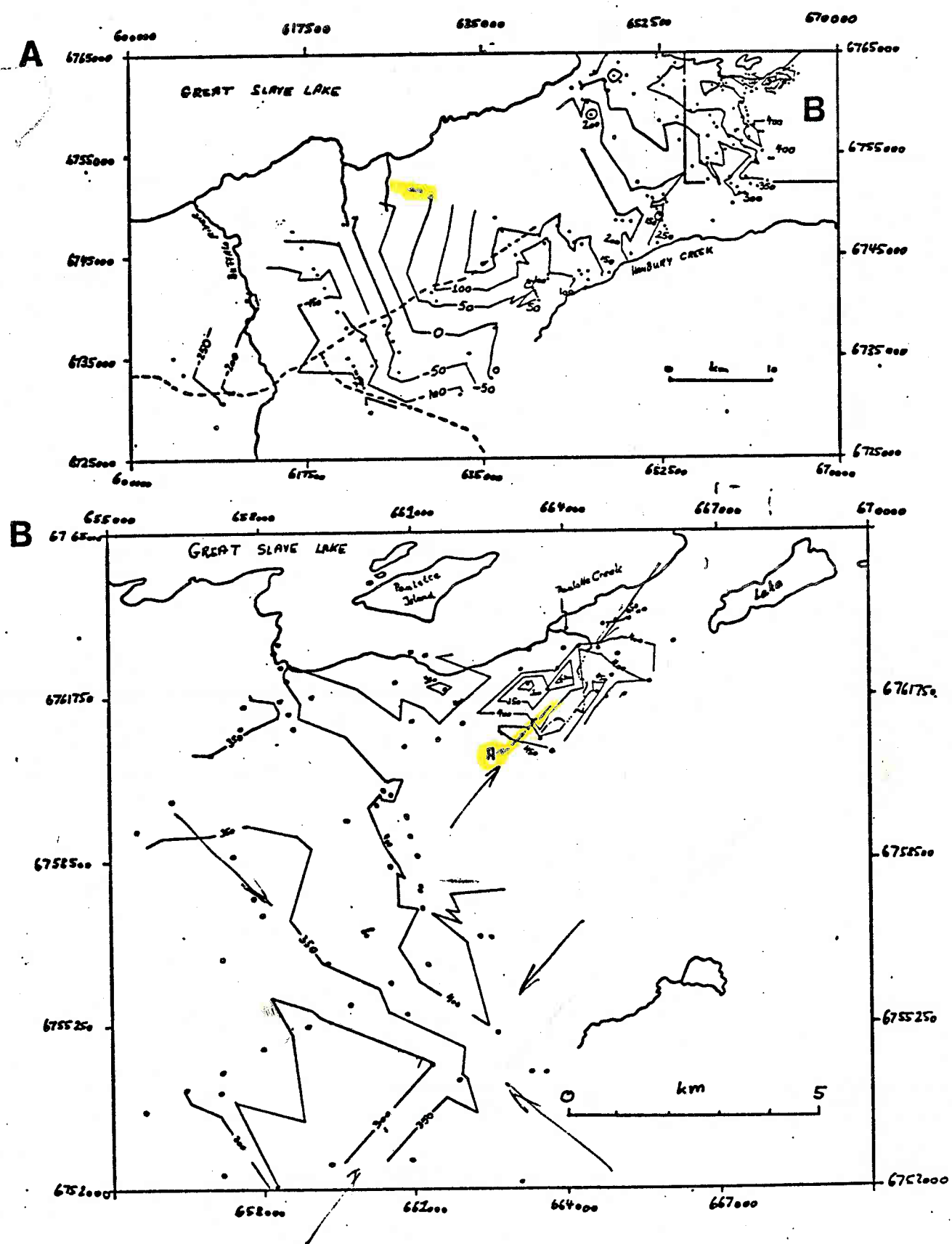
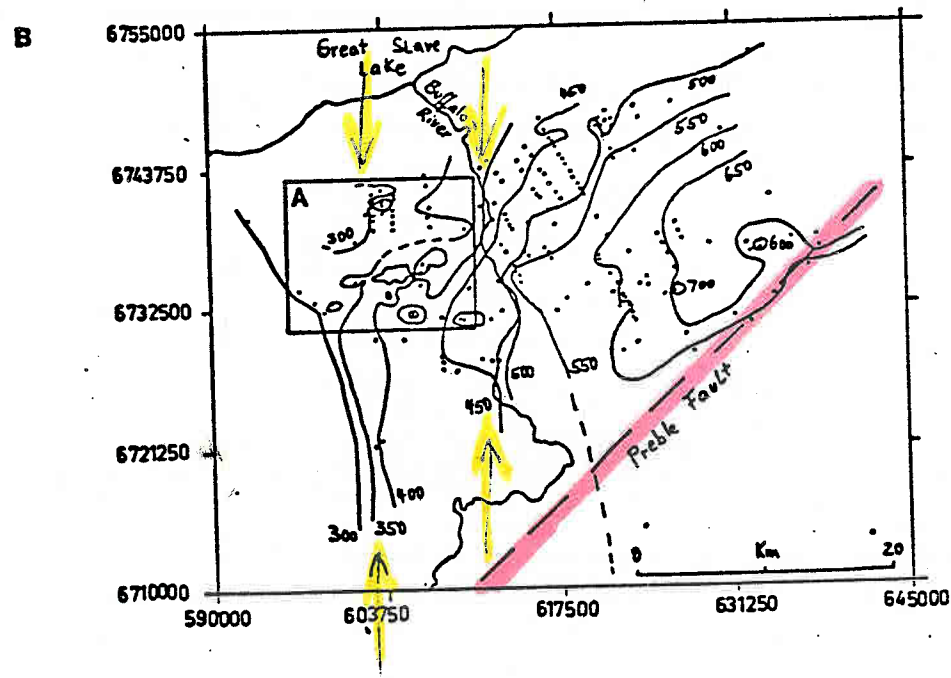
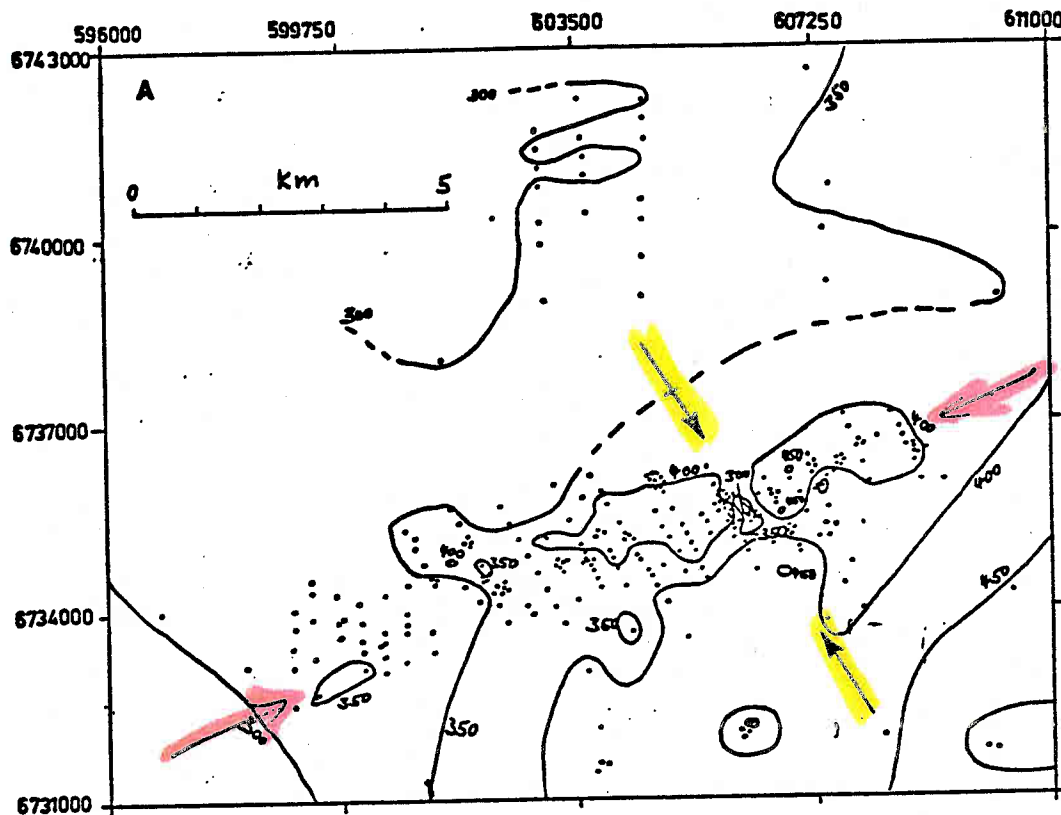
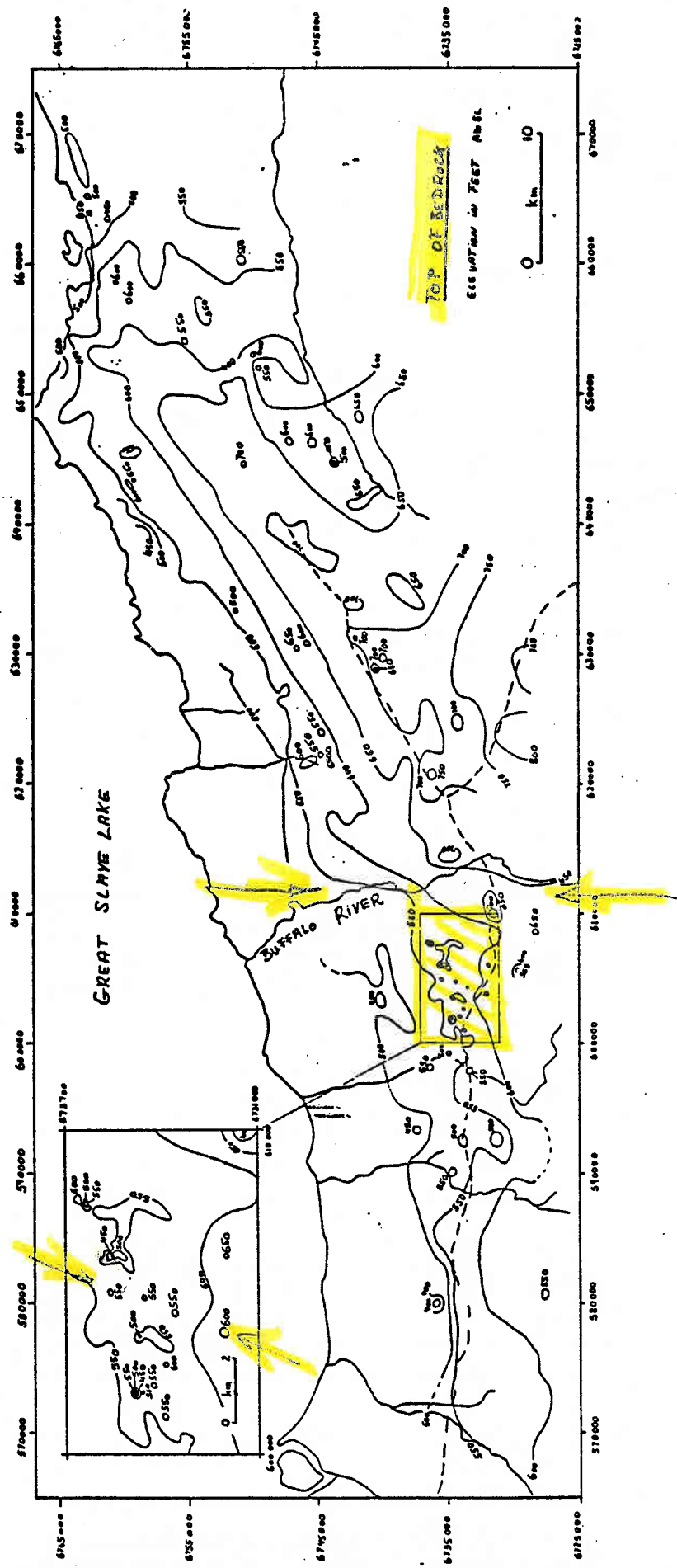


FIG. 3-13



Top of Amco Shale [Elevation in feet]

FIG. 3-15



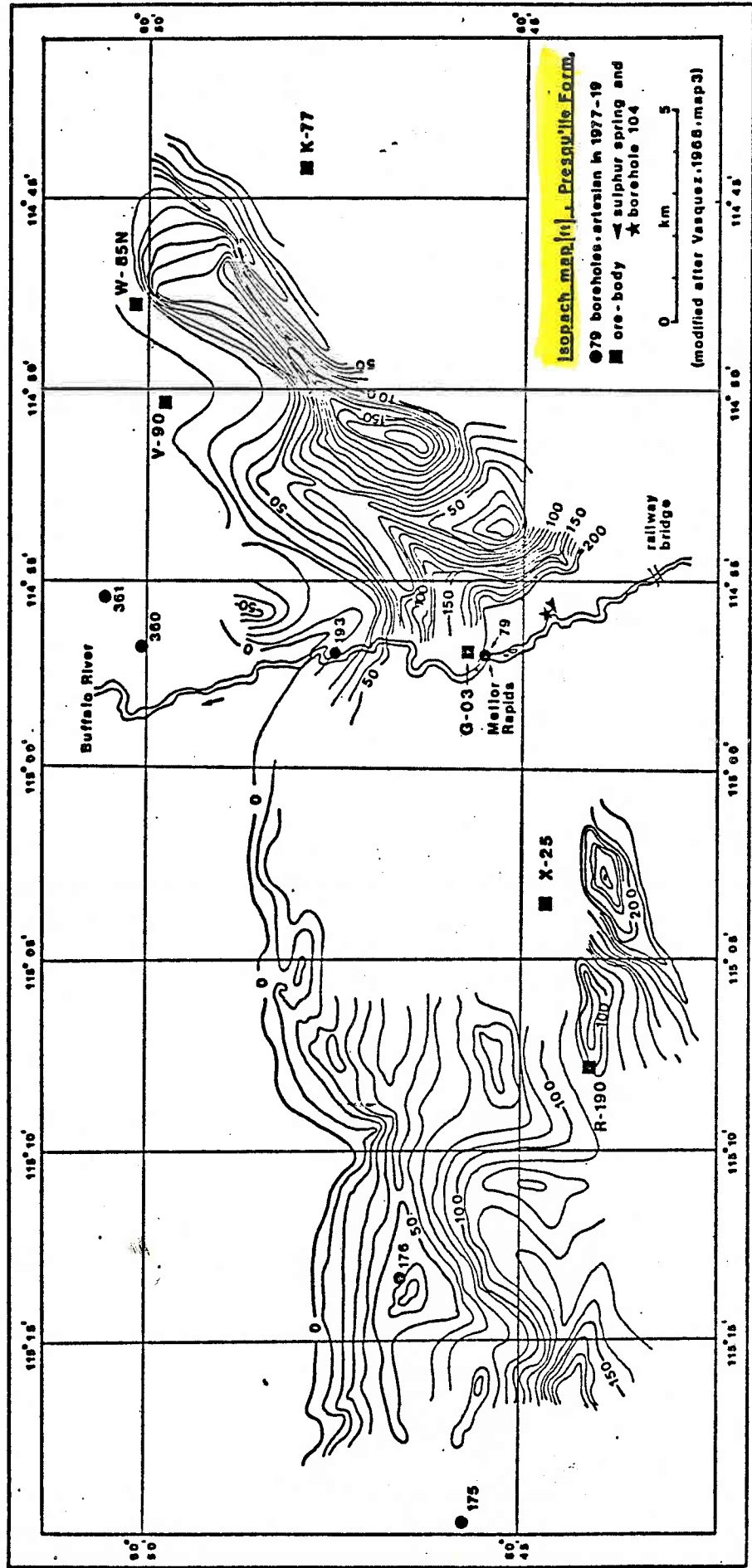


FIG. 3-16

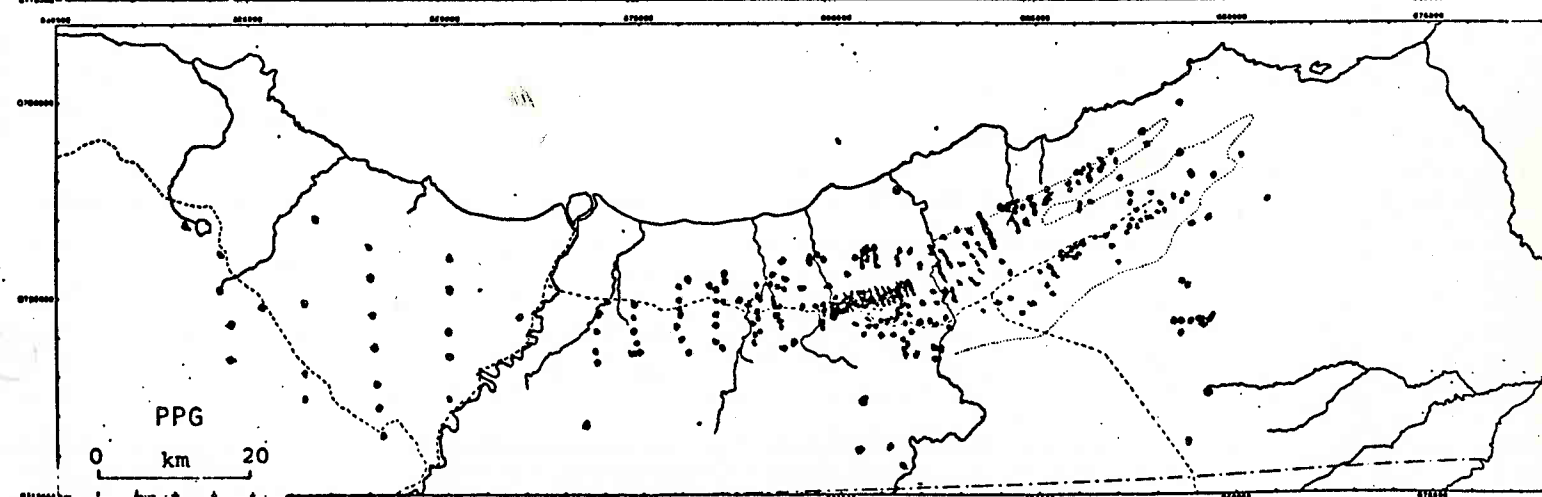
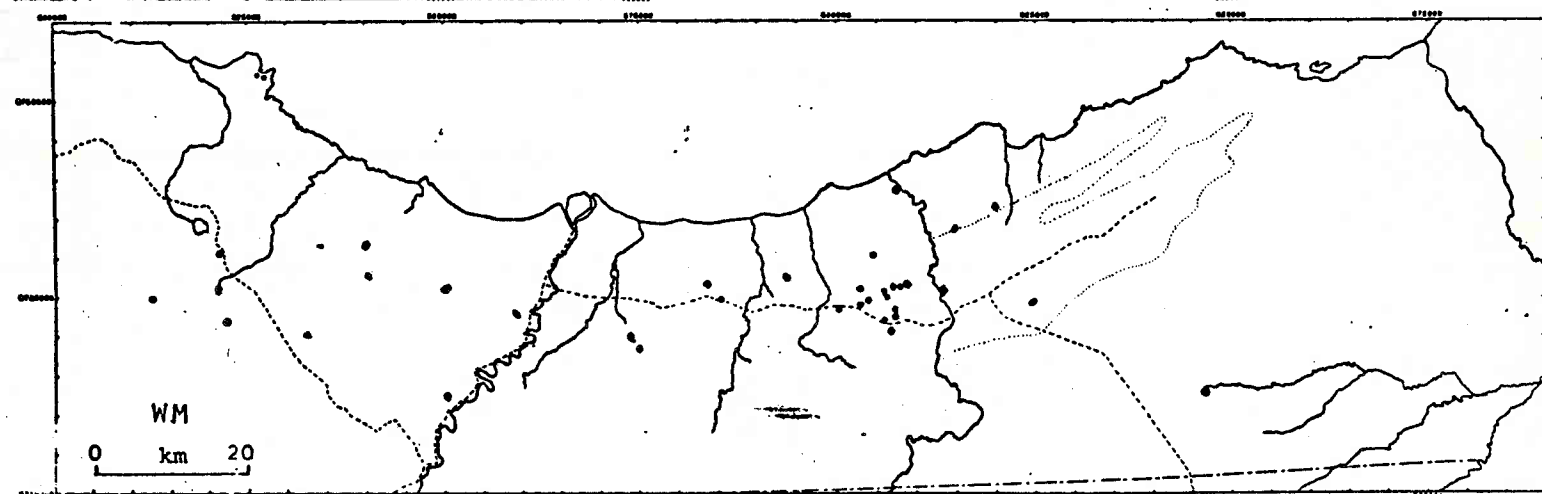
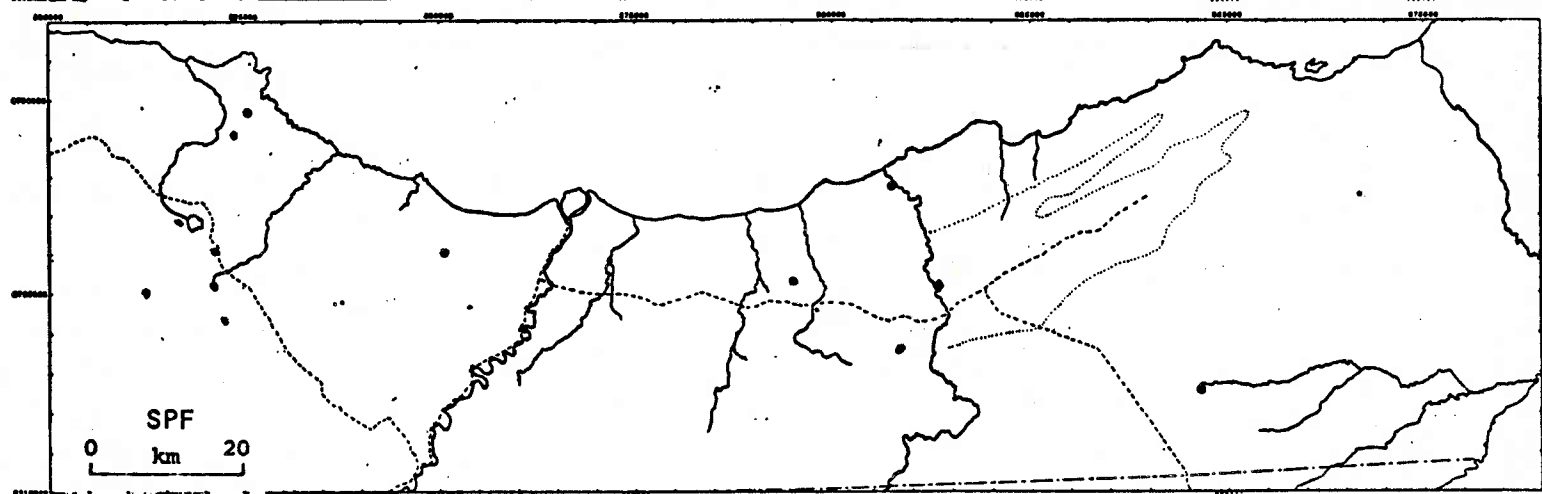
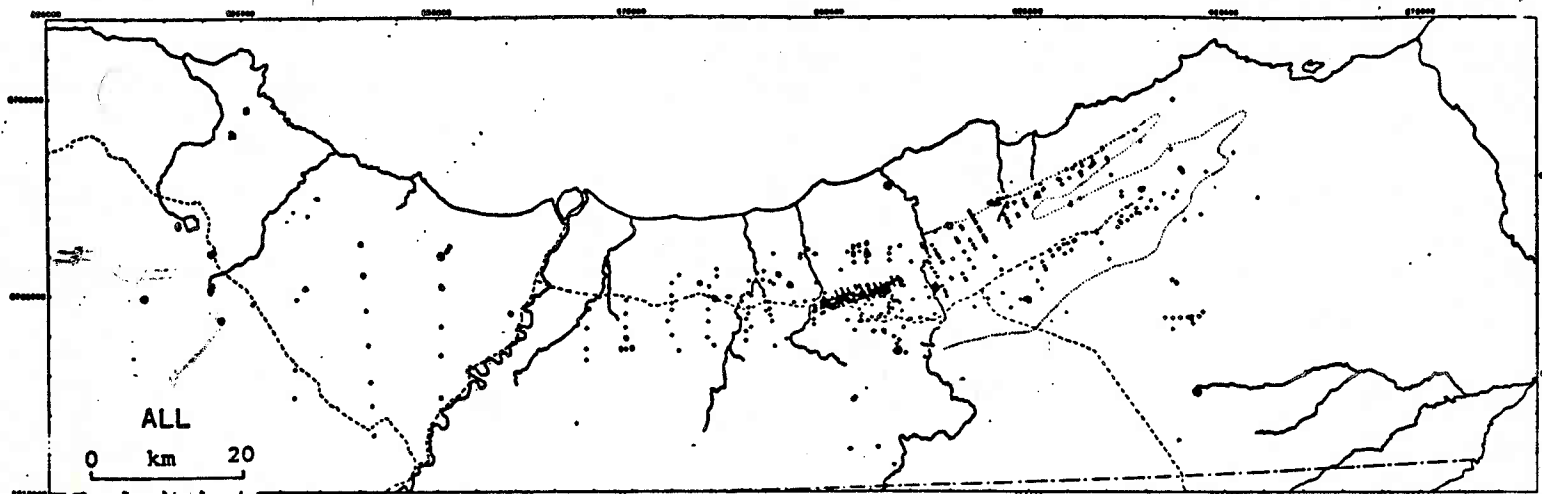


FIG. 3-18

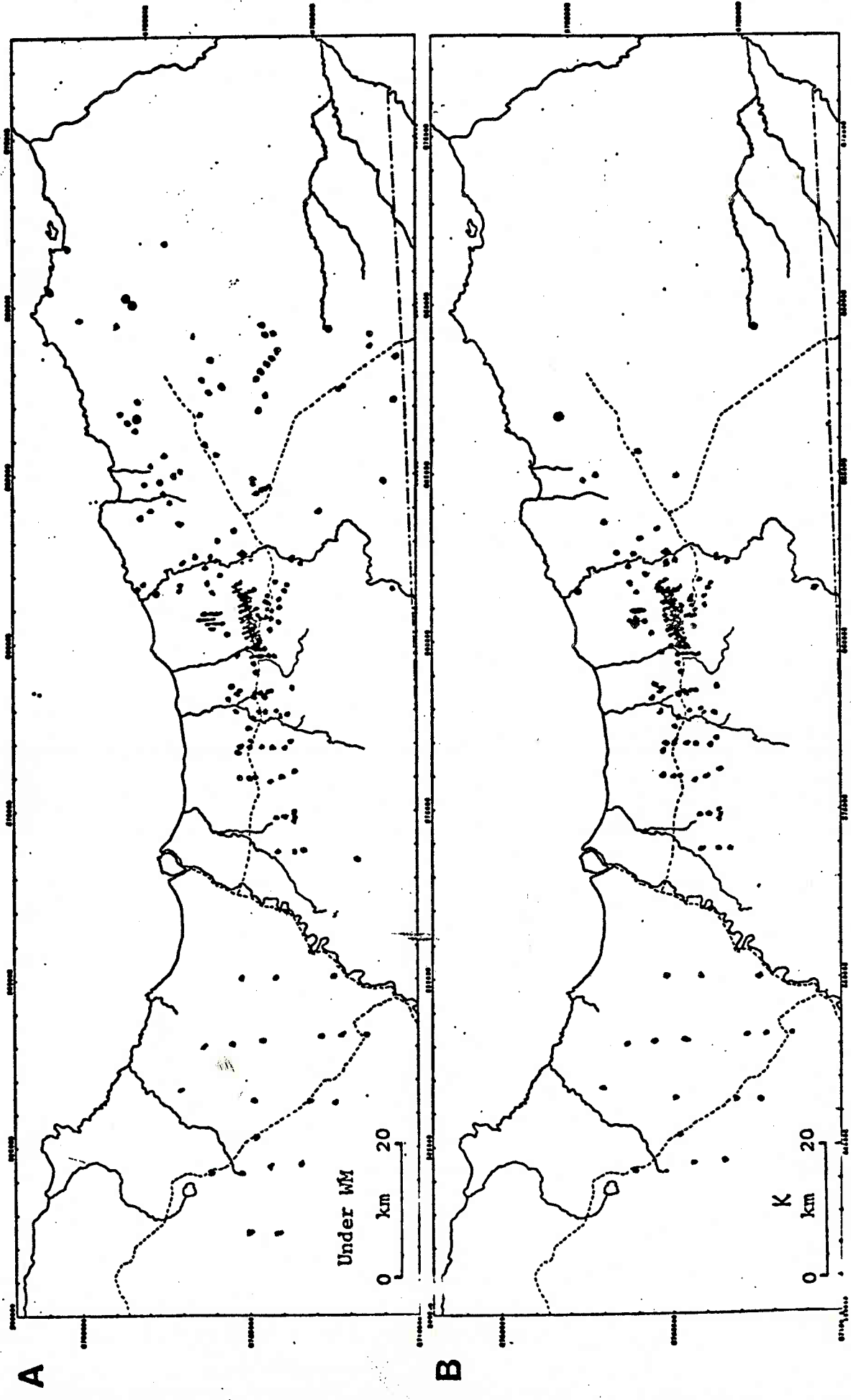
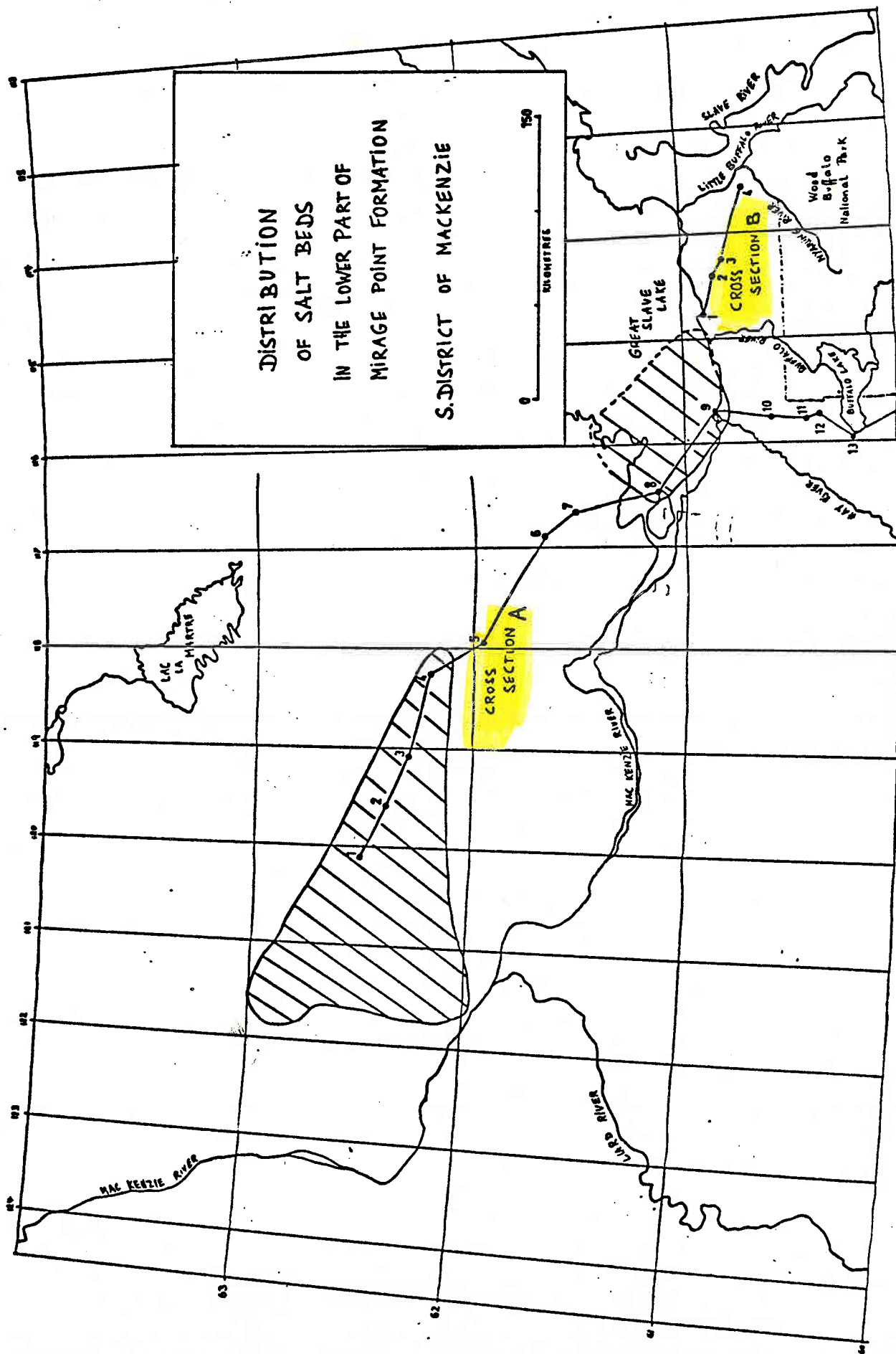


FIG. 3-19



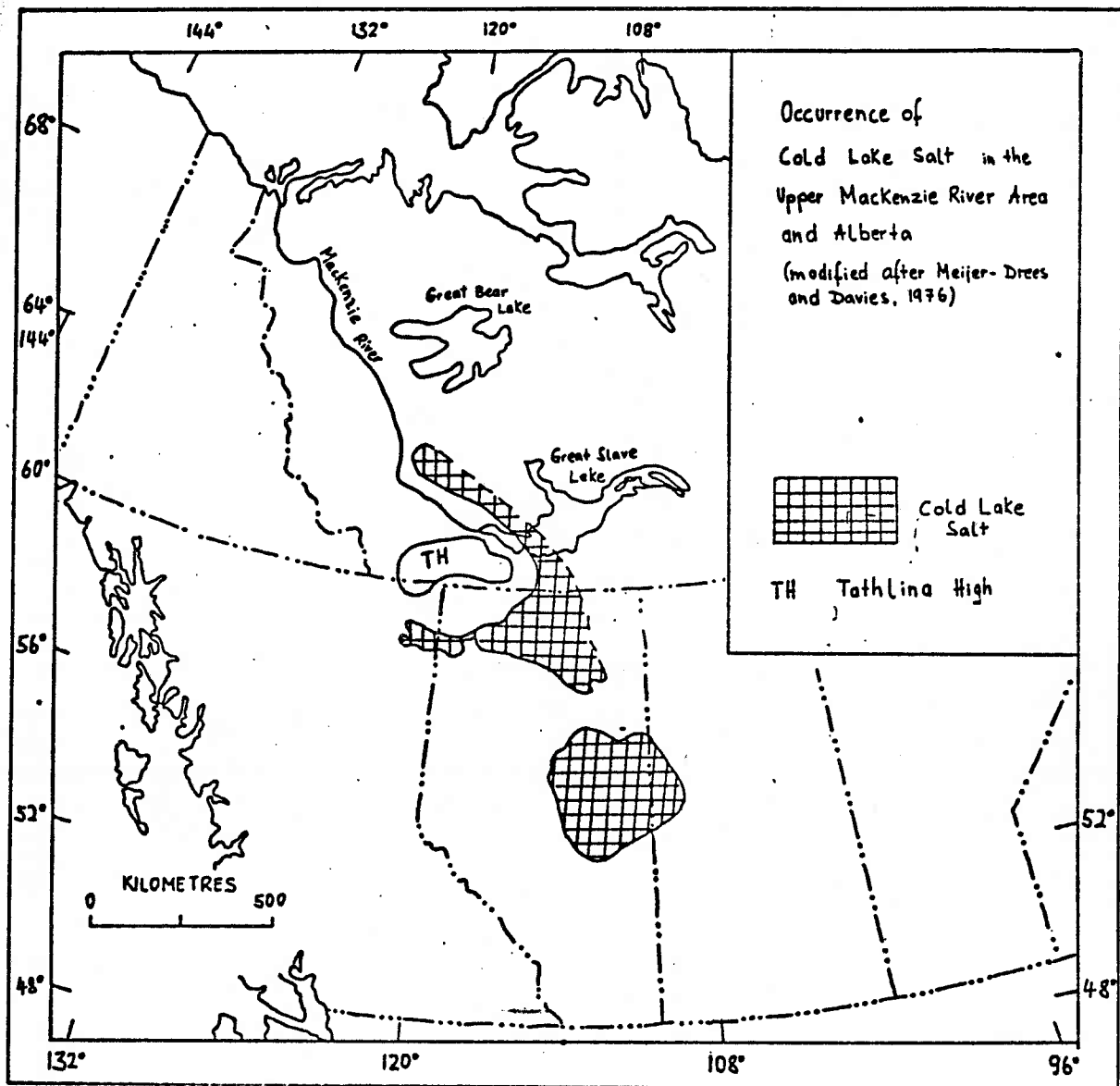


FIG. 3-20

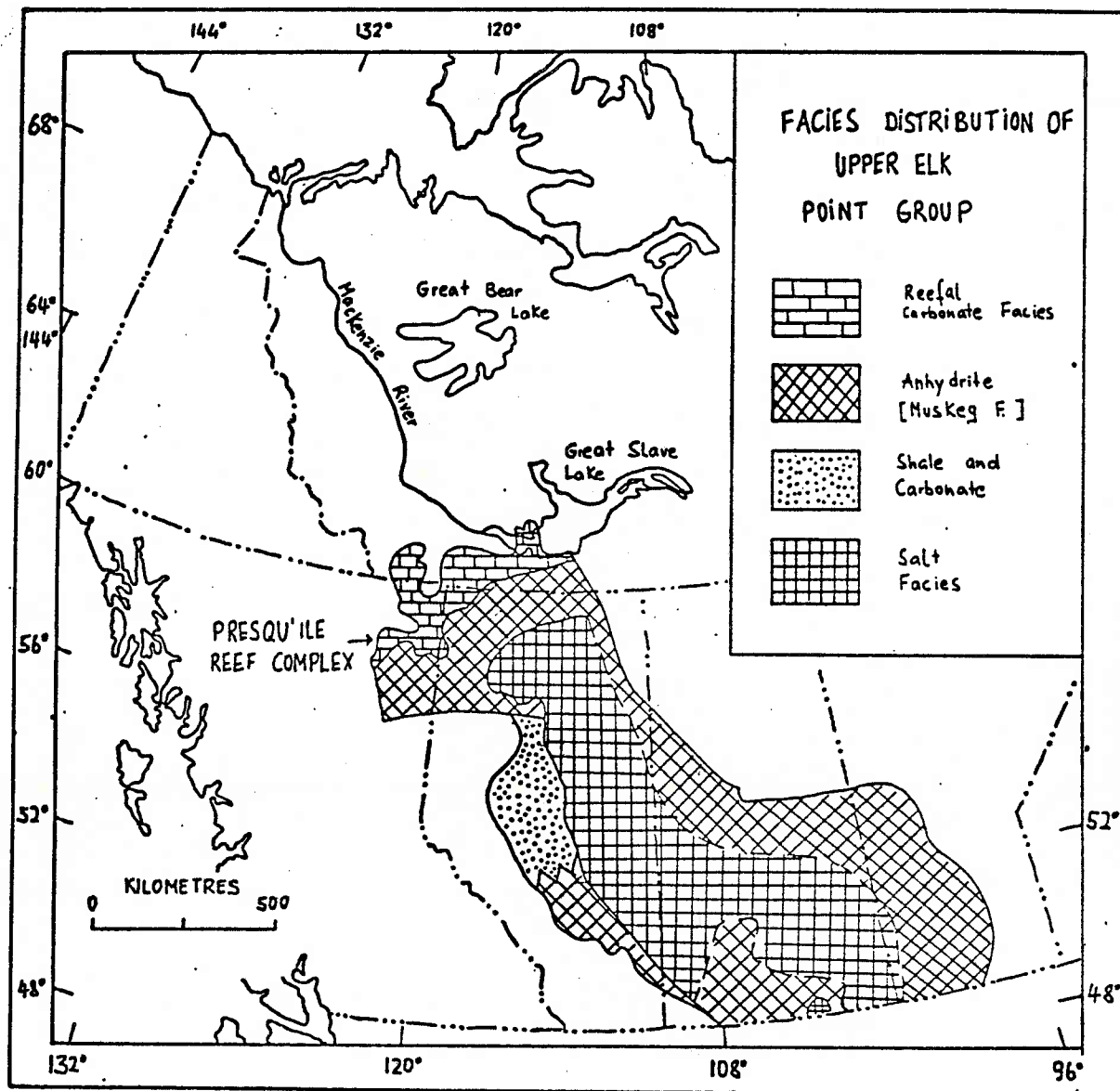


FIG. 3-21

**SALT SOLUTION,
EAST CENTRAL ALBERTA**

W

X'

X

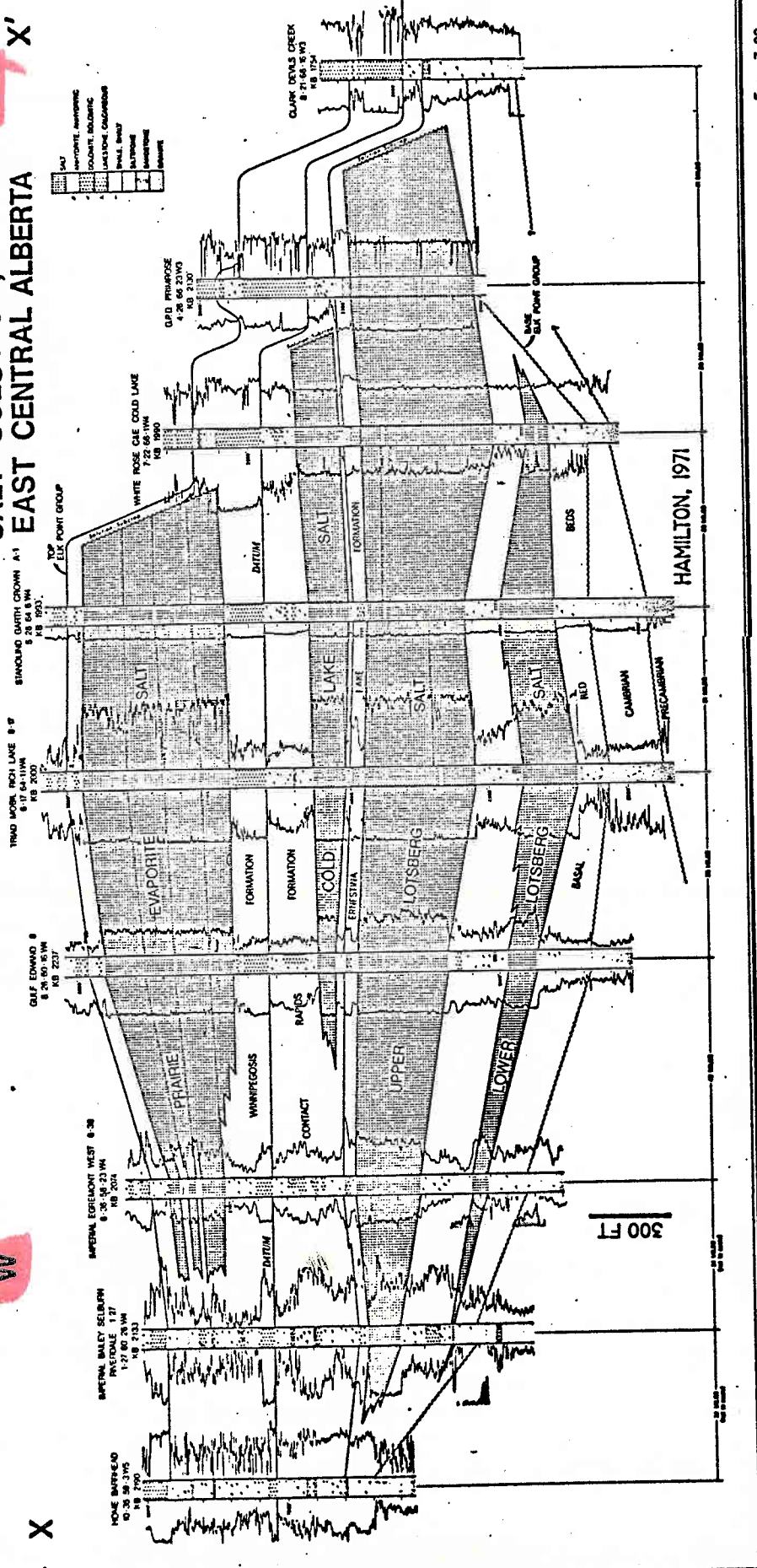
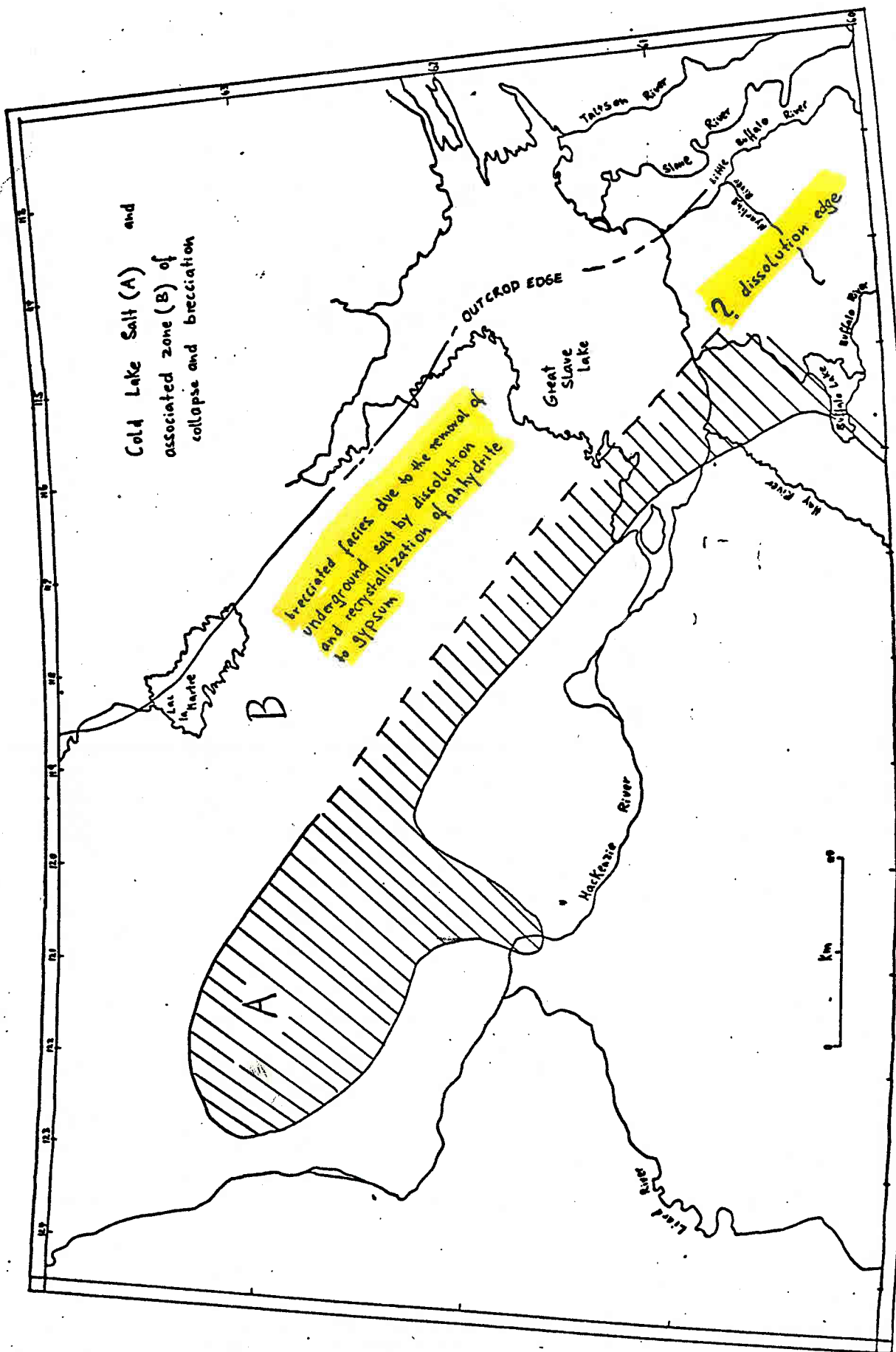


FIG. 3-22

FIG. 3-23



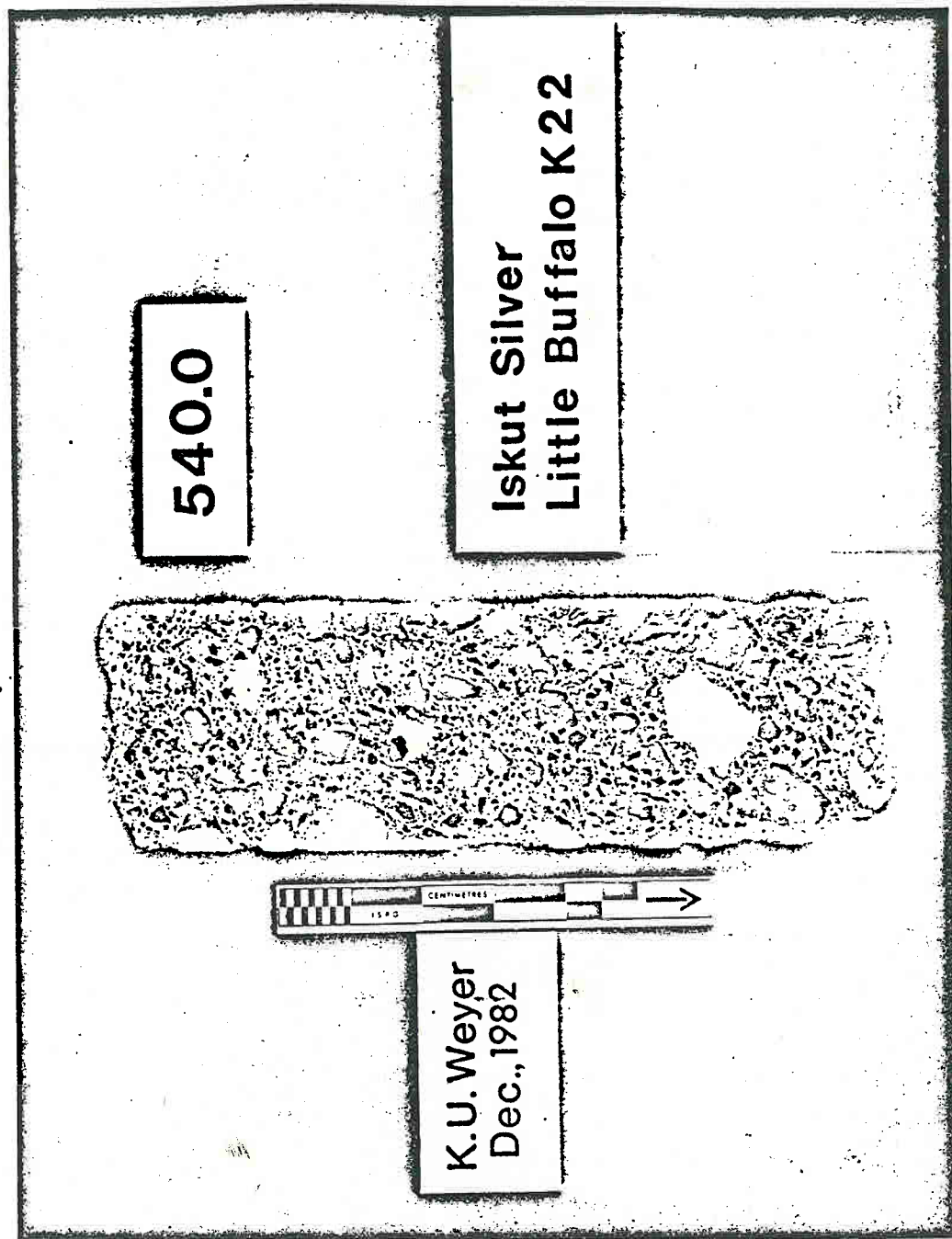


FIG. 3-24

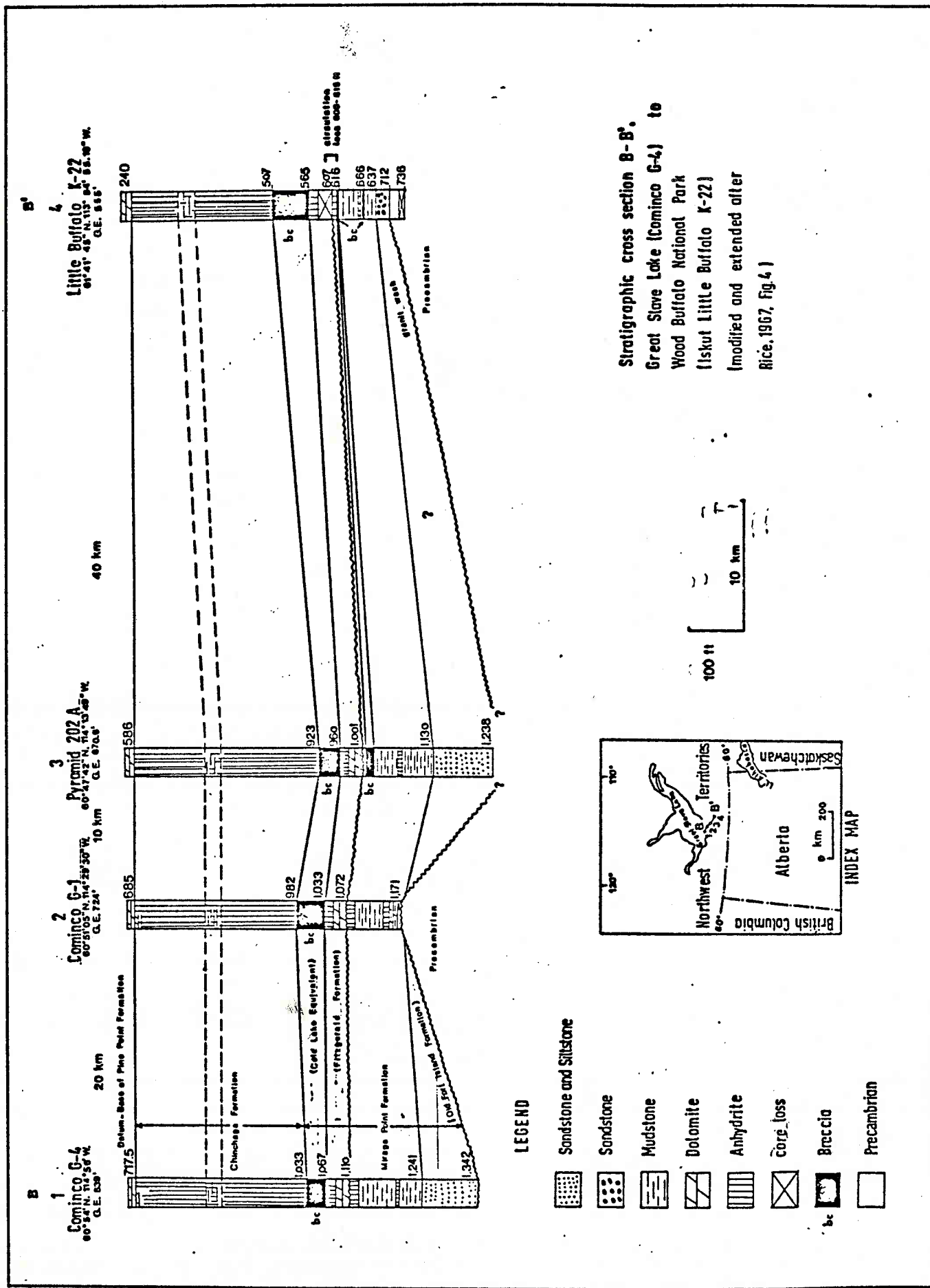
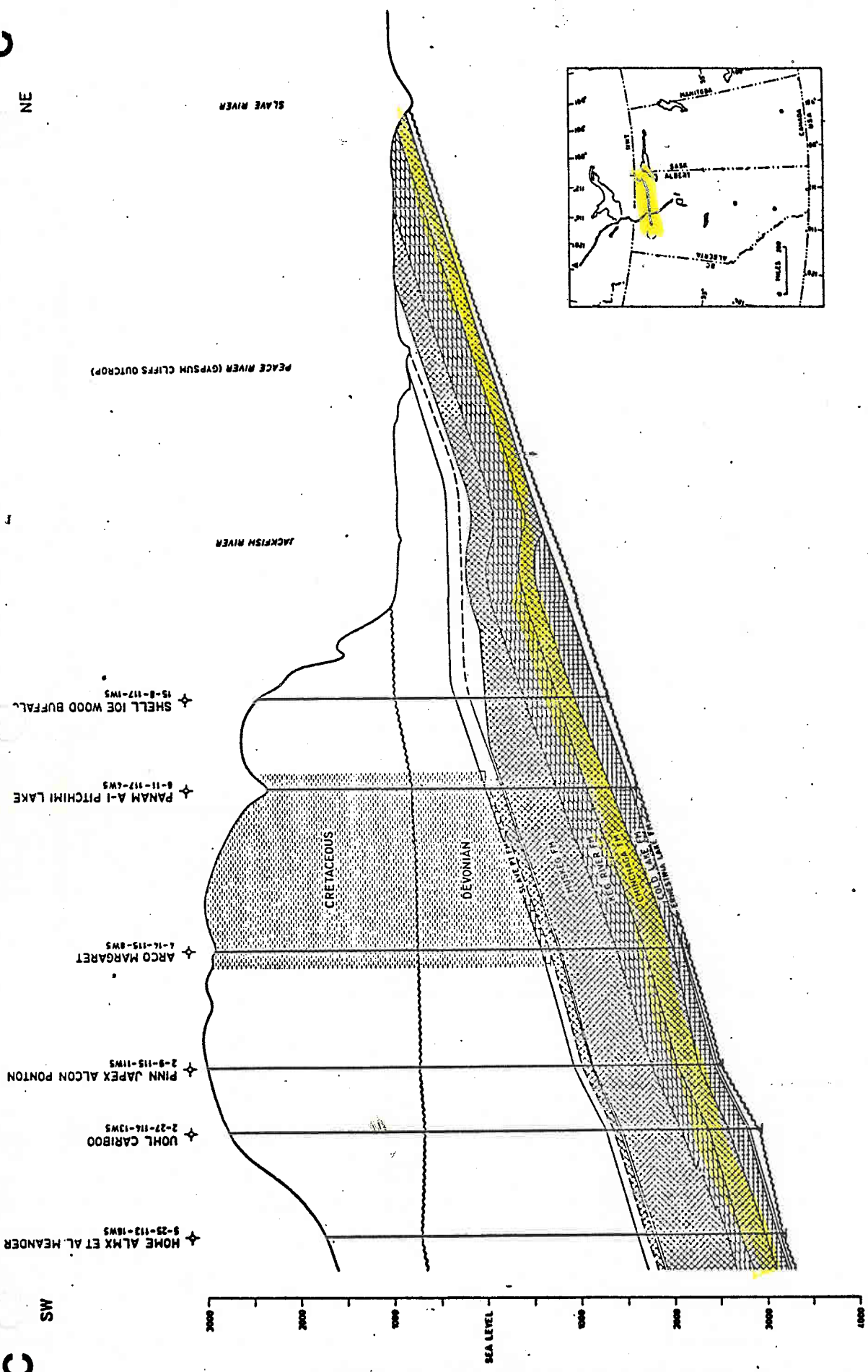


FIG. 3-25

FIG. 3-26



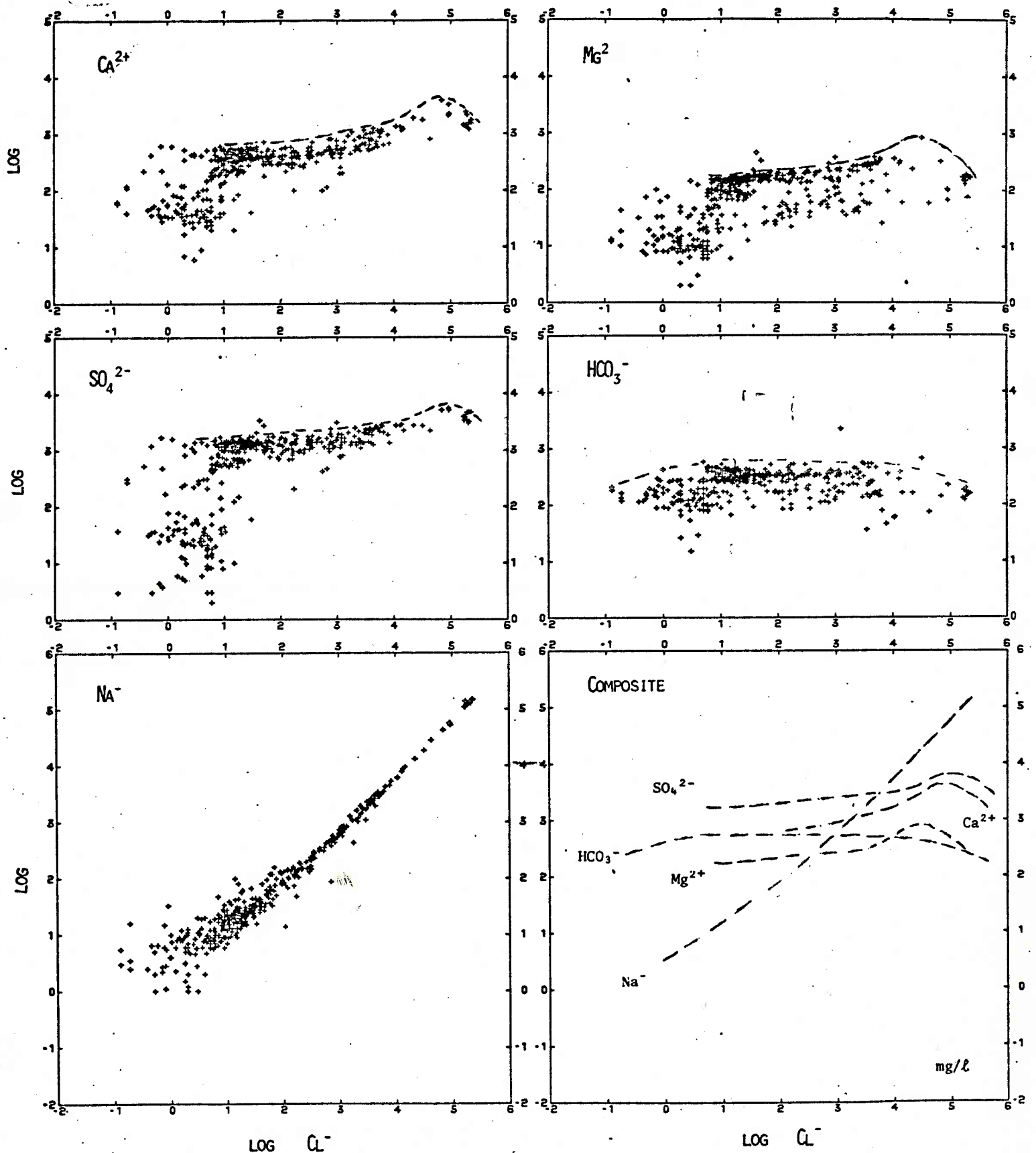
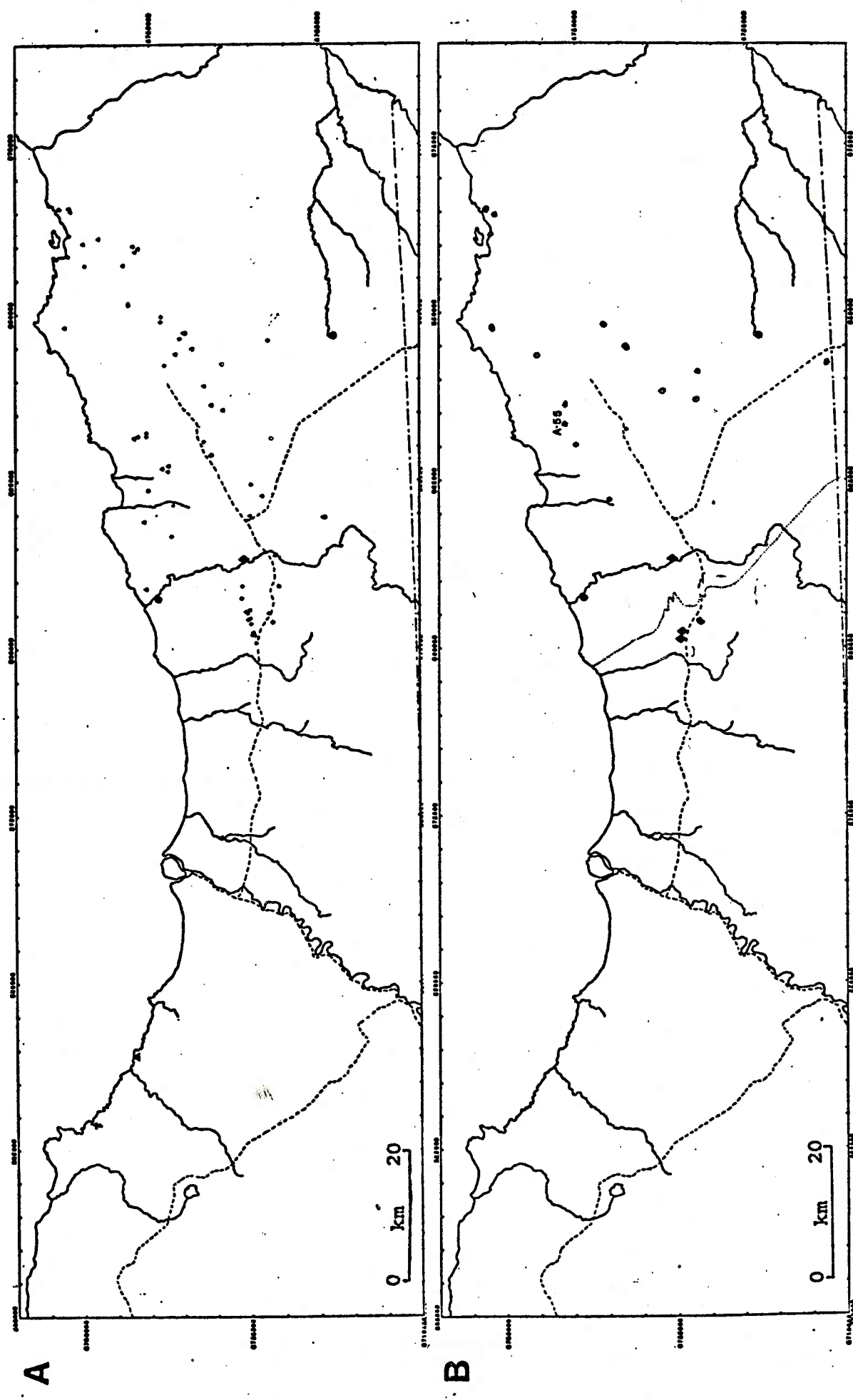


FIG. 3-28

FIG. 3-29



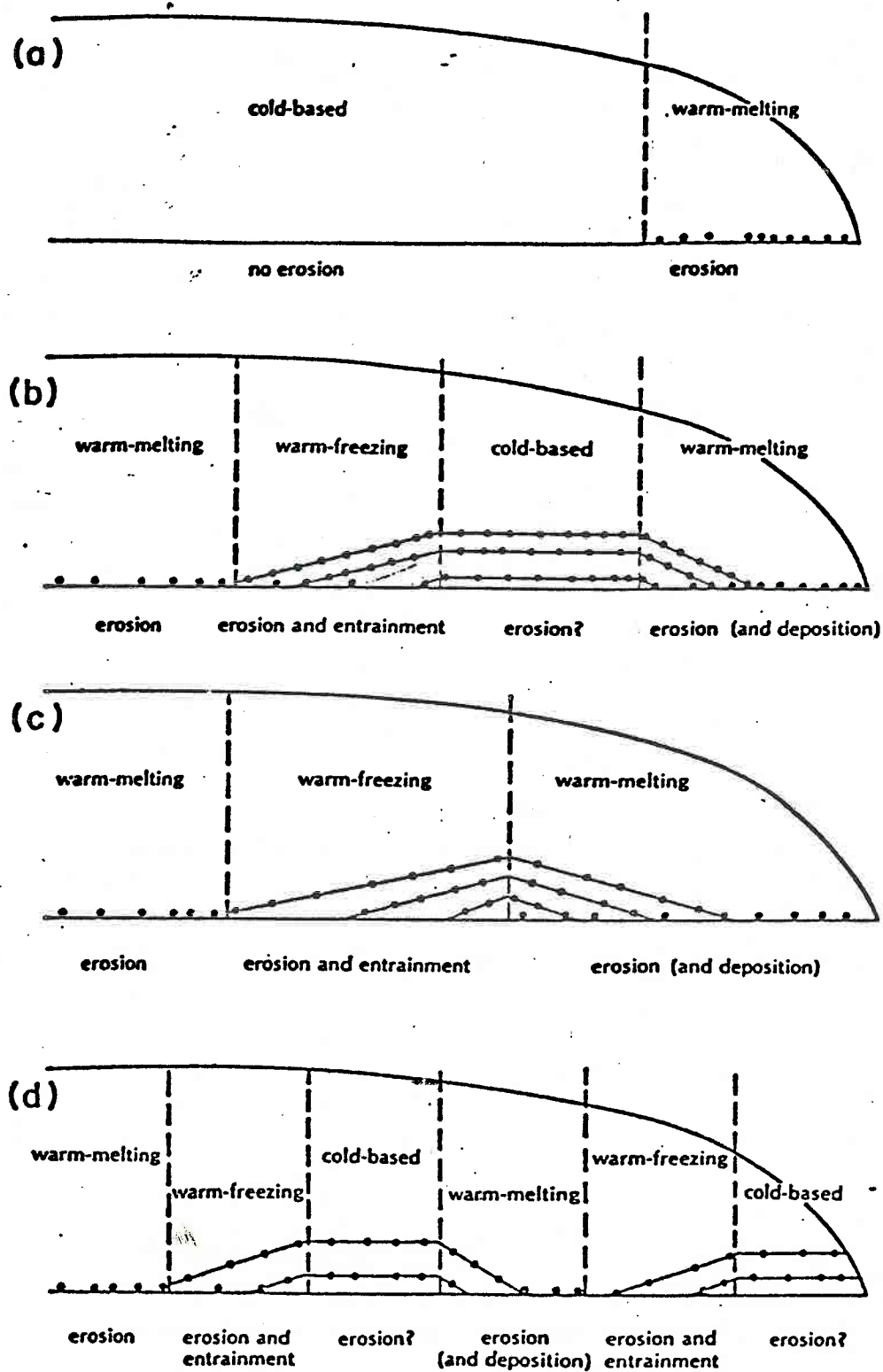


FIG. 3-30

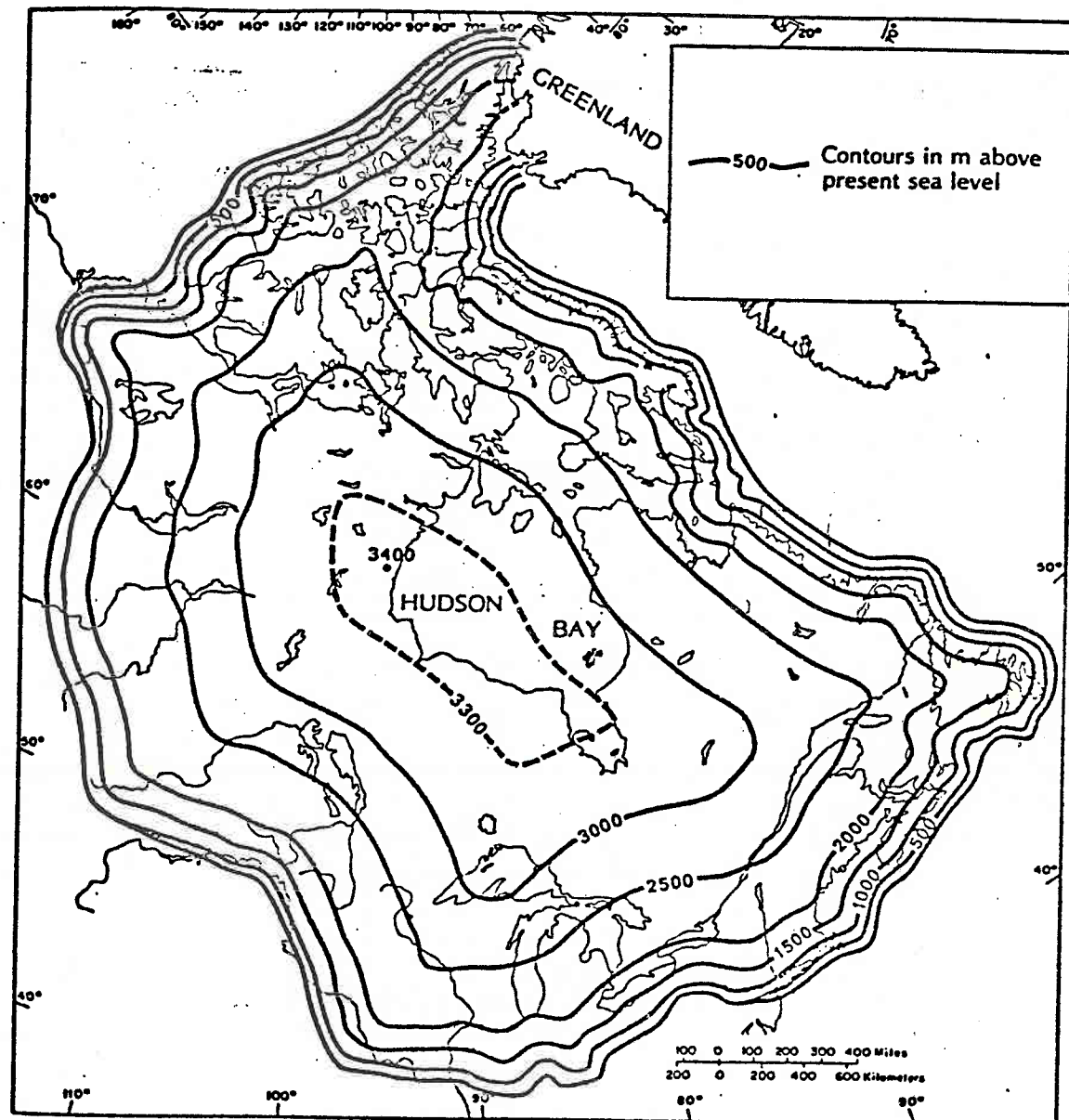


FIG. 3-31

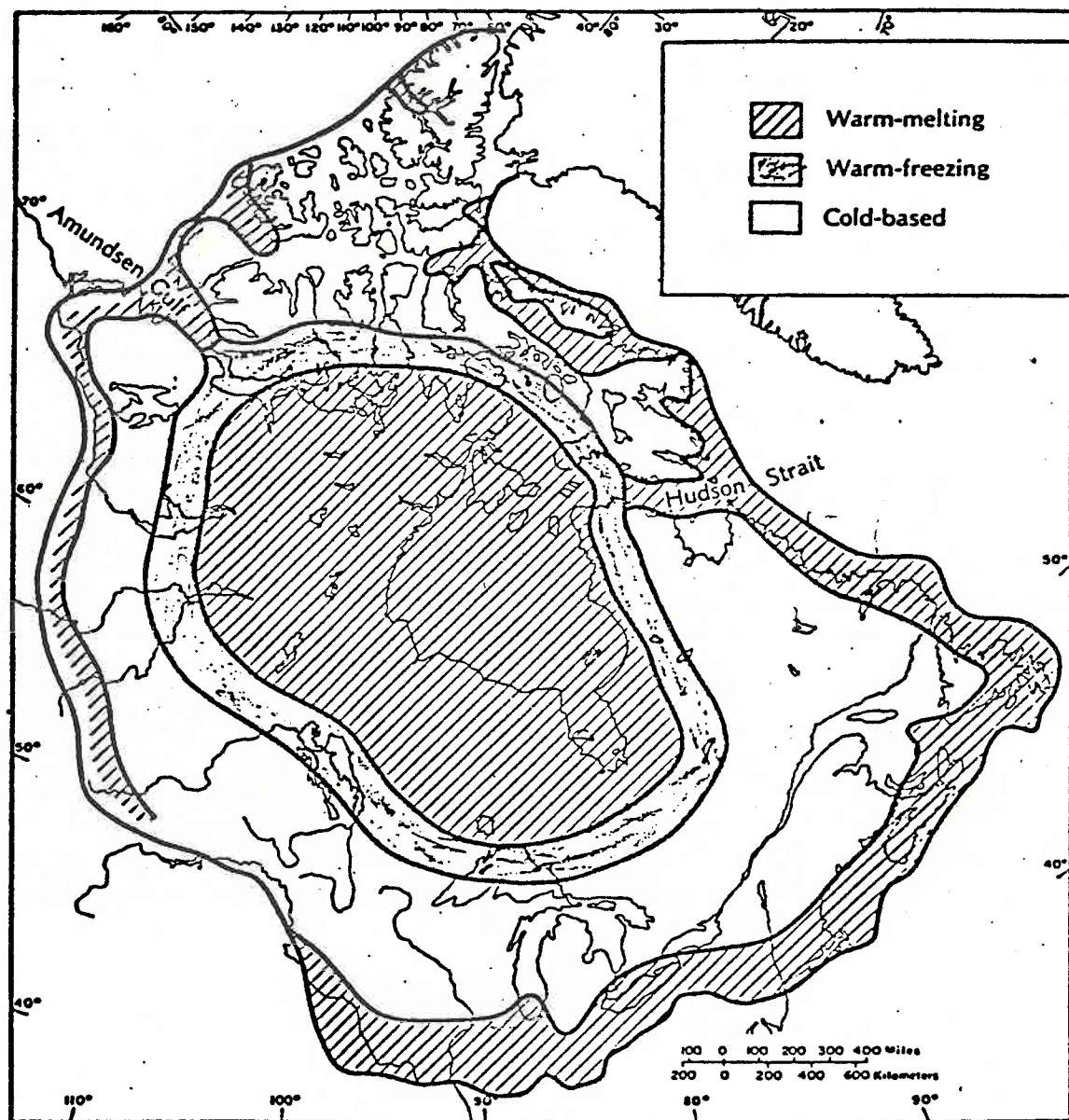


FIG. 3-32

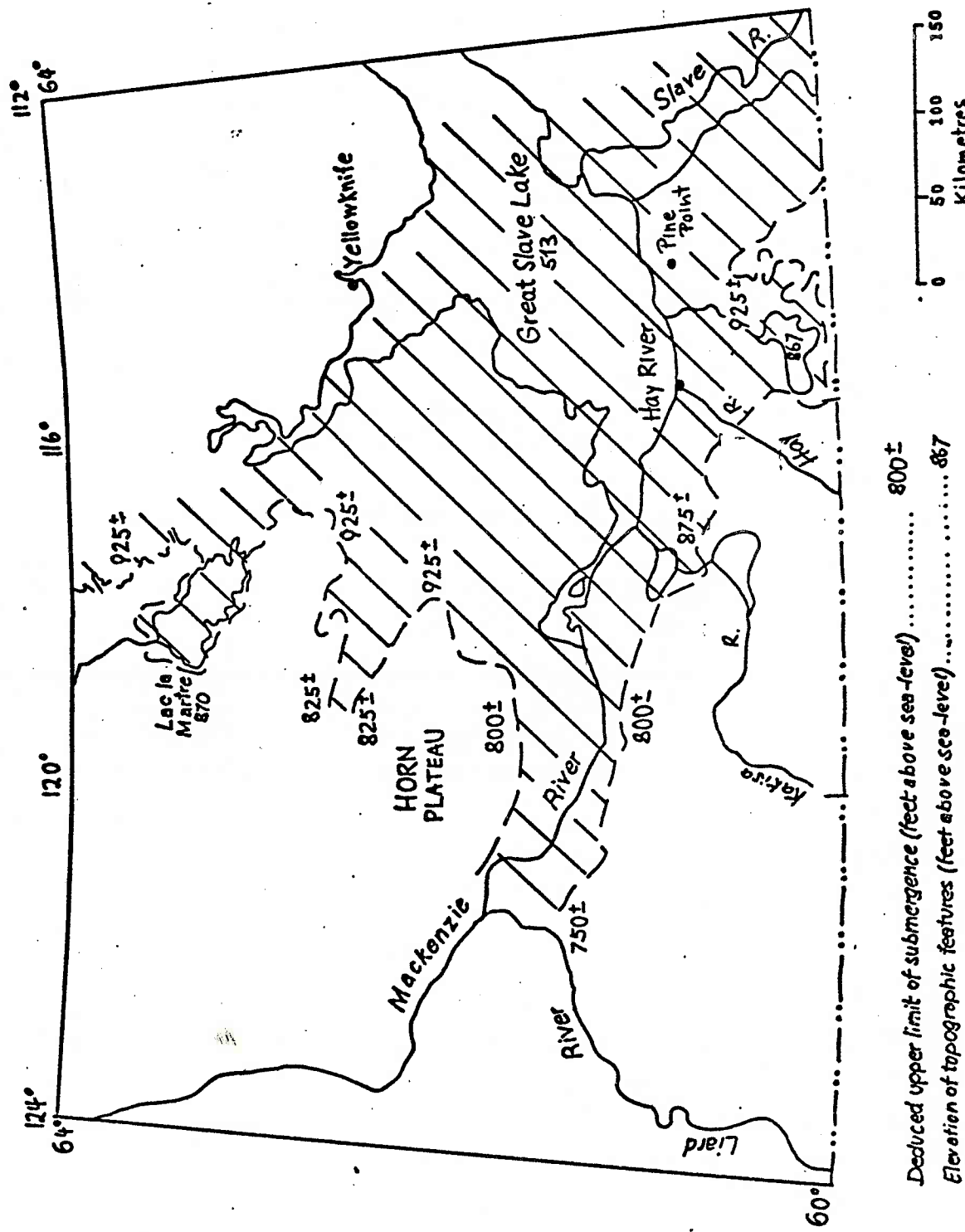


FIG. 3-33

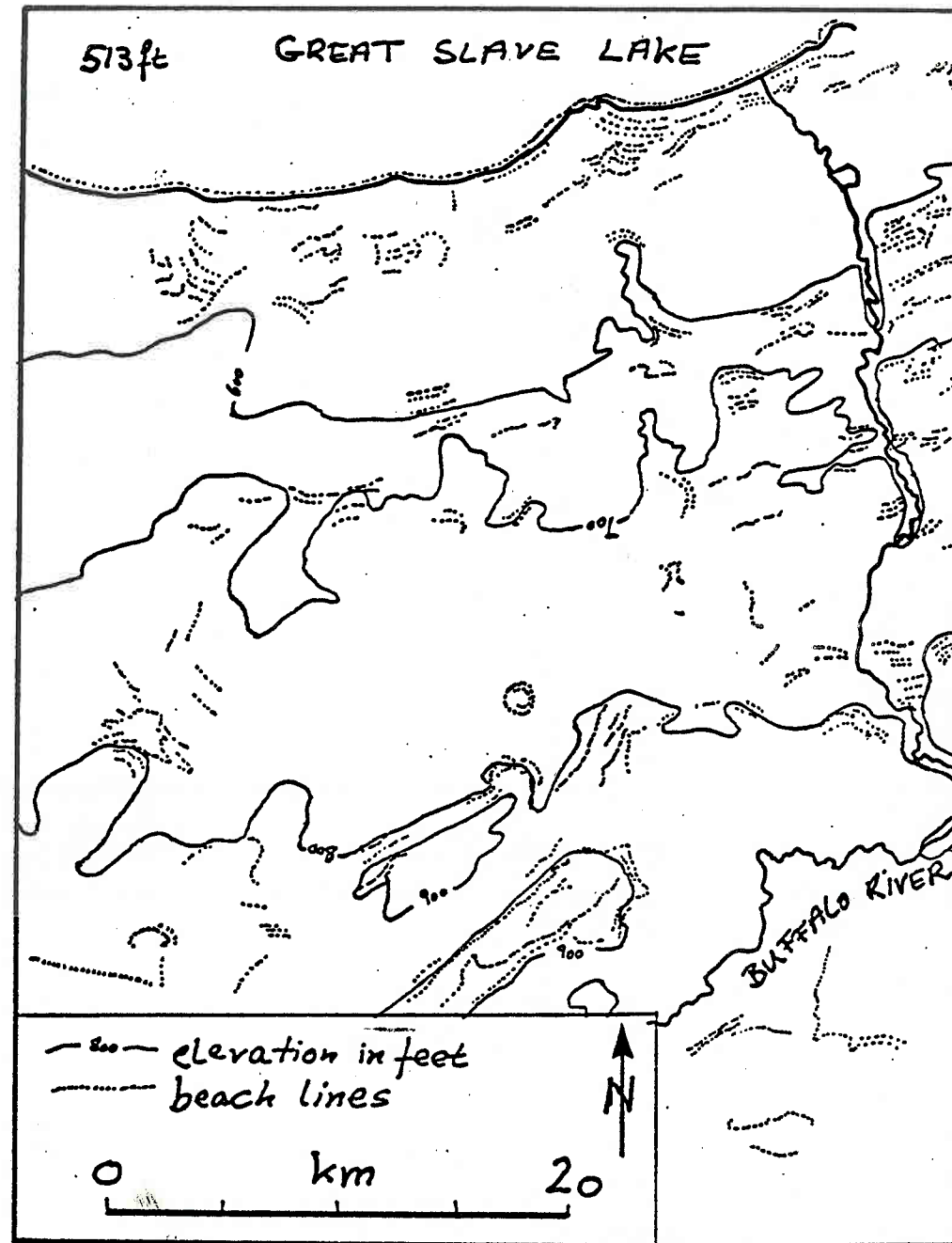
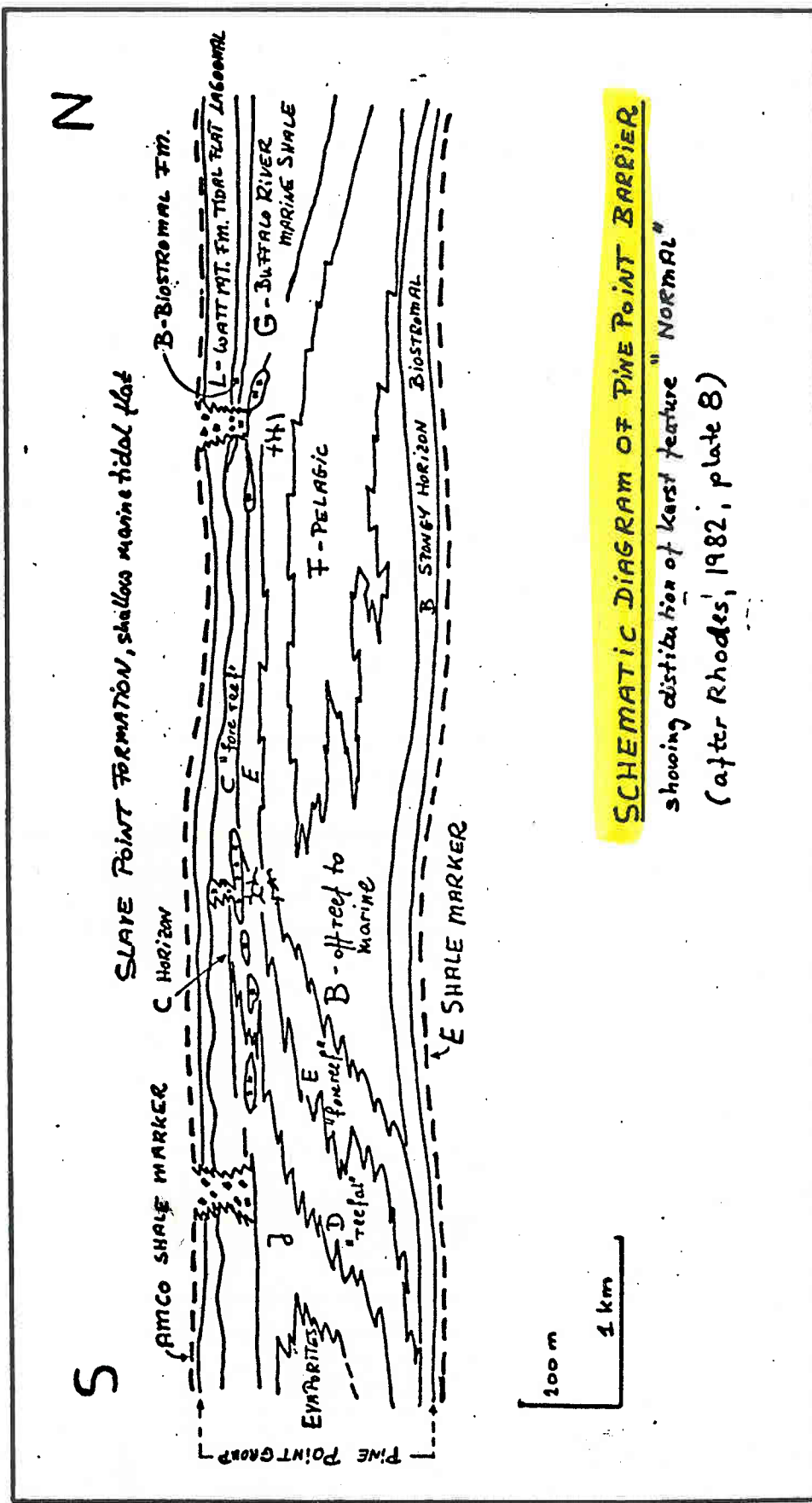


FIG. 3-34

FIG. 3-35



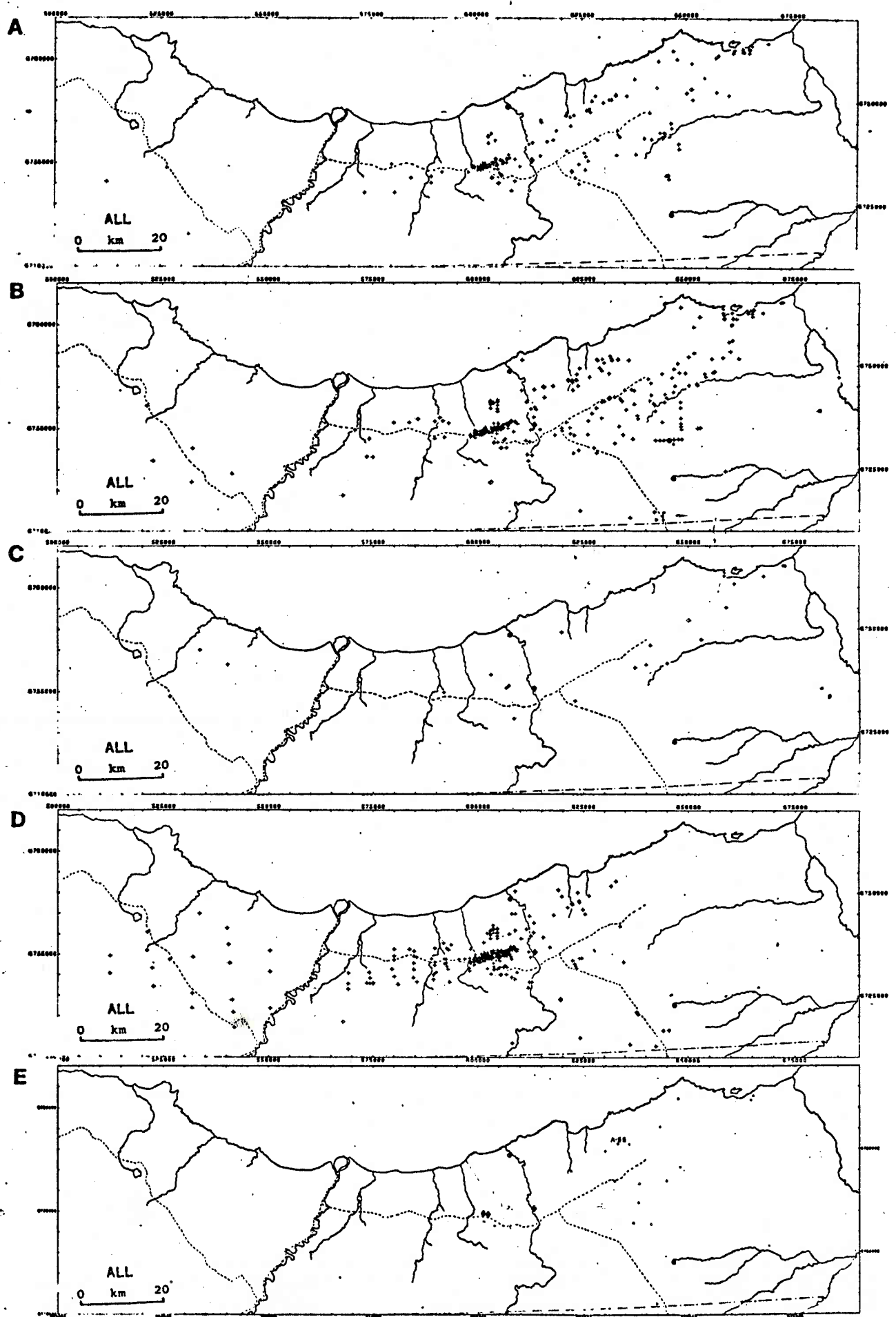
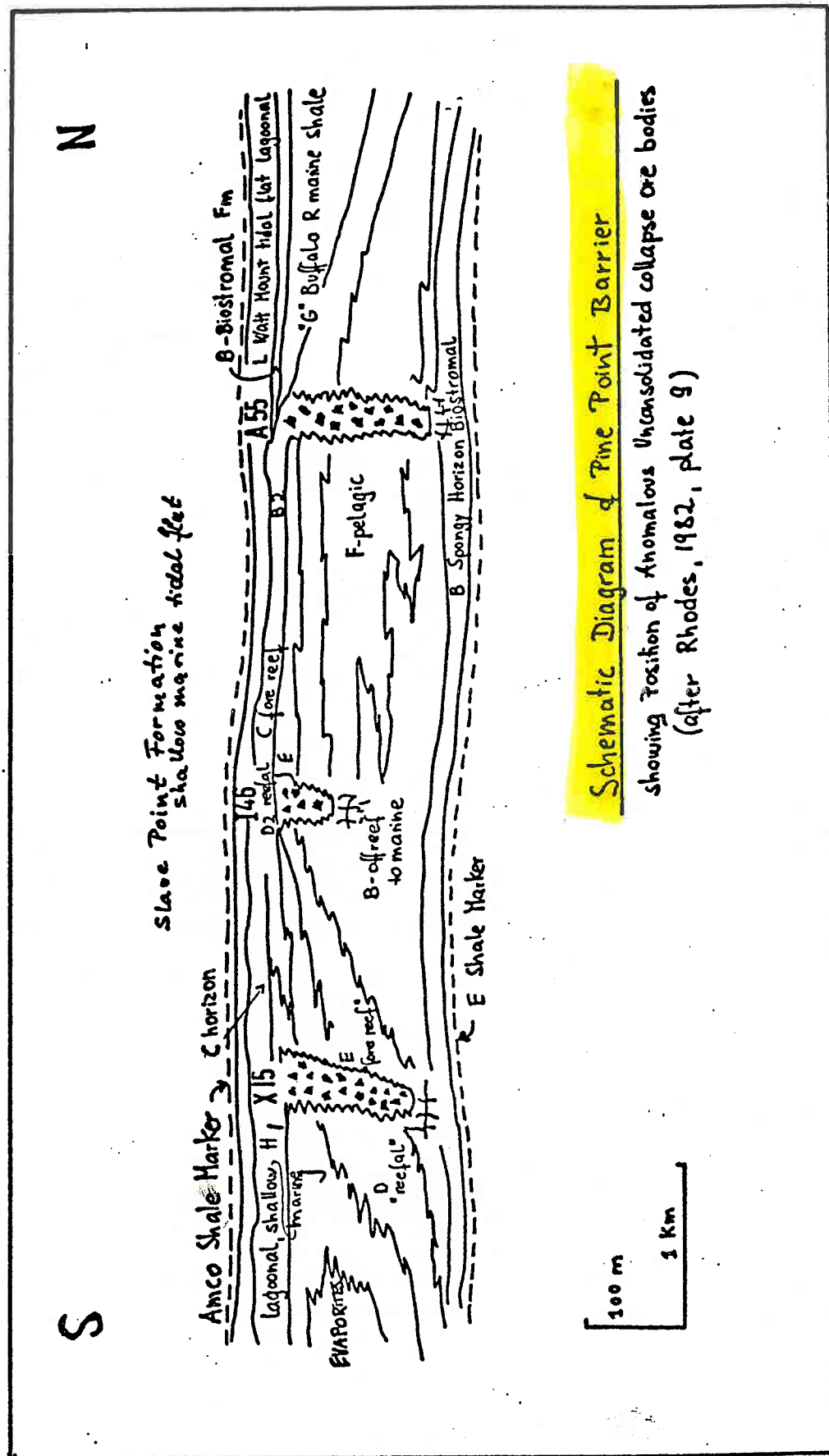
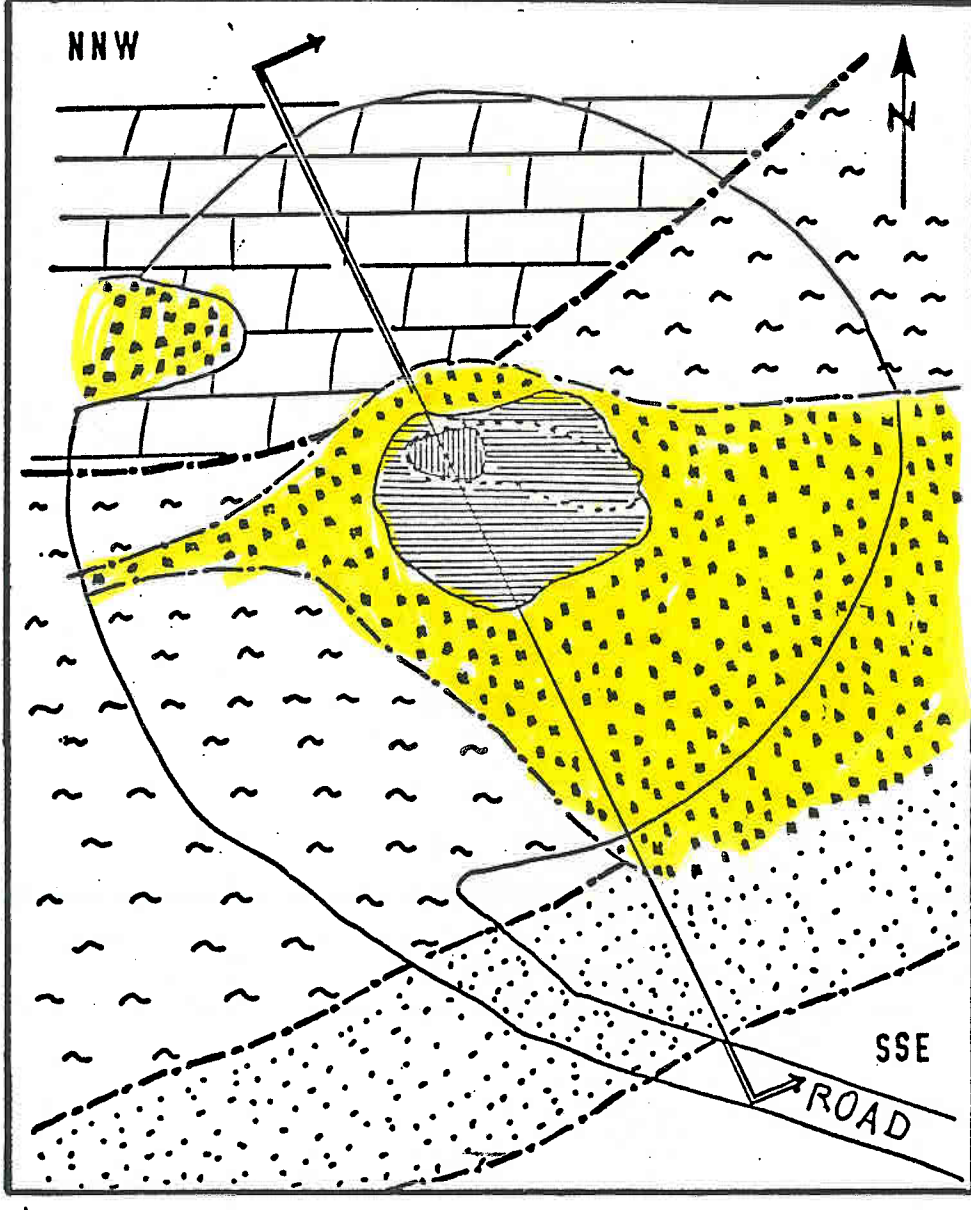


FIG. 3-37





LEGEND

- [Hatched Box] D2 Facies (Presqu'illized)
- [Wavy Line Box] BRS Facies
- [Vertical Lines Box] Ore Outline(4th Bench)
- [Diagonal Lines Box] Ore Outline (14th Bench)

- [Yellow Box] Collapse (Subcrop)
- [Dotted Box] Paleokarst Channel
- [Circle Box] Collapse (14th Bench)

MAJOR GEOLOGICAL FEATURES OF THE
A-55 ORE BODY (AFTER ALLDRICK, 1982, FIGS. 2+4)

FIG. 3-38

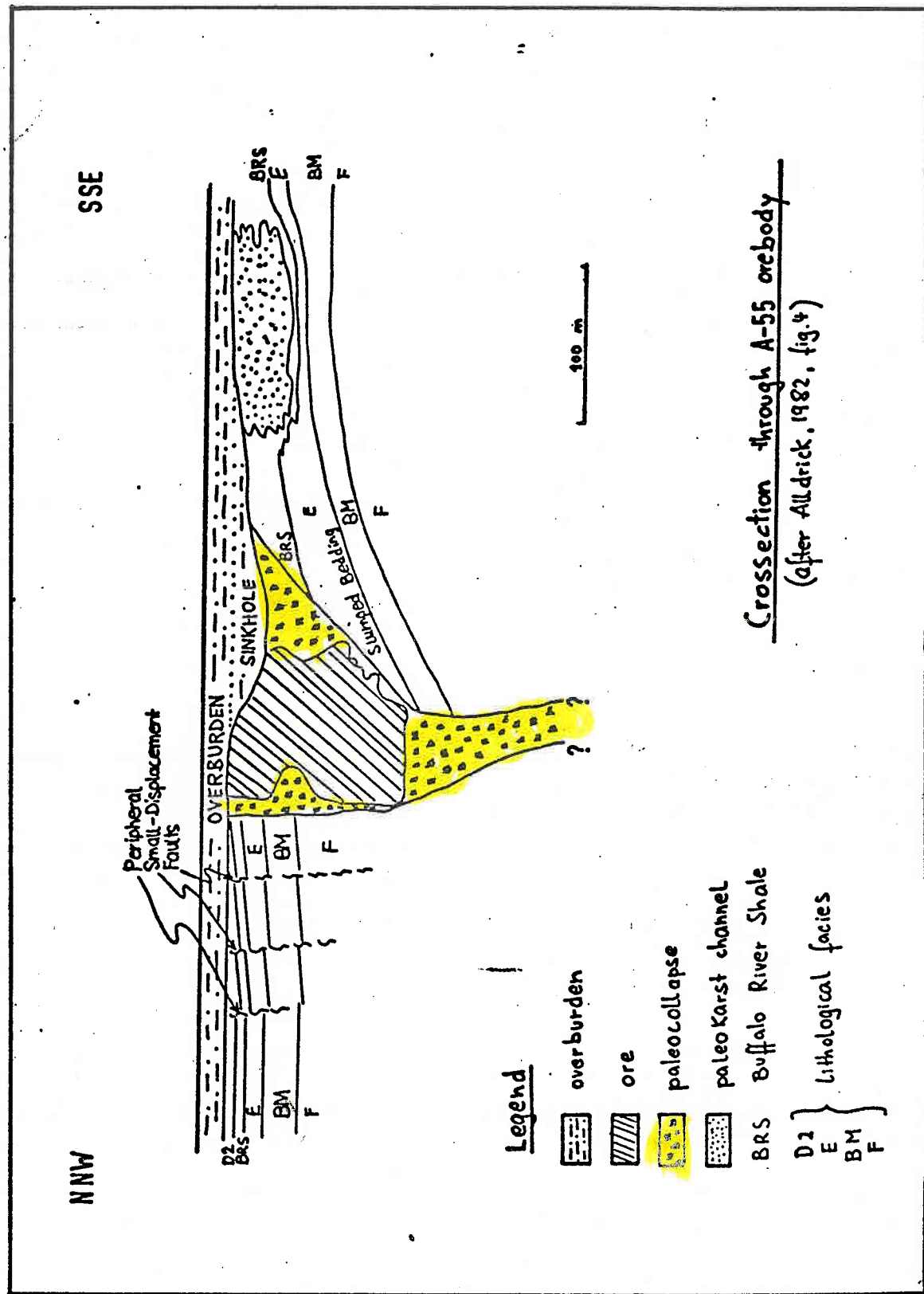


FIG. 3-39

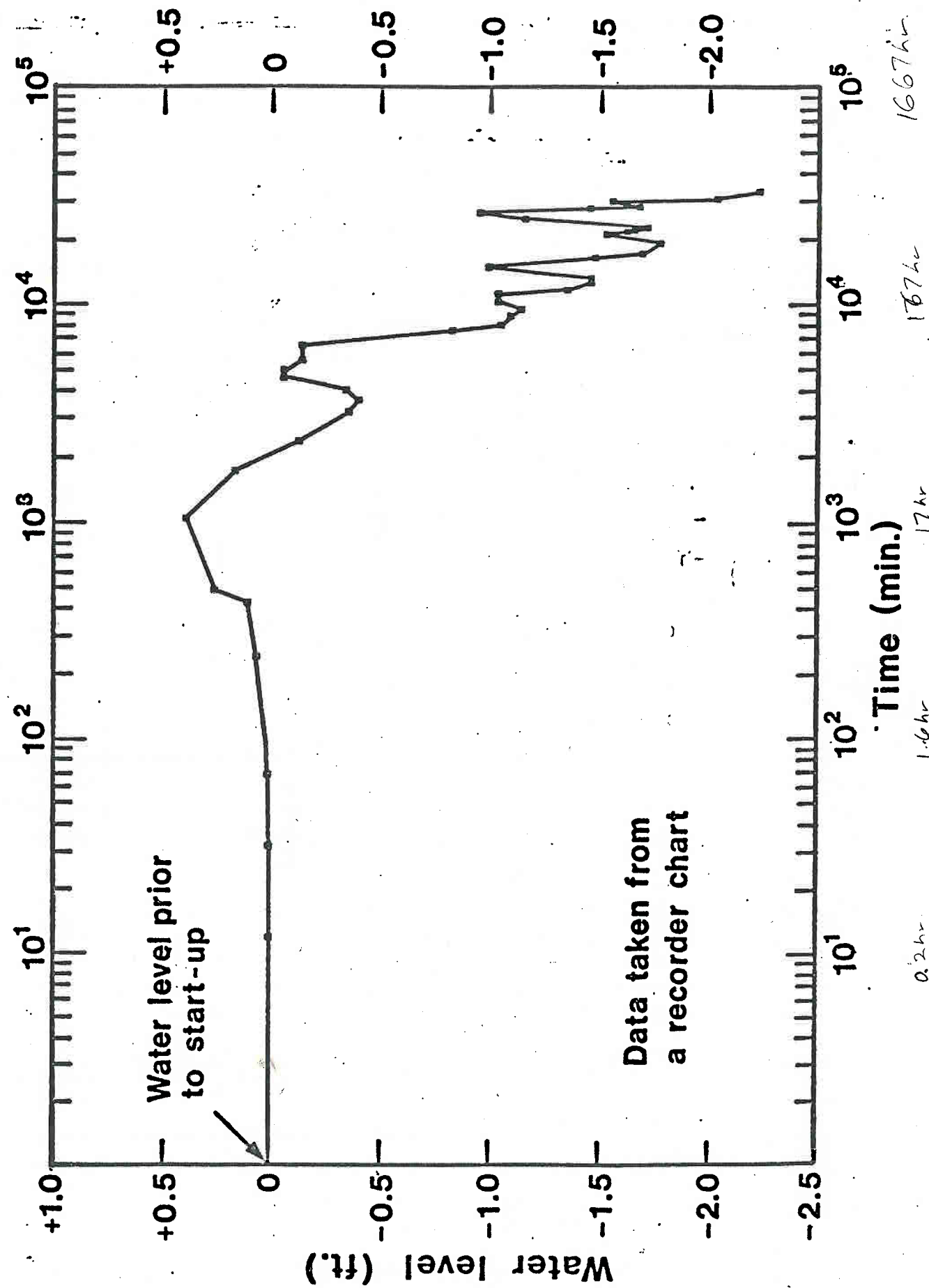


FIG. 3-40

FIG. 3-41

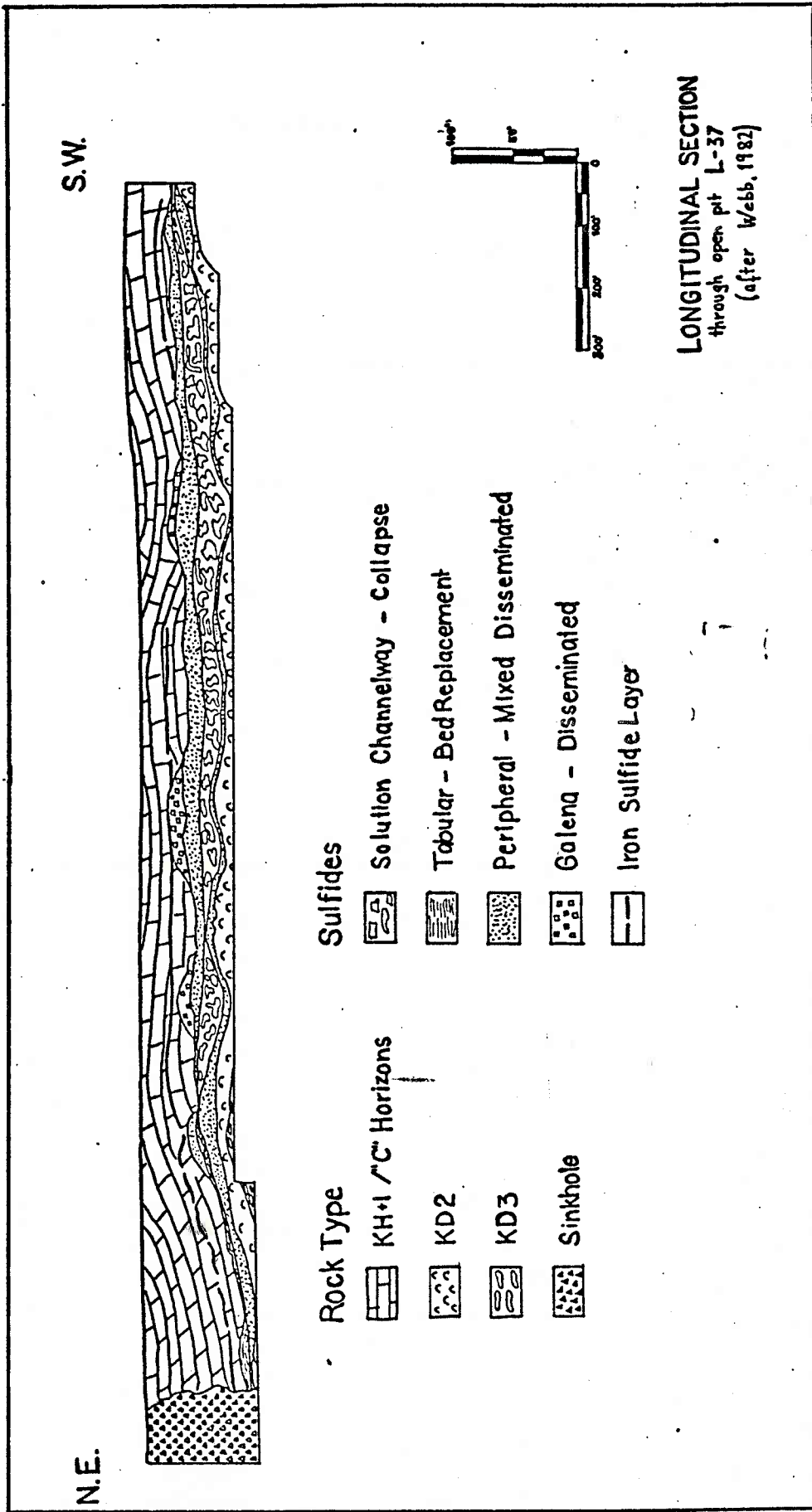
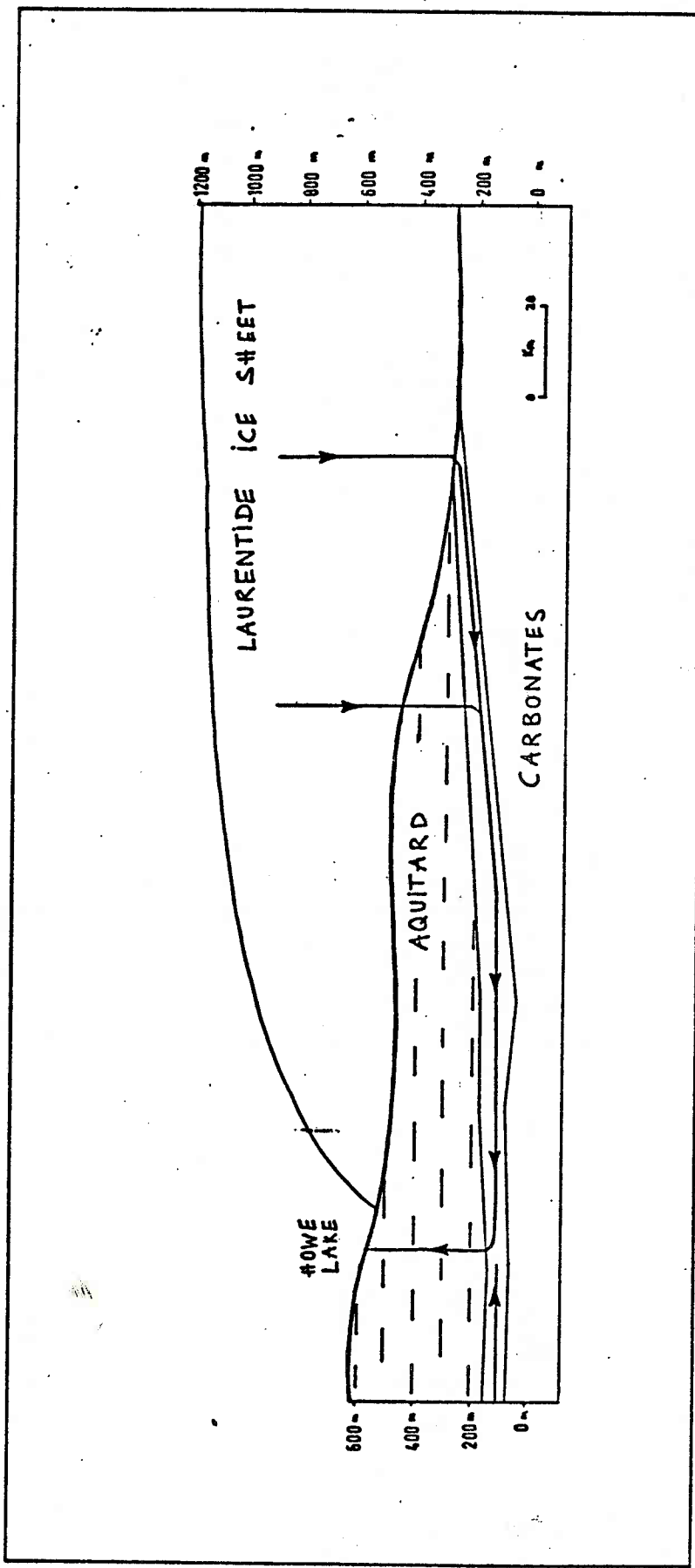
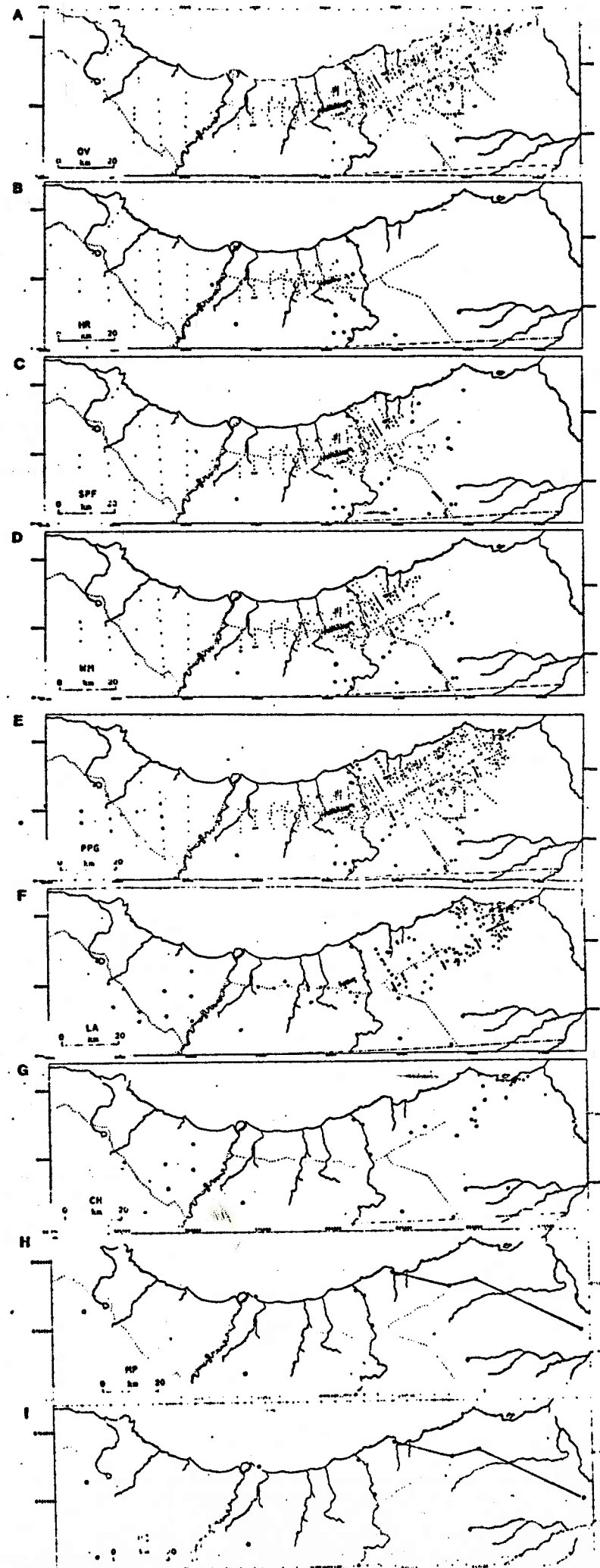
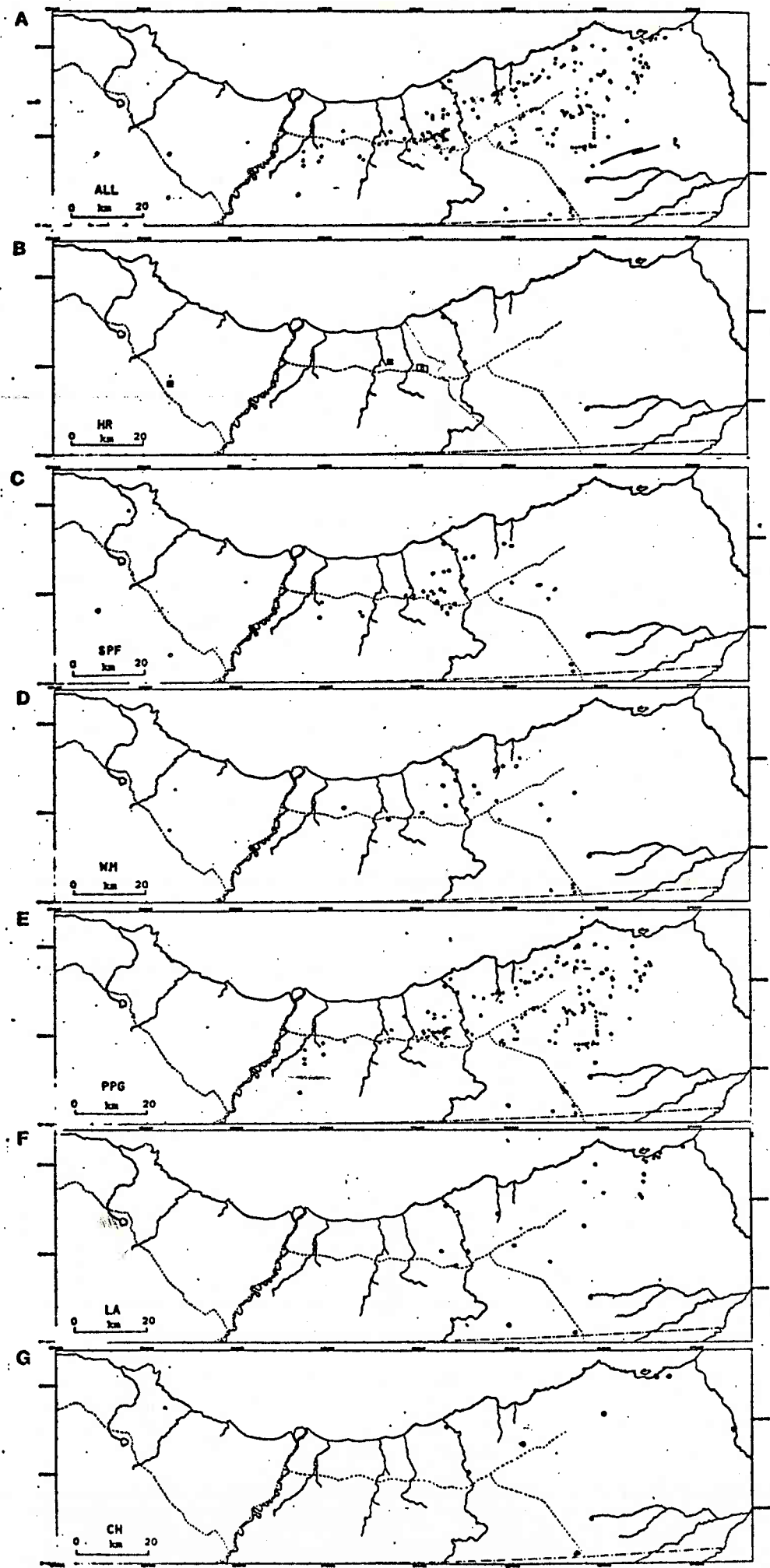


FIG. 3-42







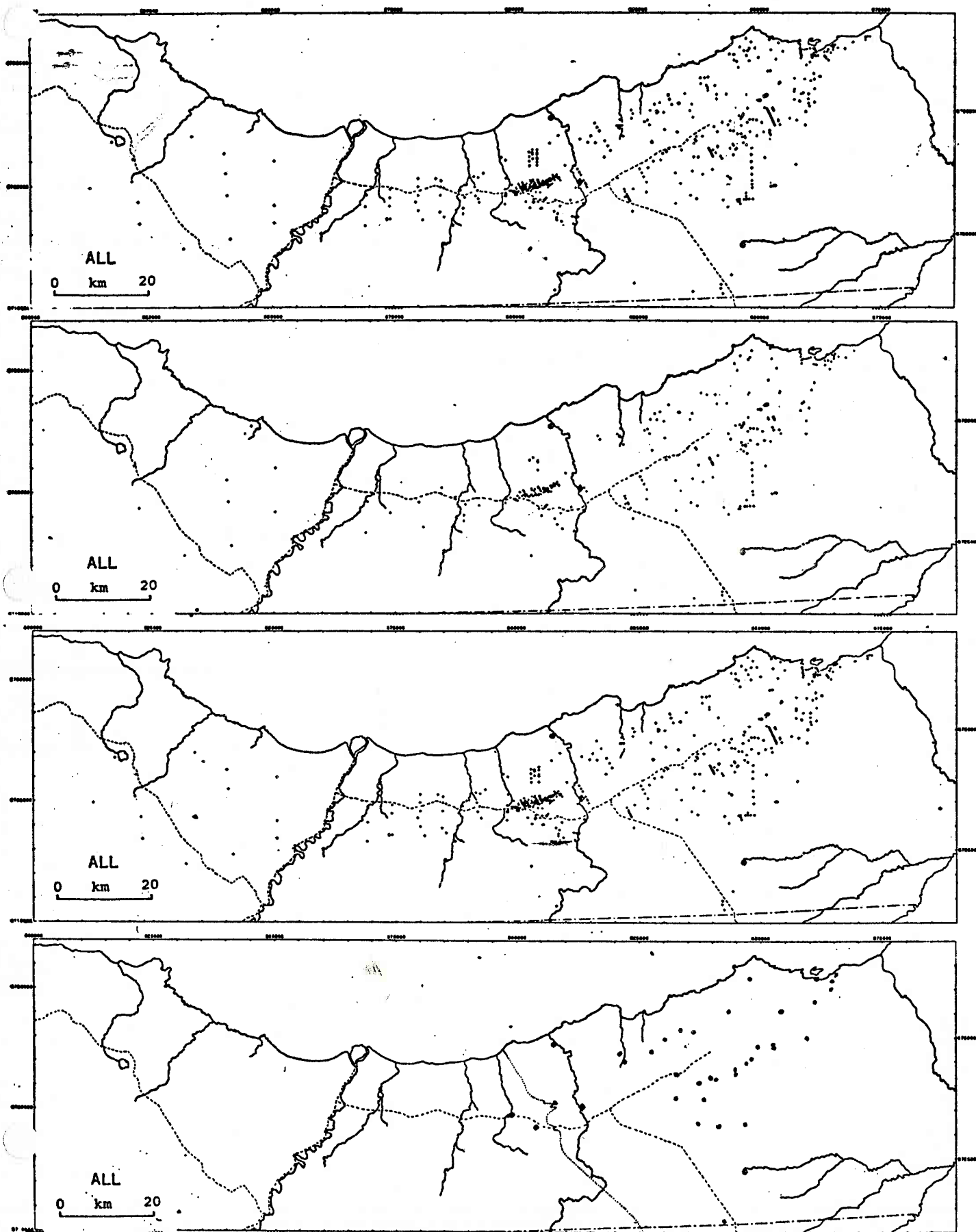
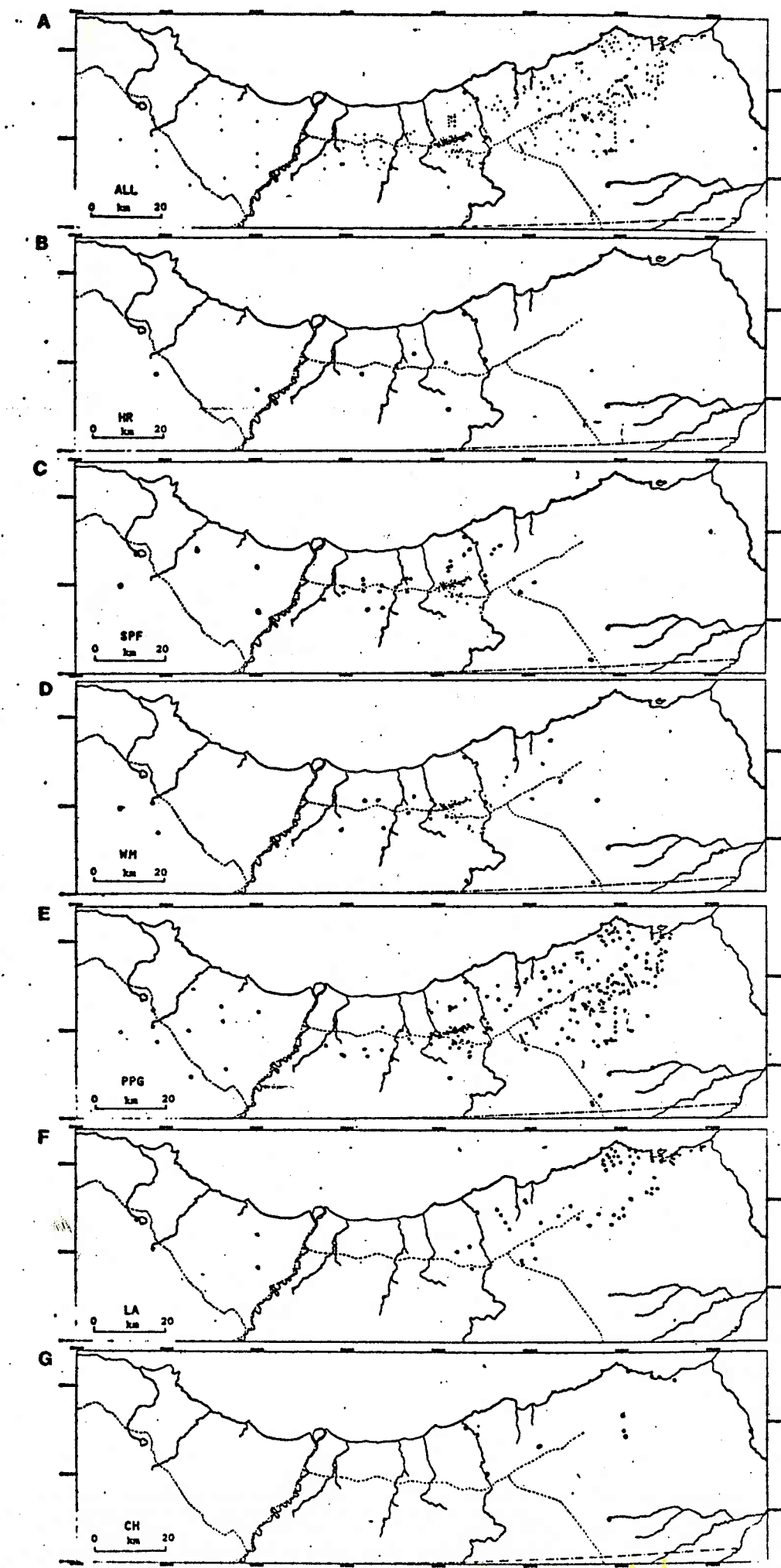
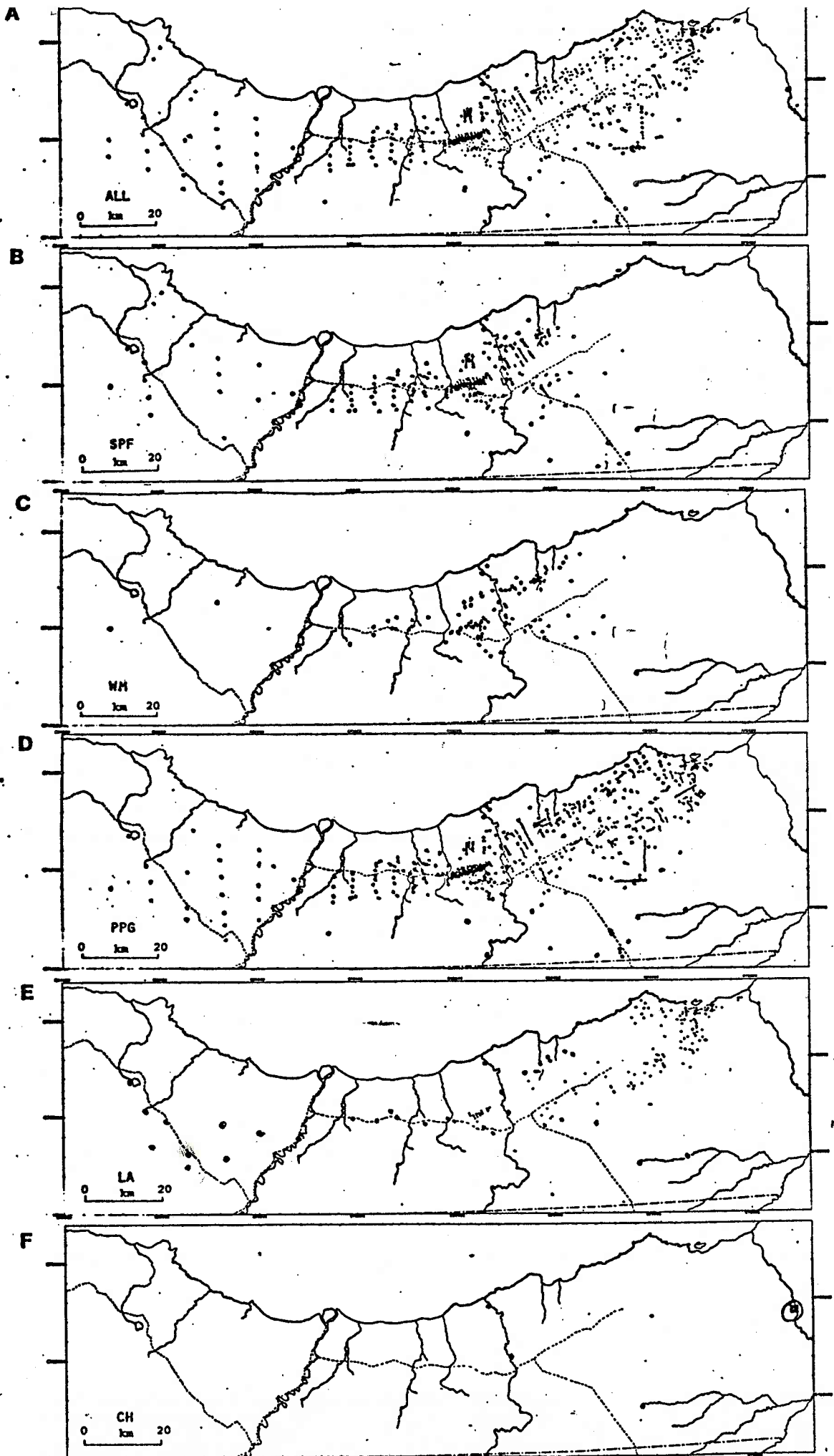


FIG. 3-45



ABEAI



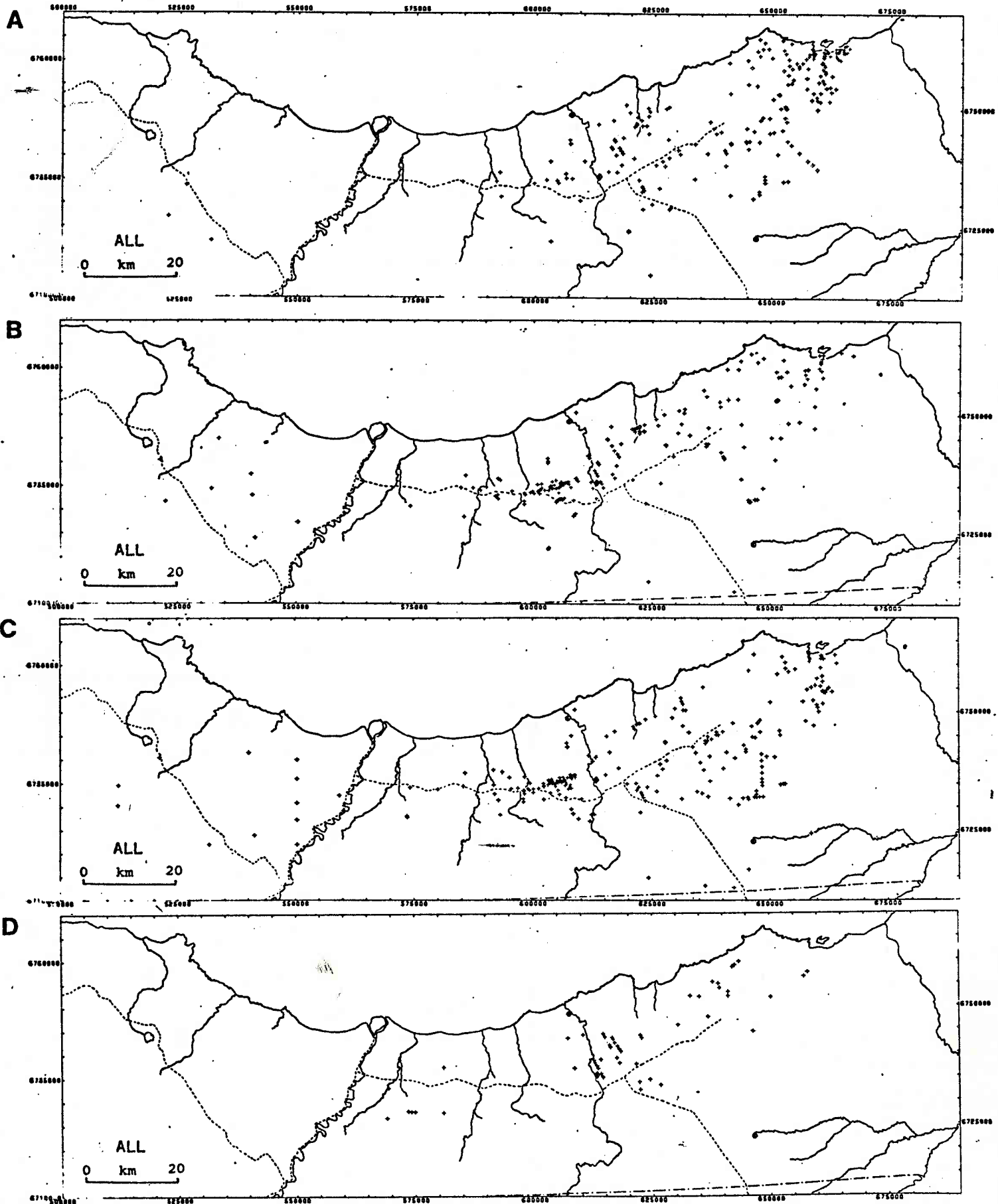


FIG. 3-48

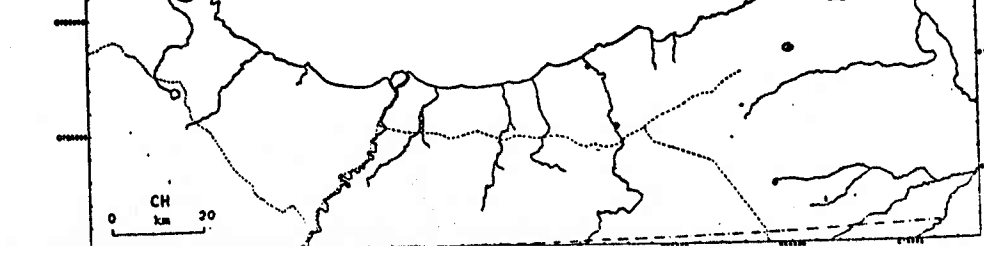
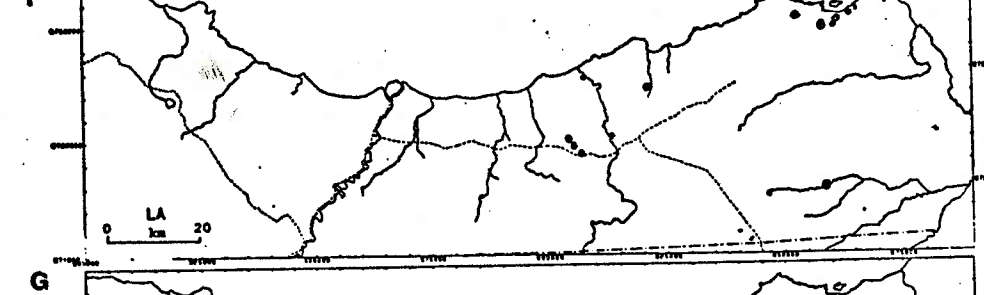
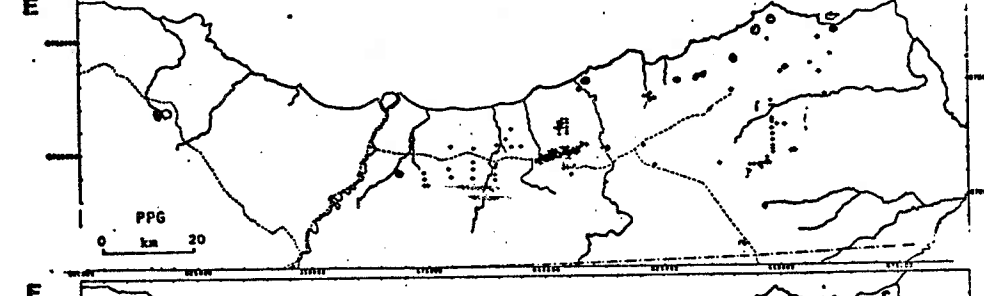
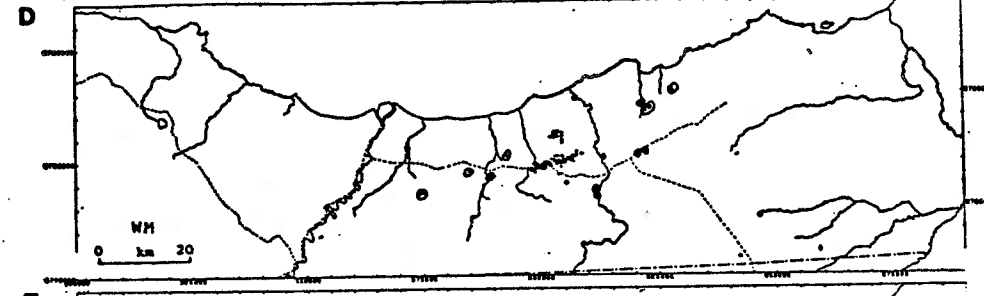
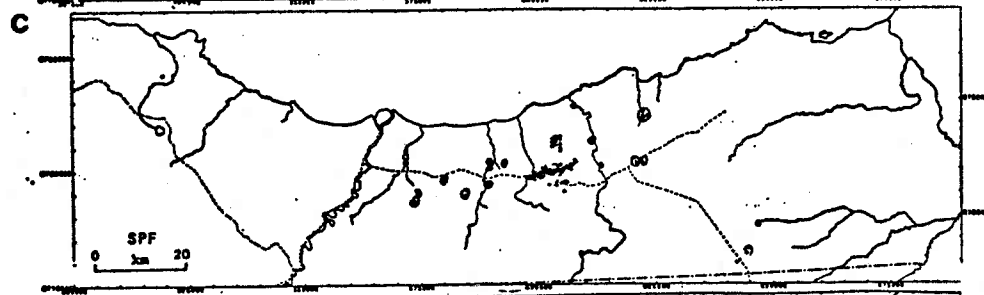
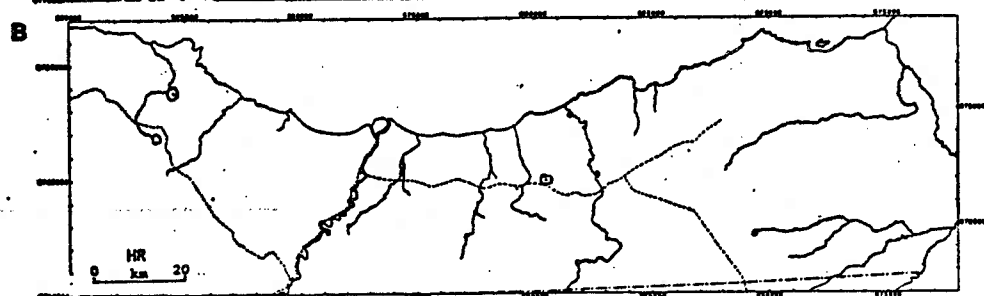
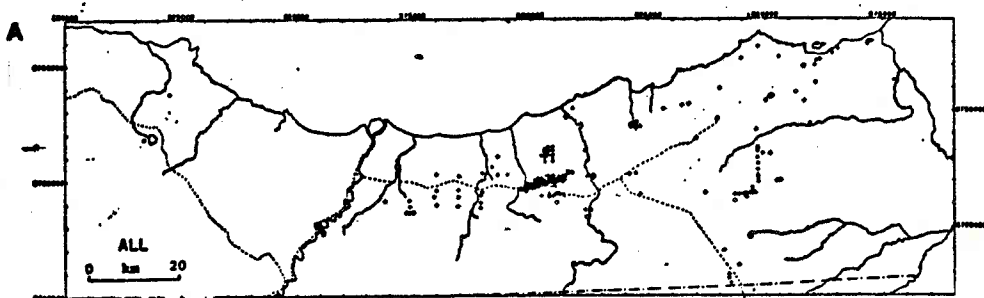
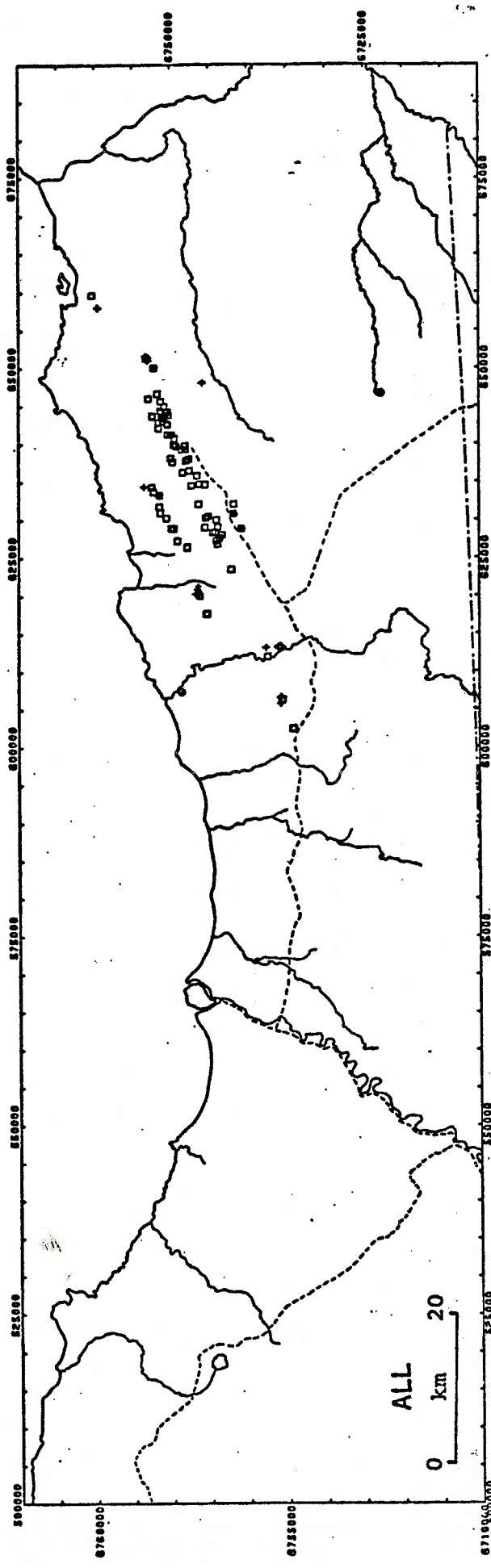
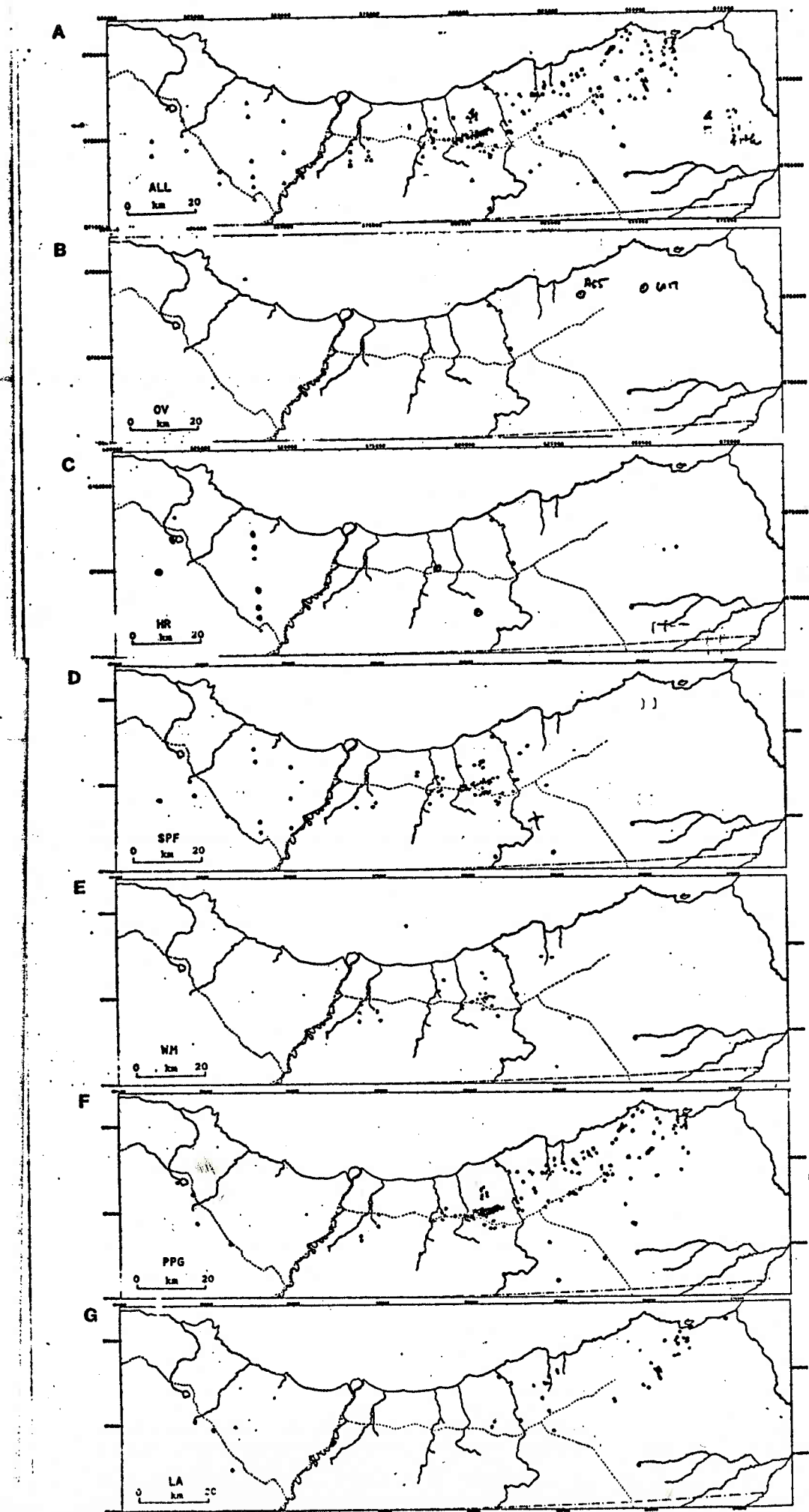
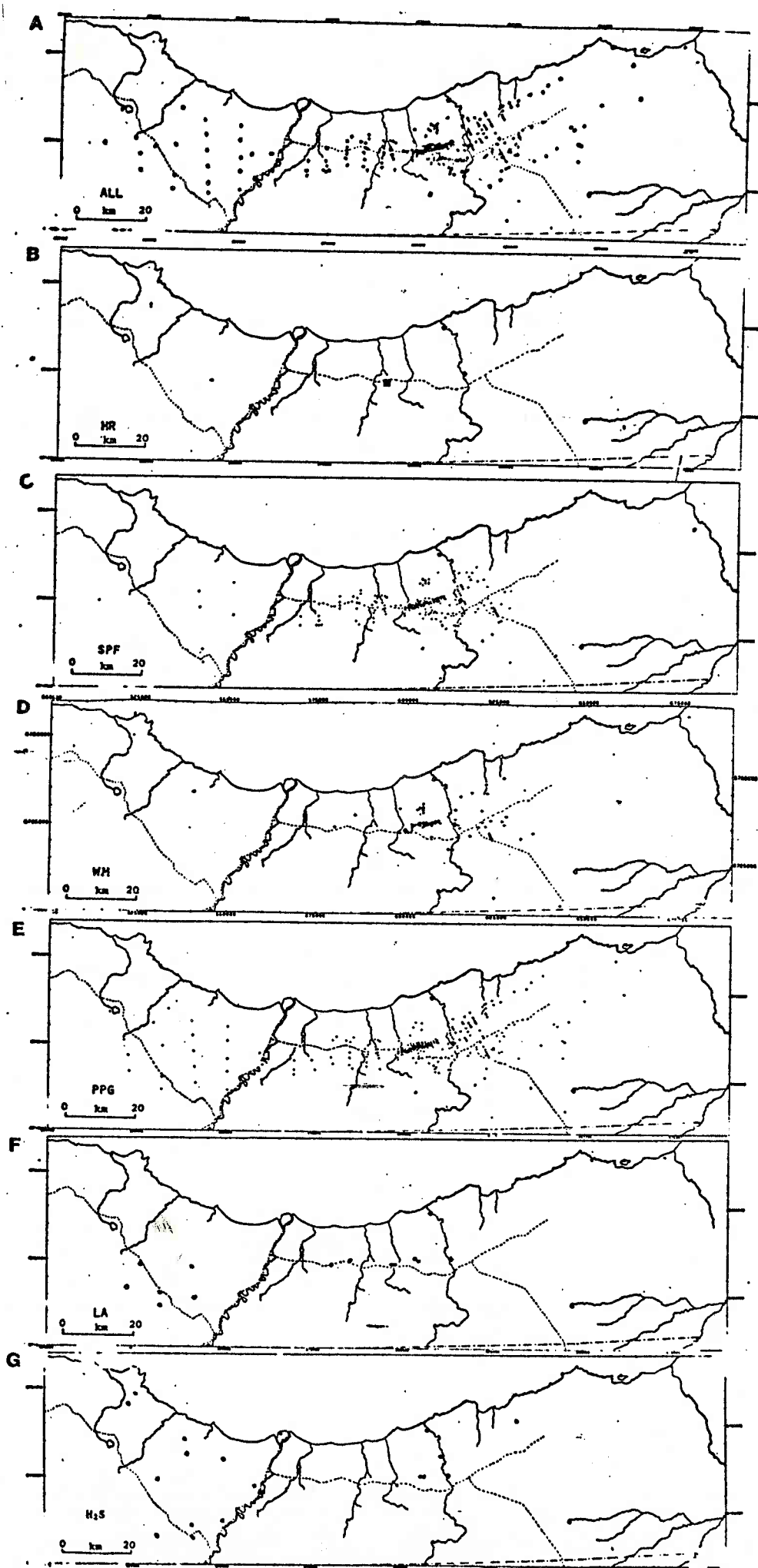
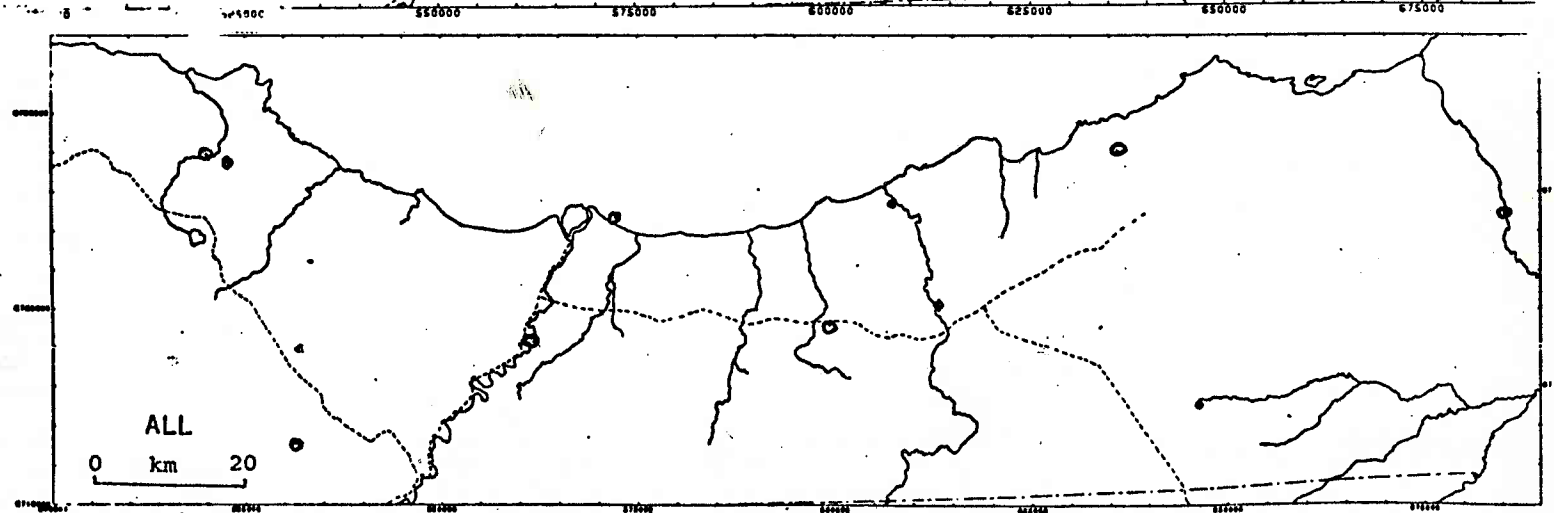
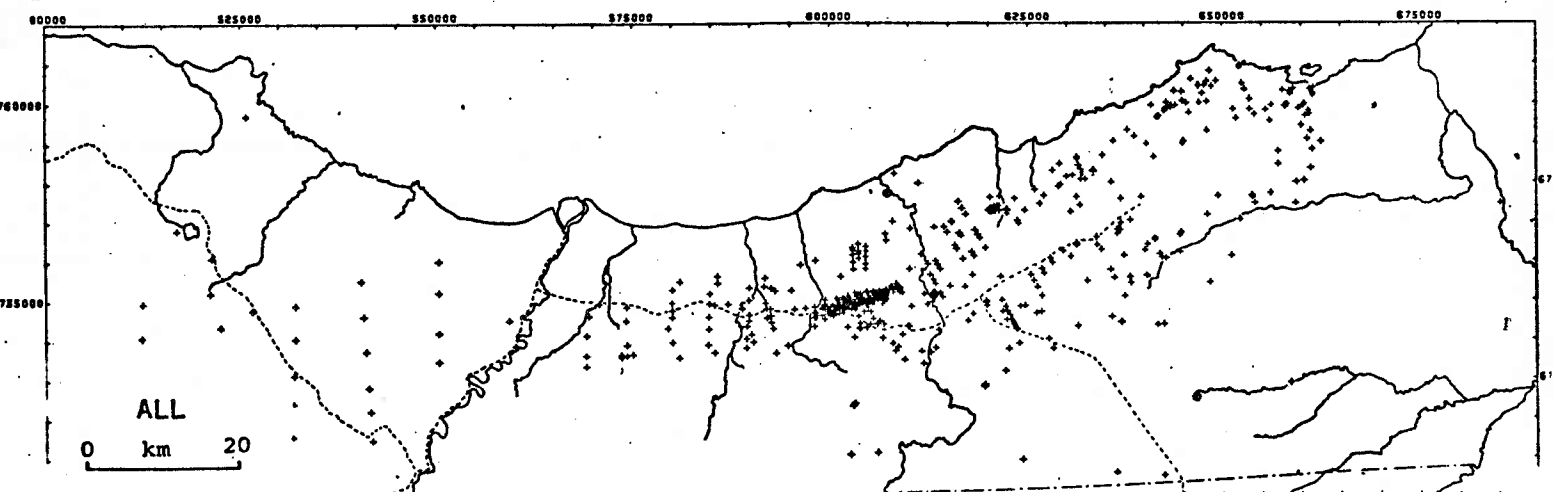
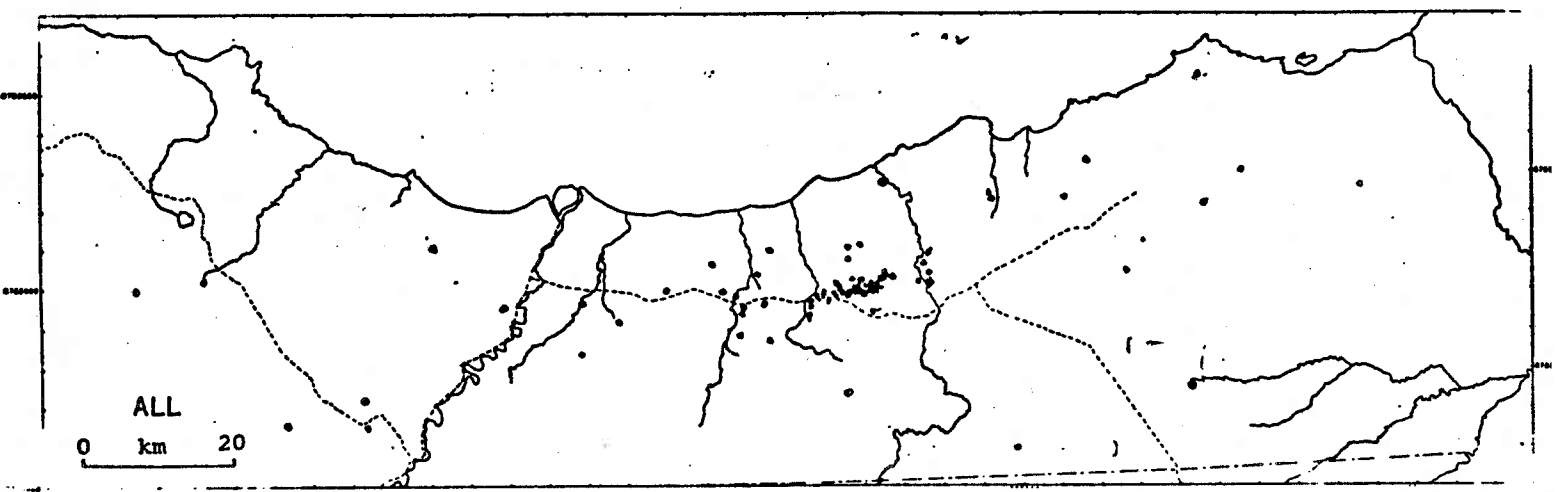
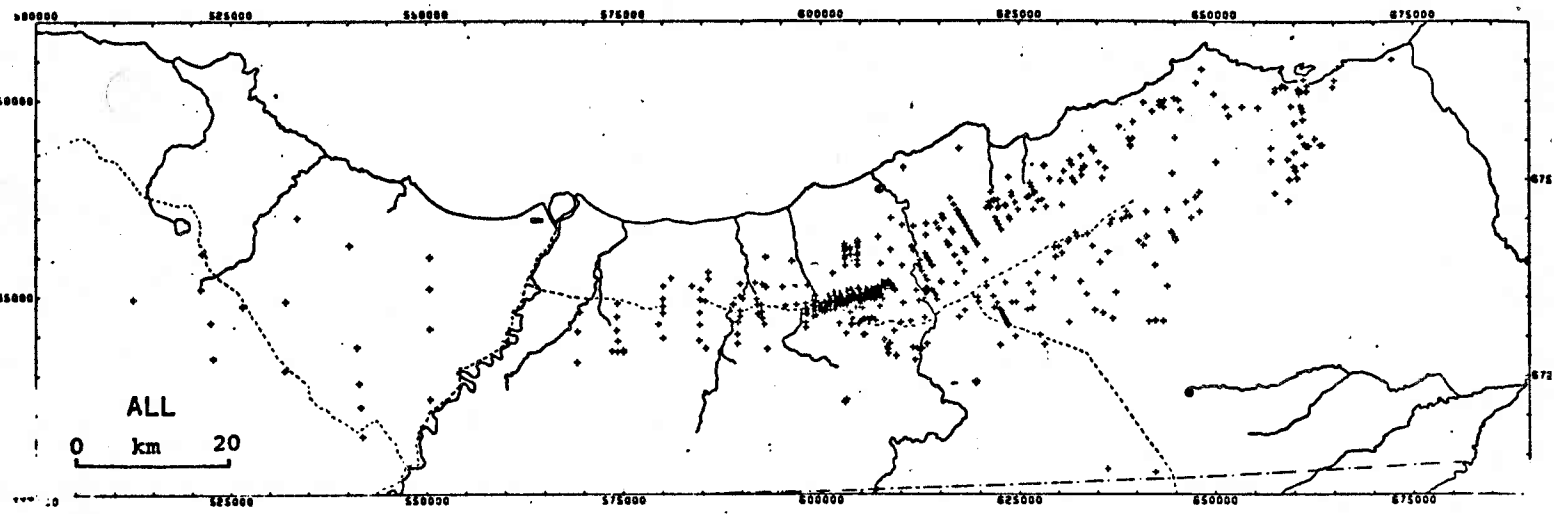


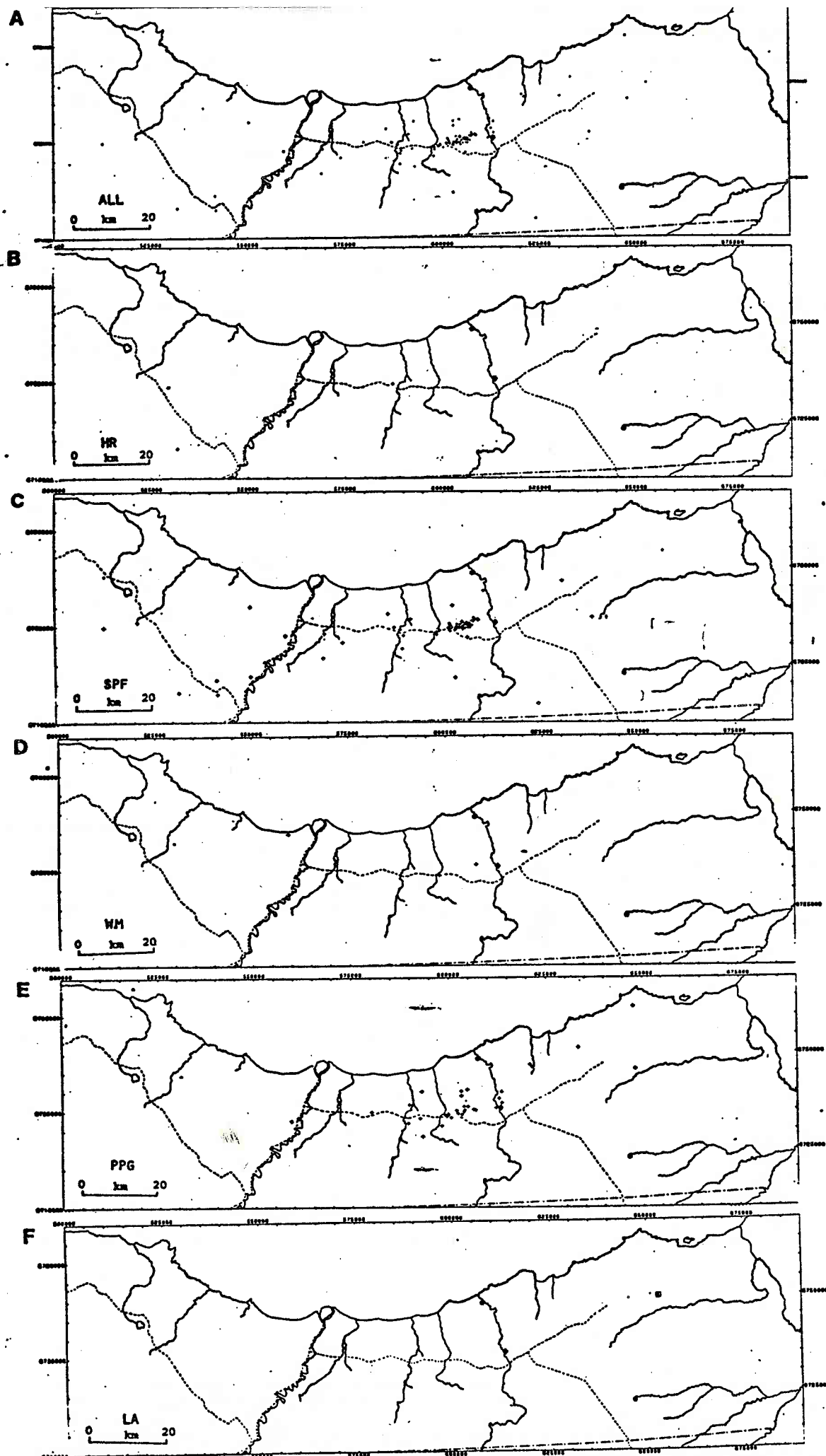
FIG. 3-50

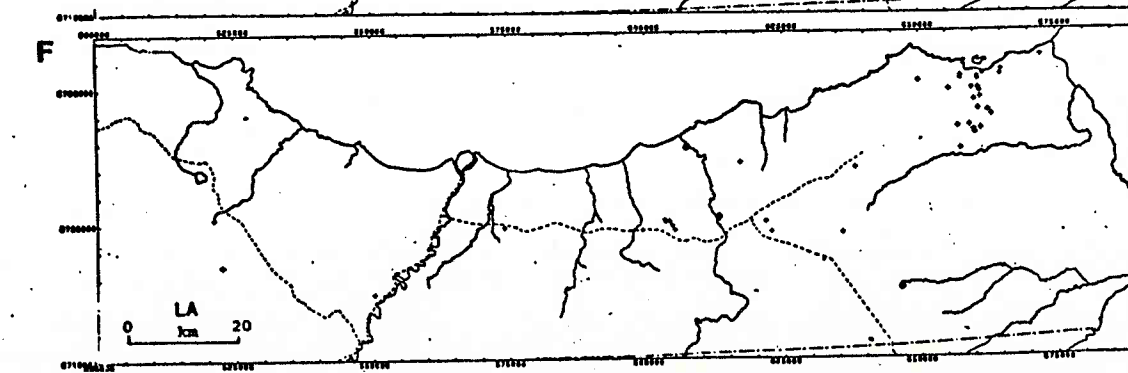
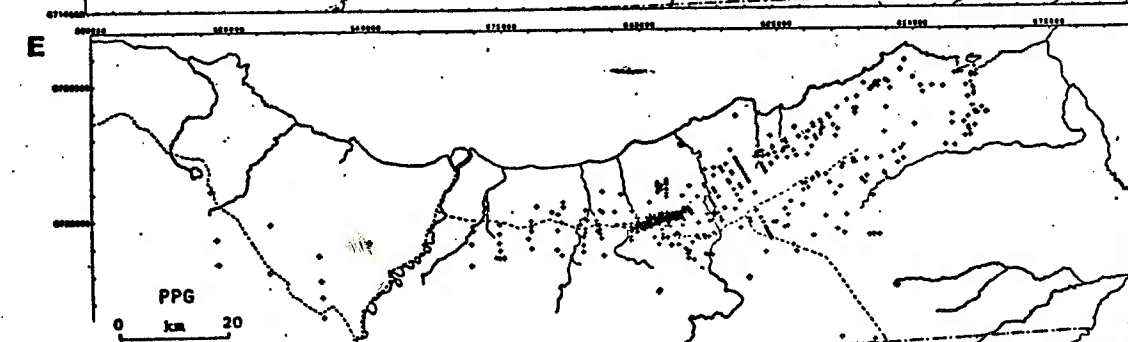
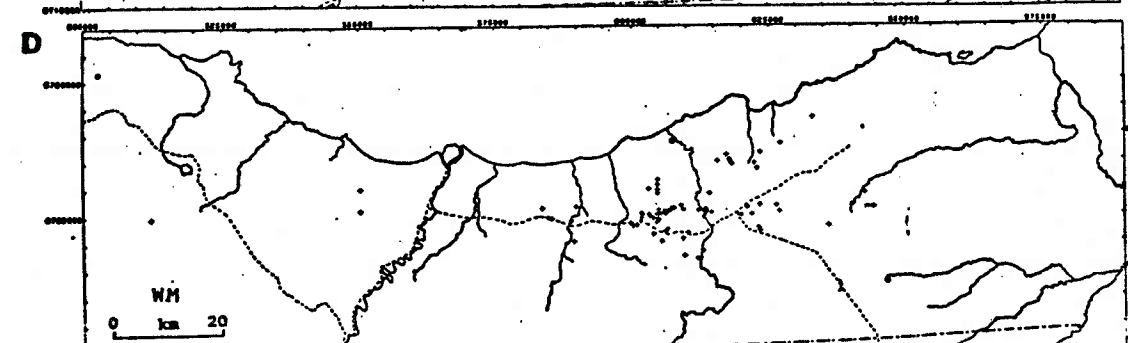
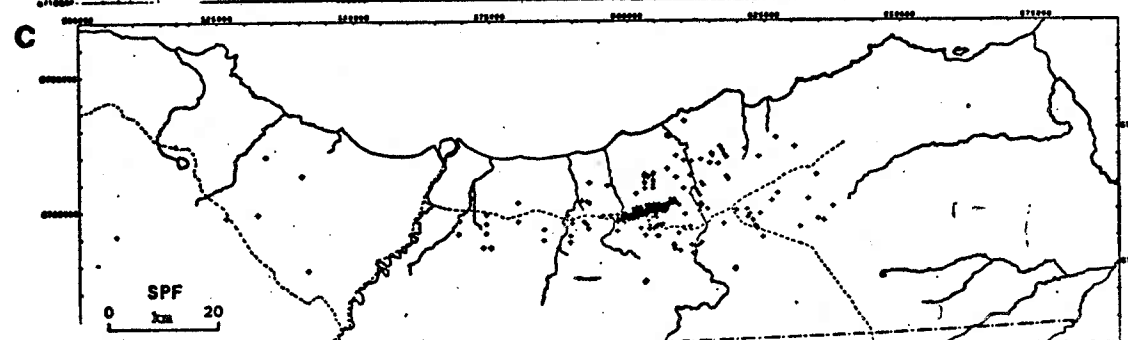
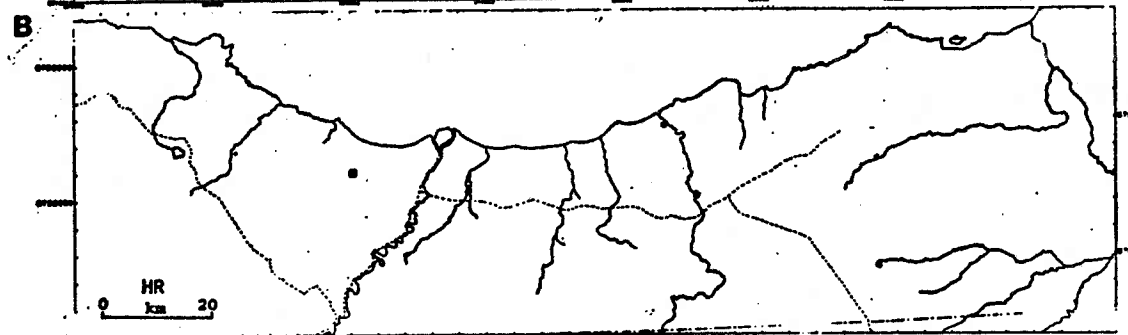
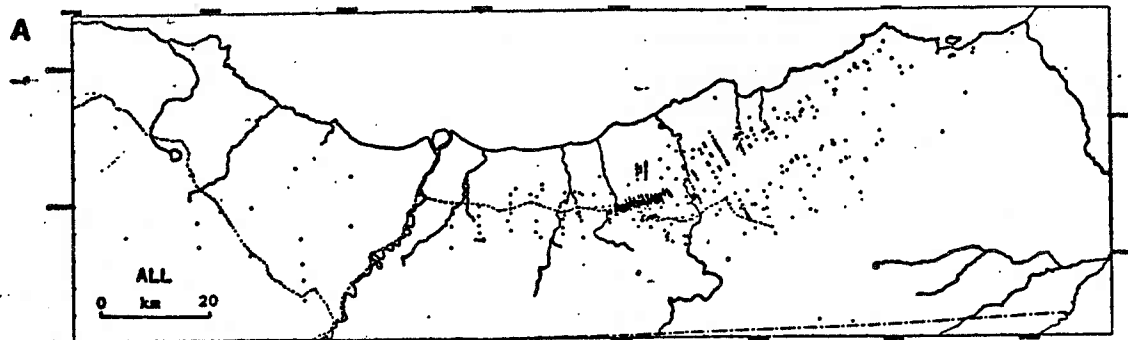






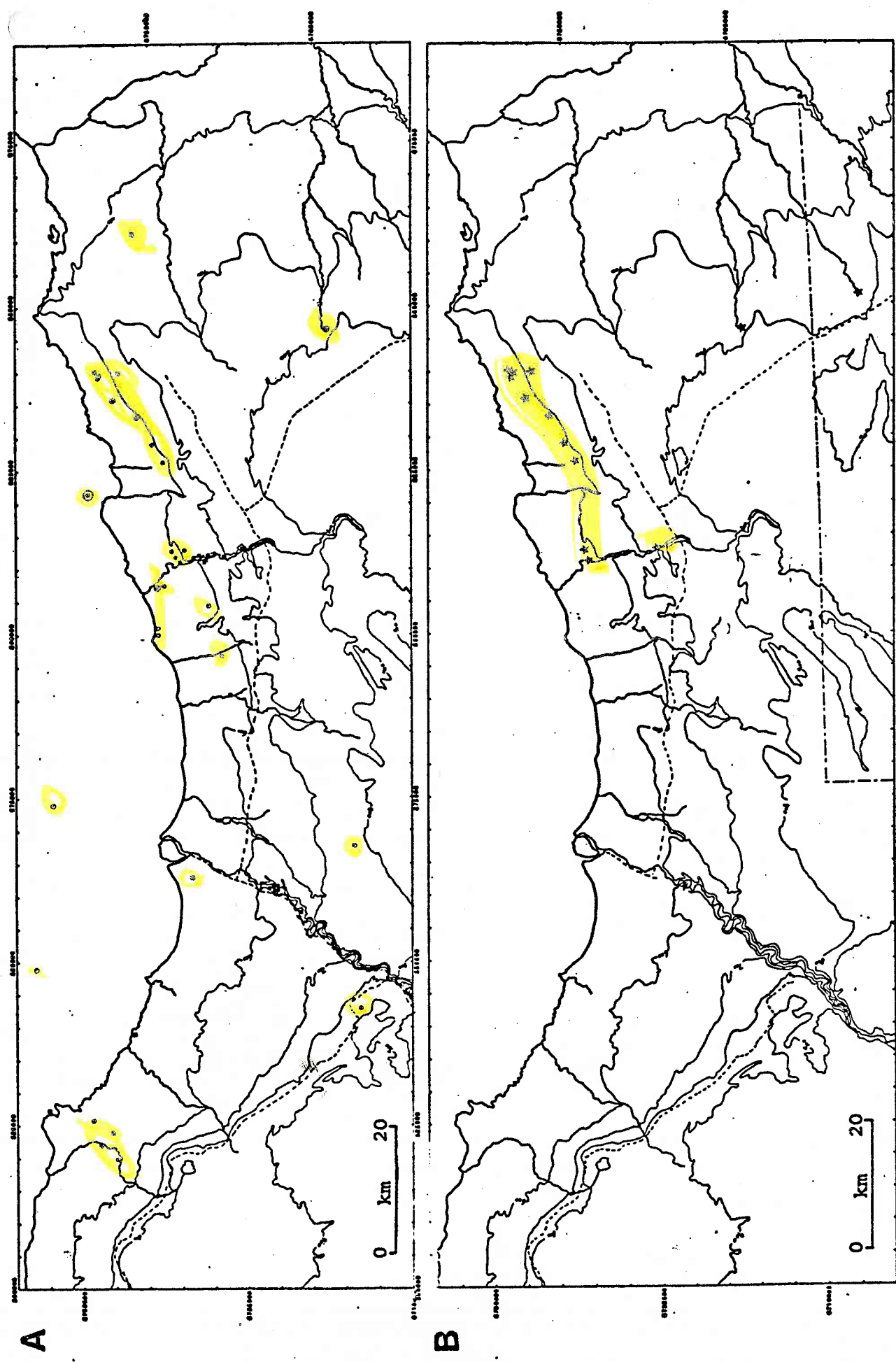






ARTESIAN HOLES

FIG. 4-1



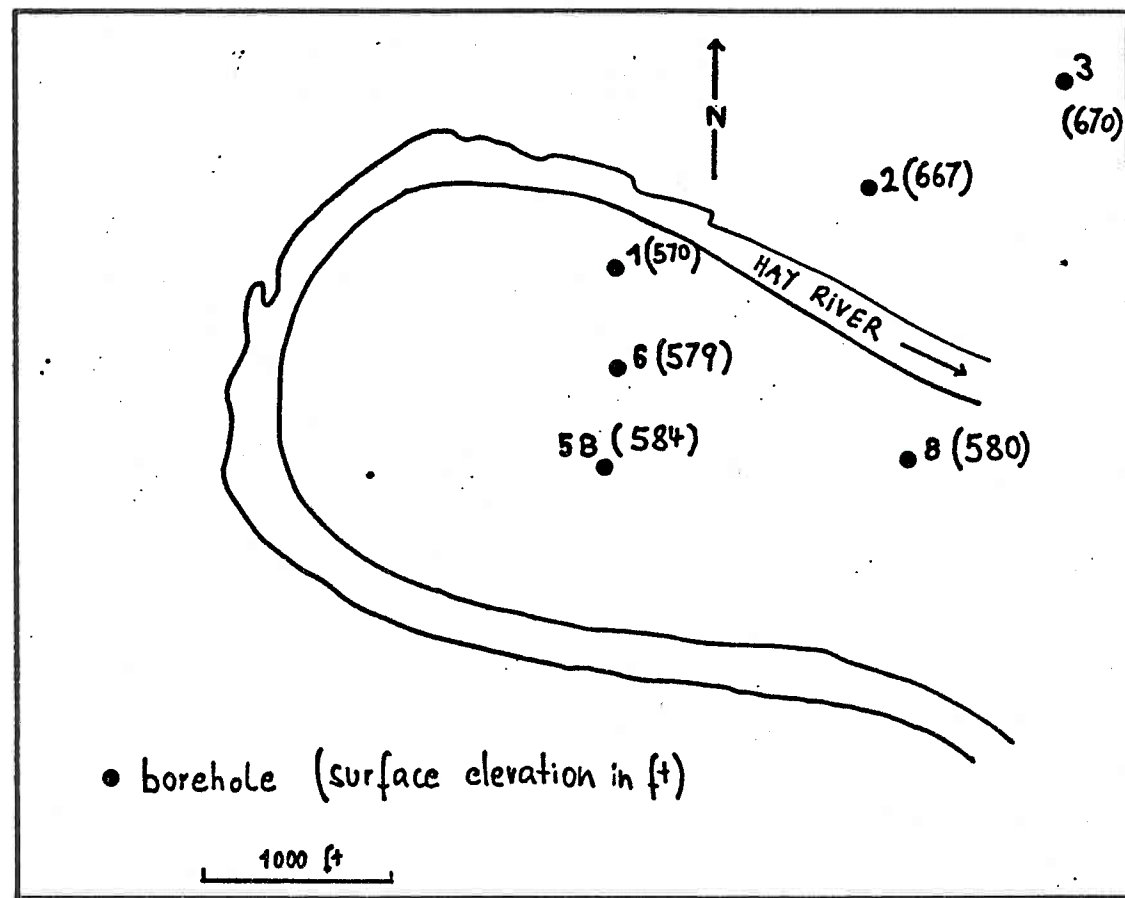


FIG. 4-2

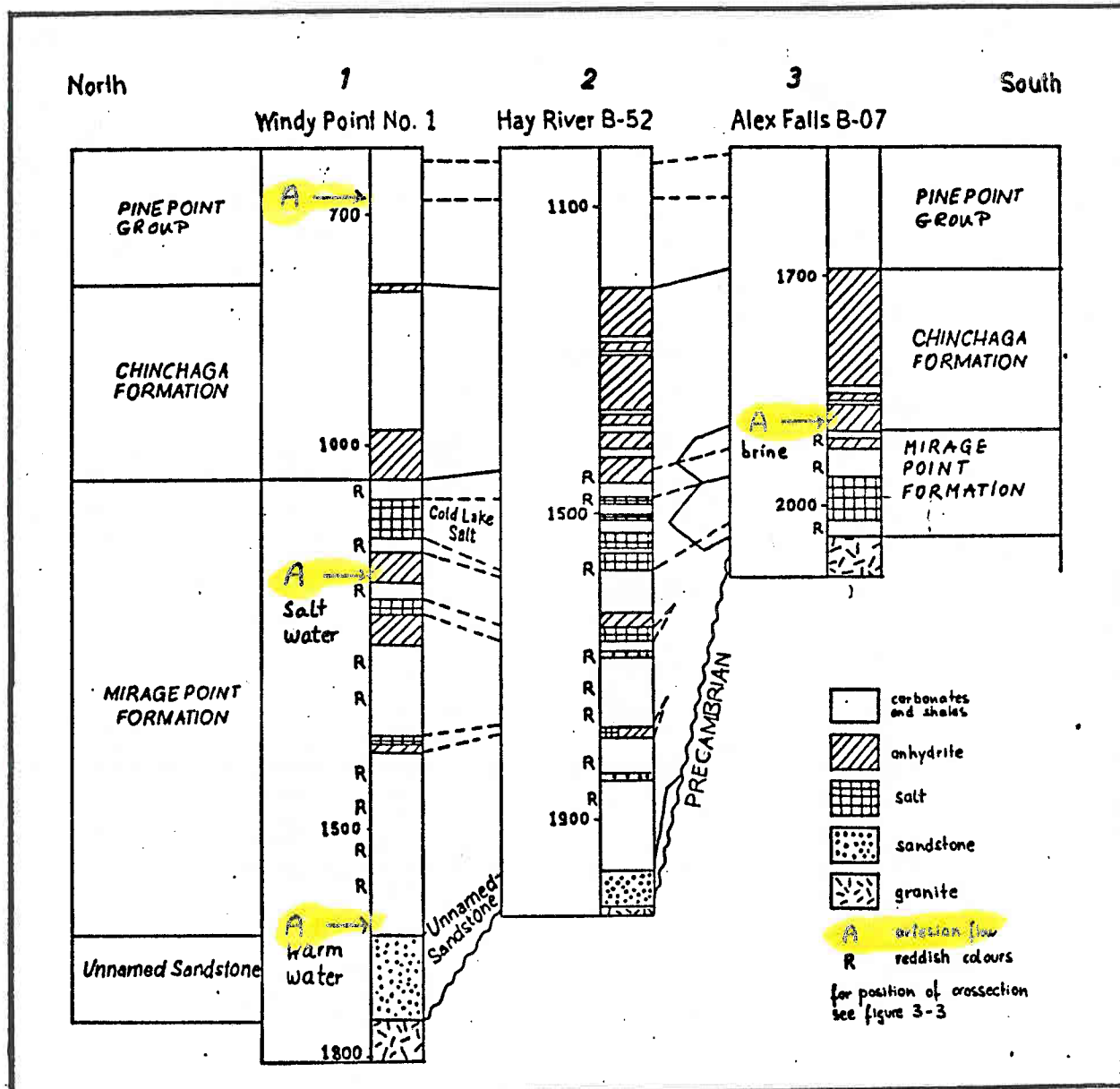


FIG. 4-3

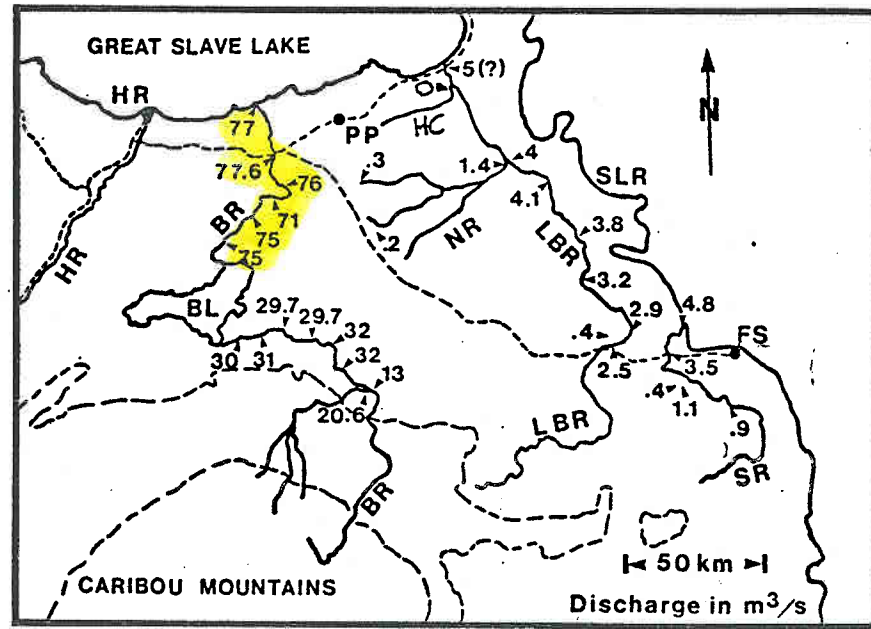
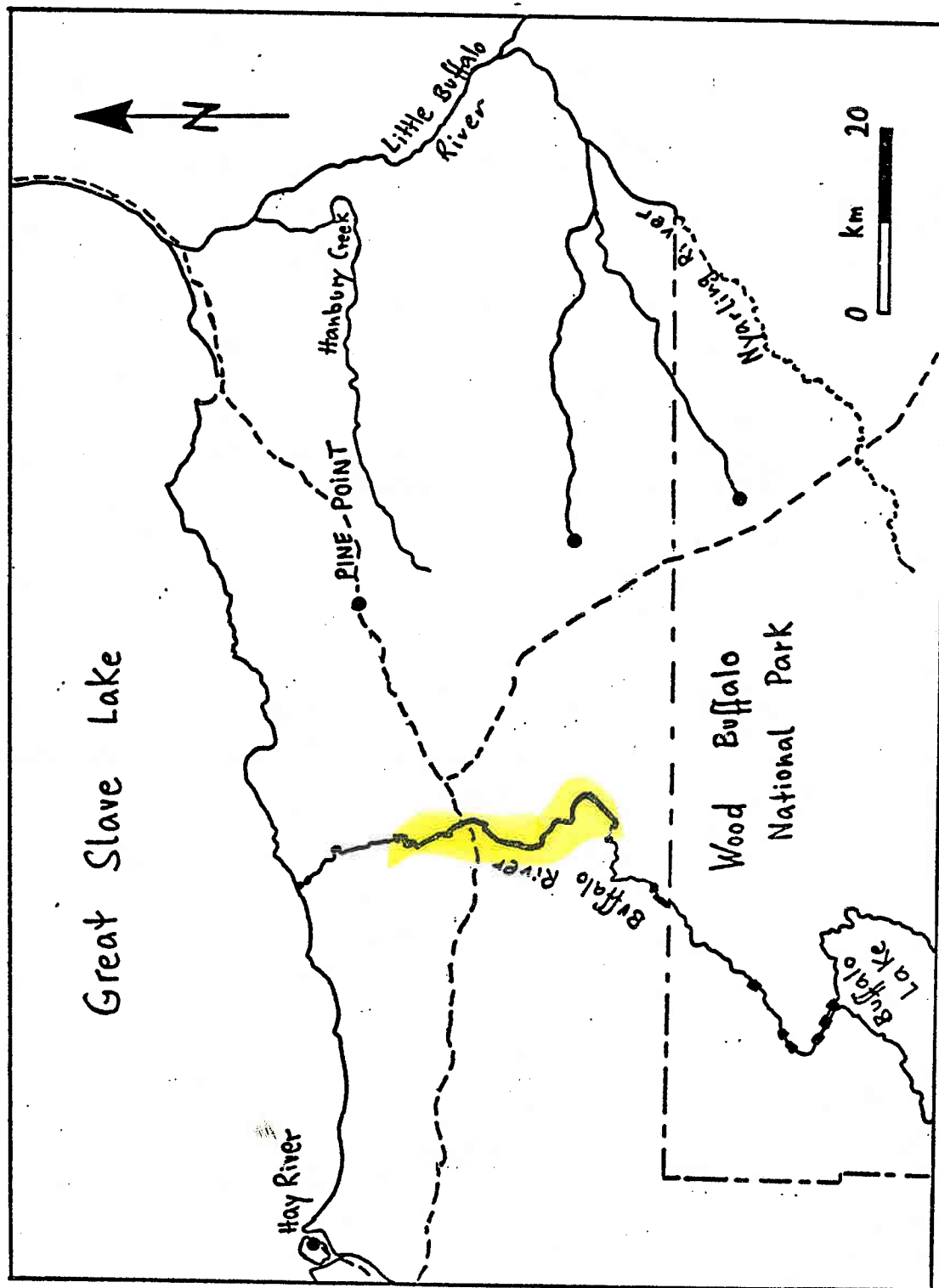


FIG. 4-4

FIG. 4-5



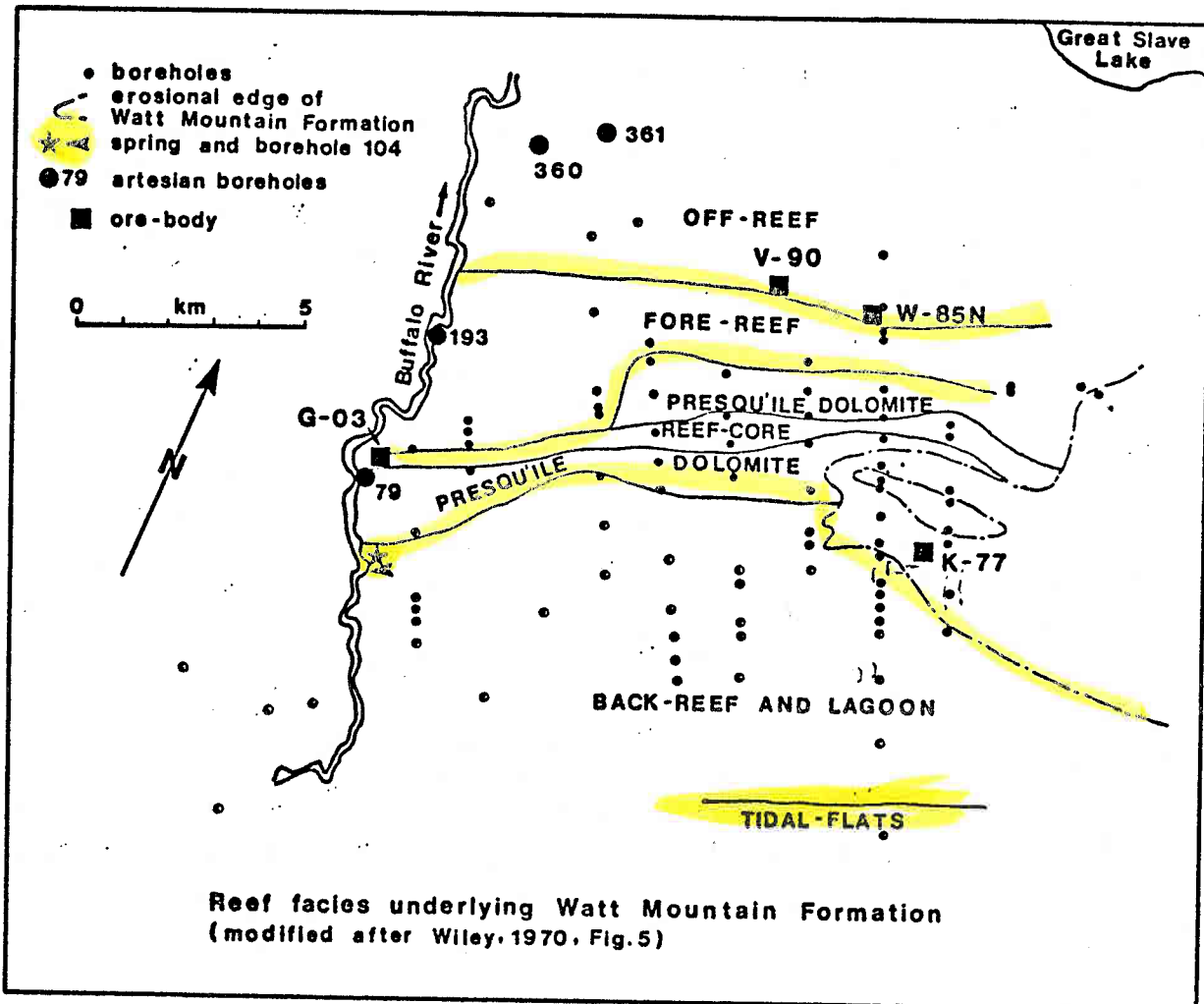
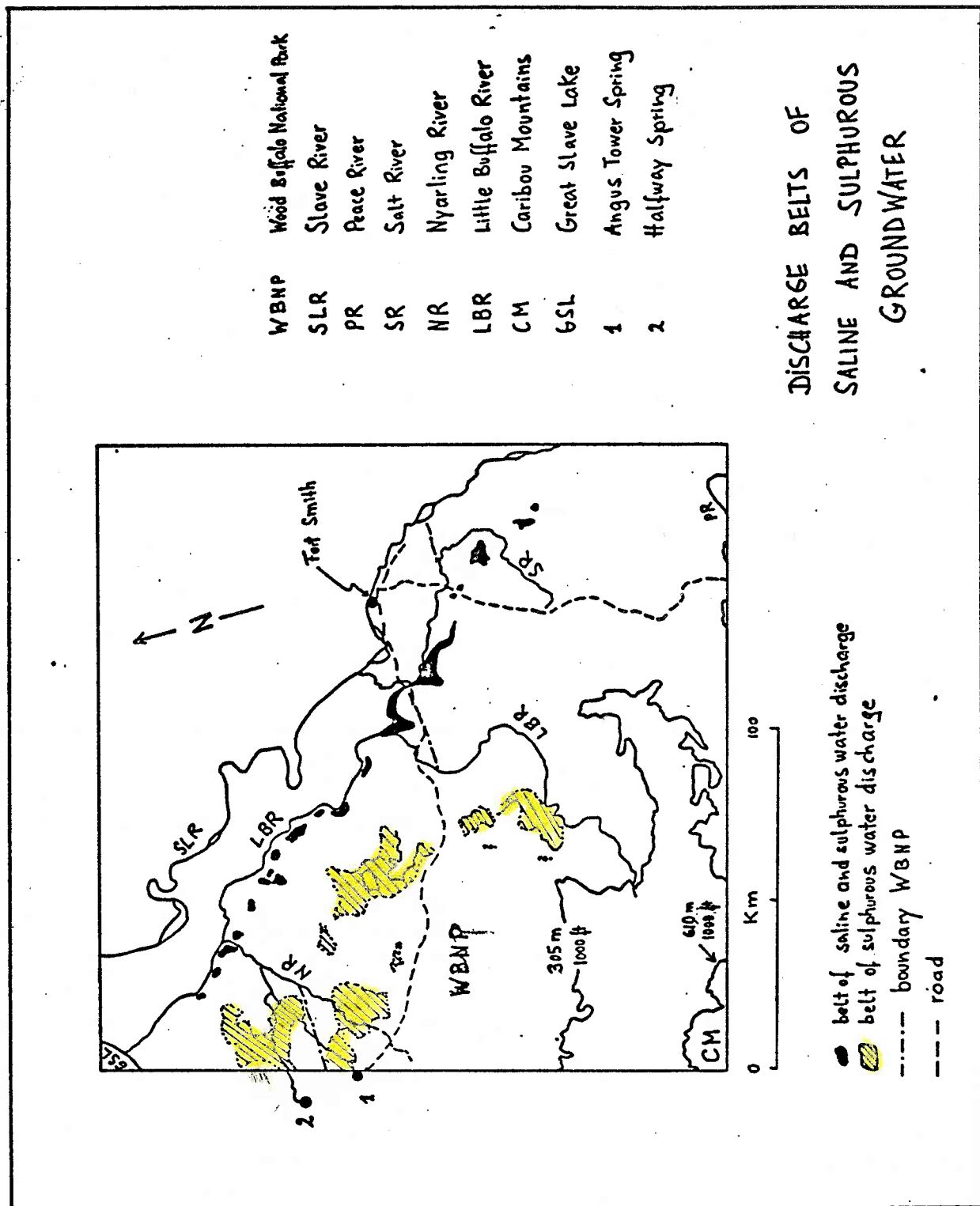


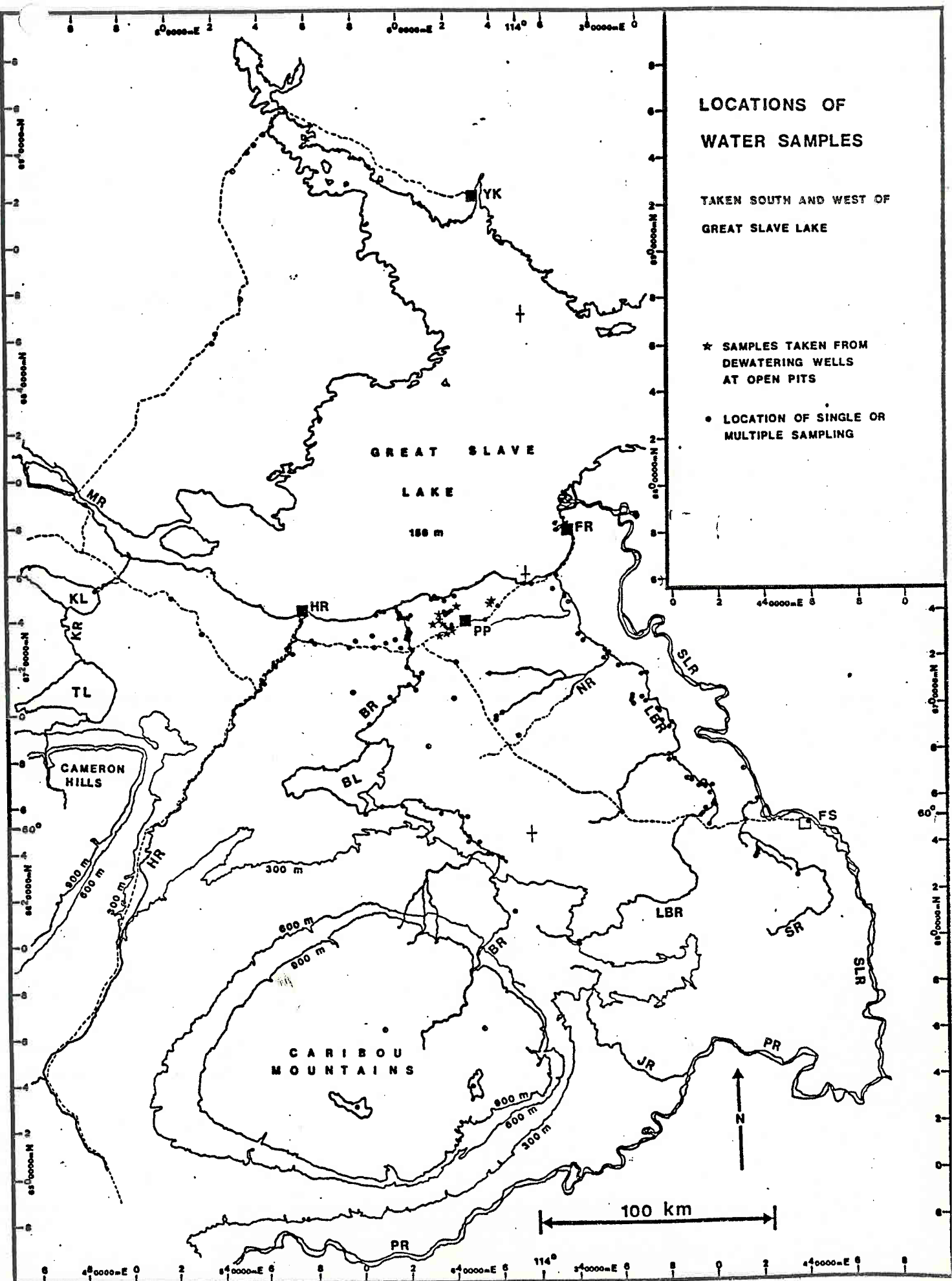
FIG. 4-6



FIG. 4-7

FIG. 4-8





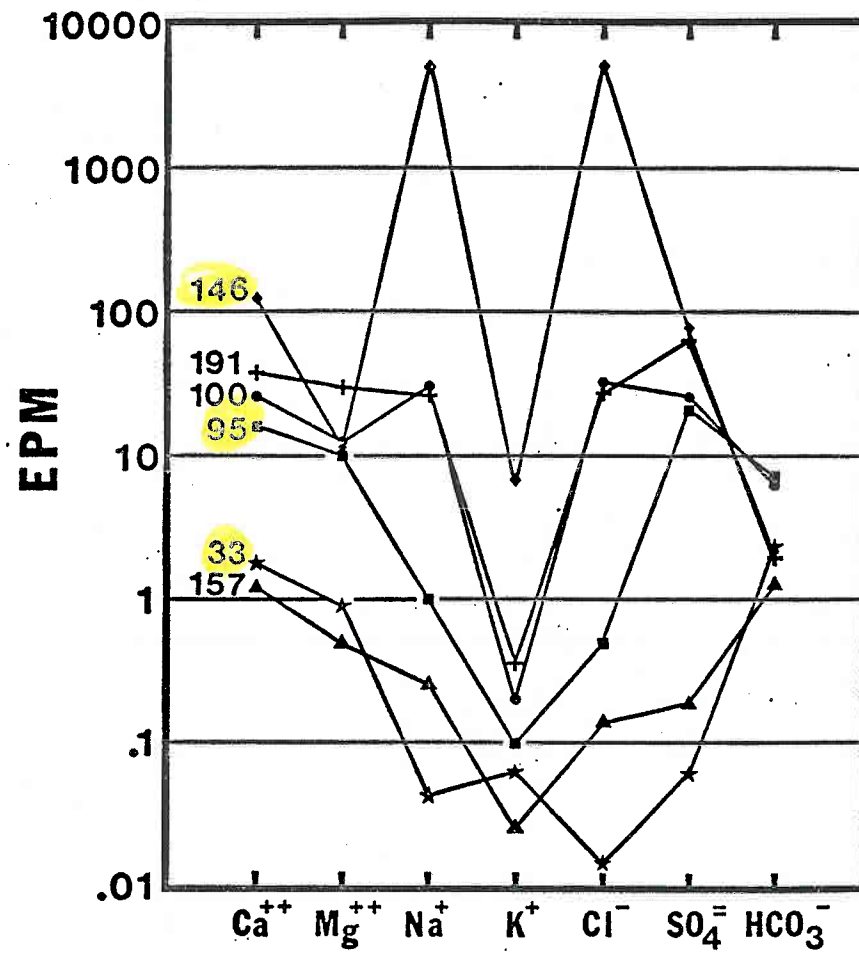


FIG. 4-10

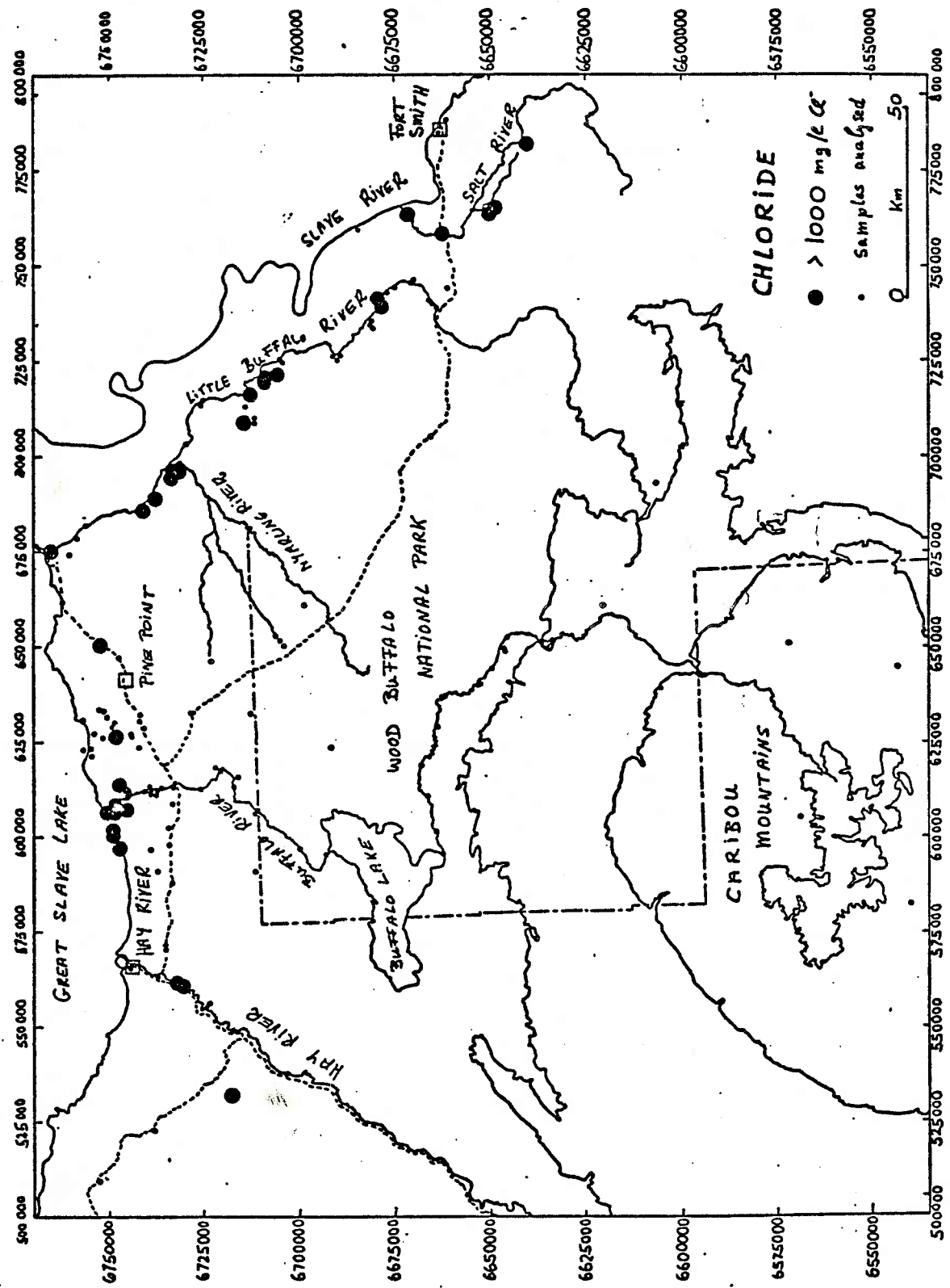
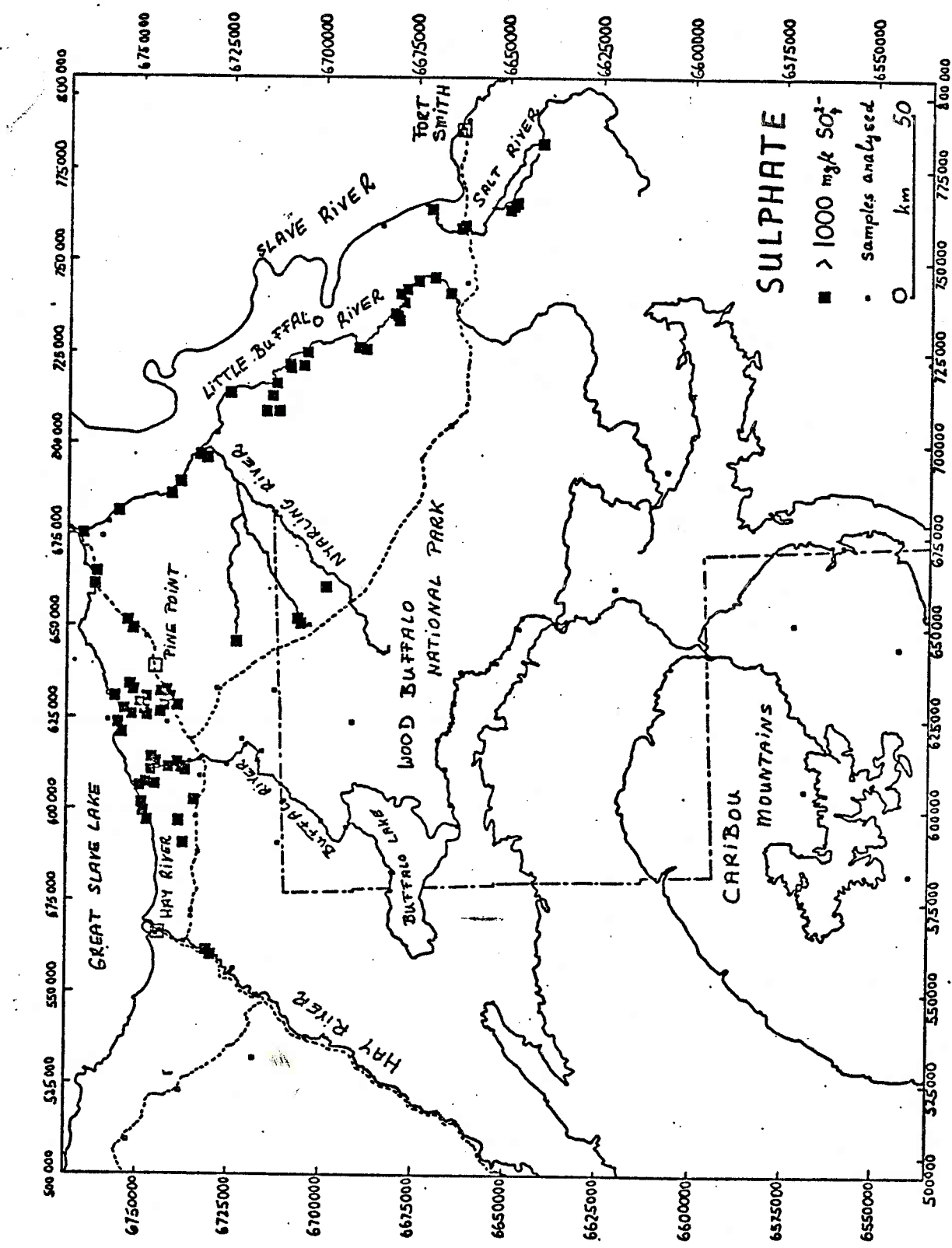


FIG. 4-11

FIG. 4-12



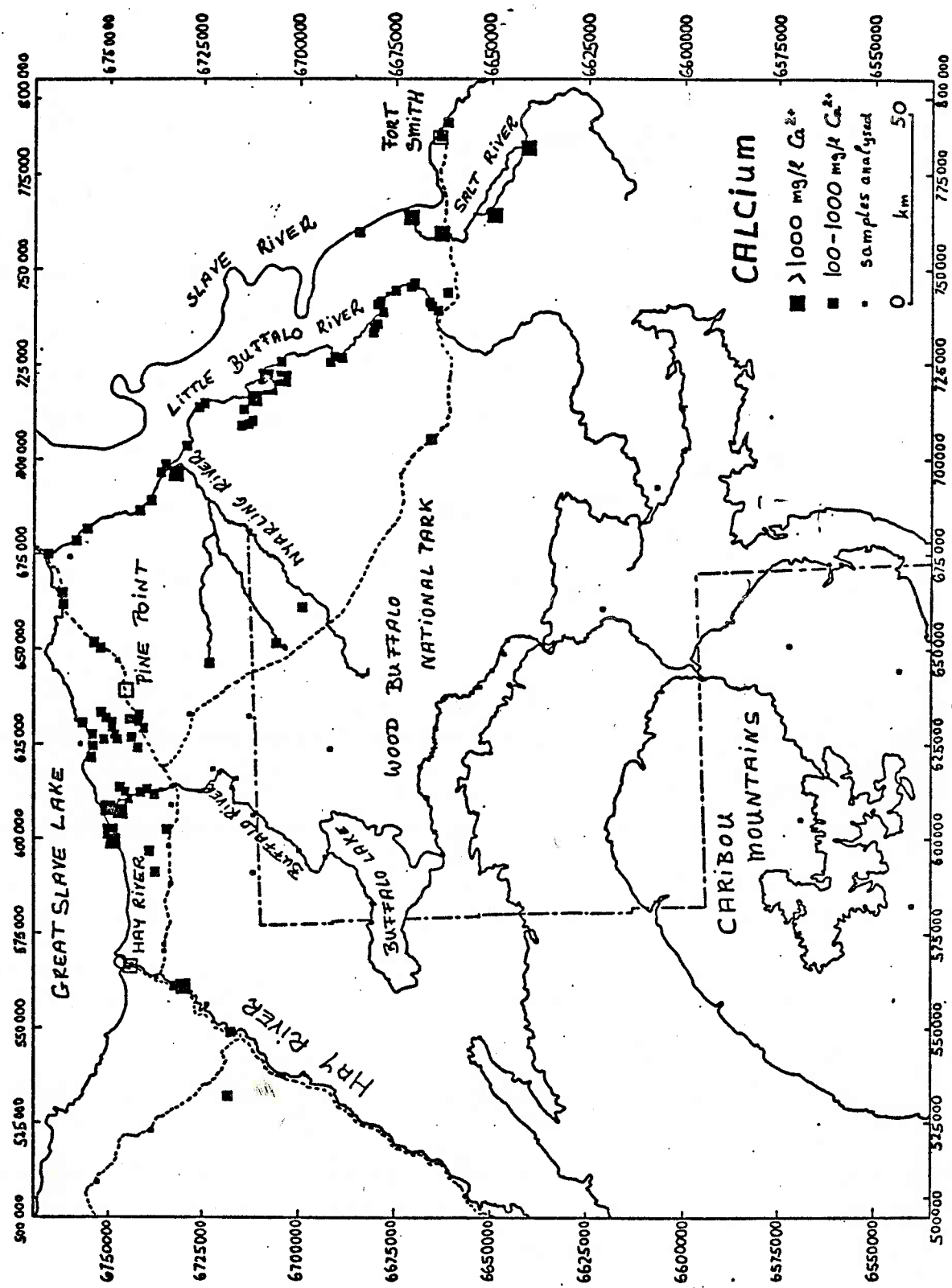
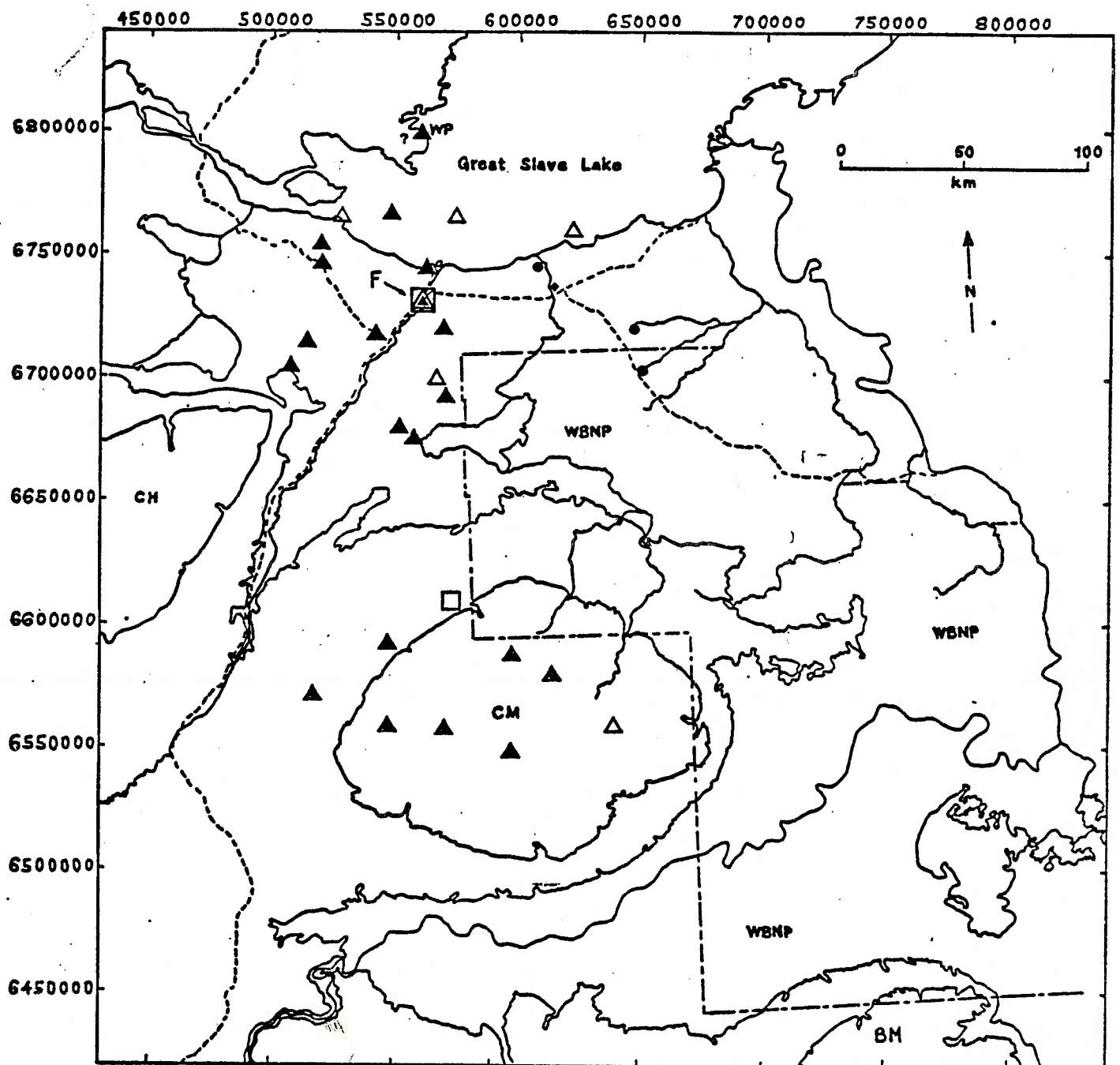
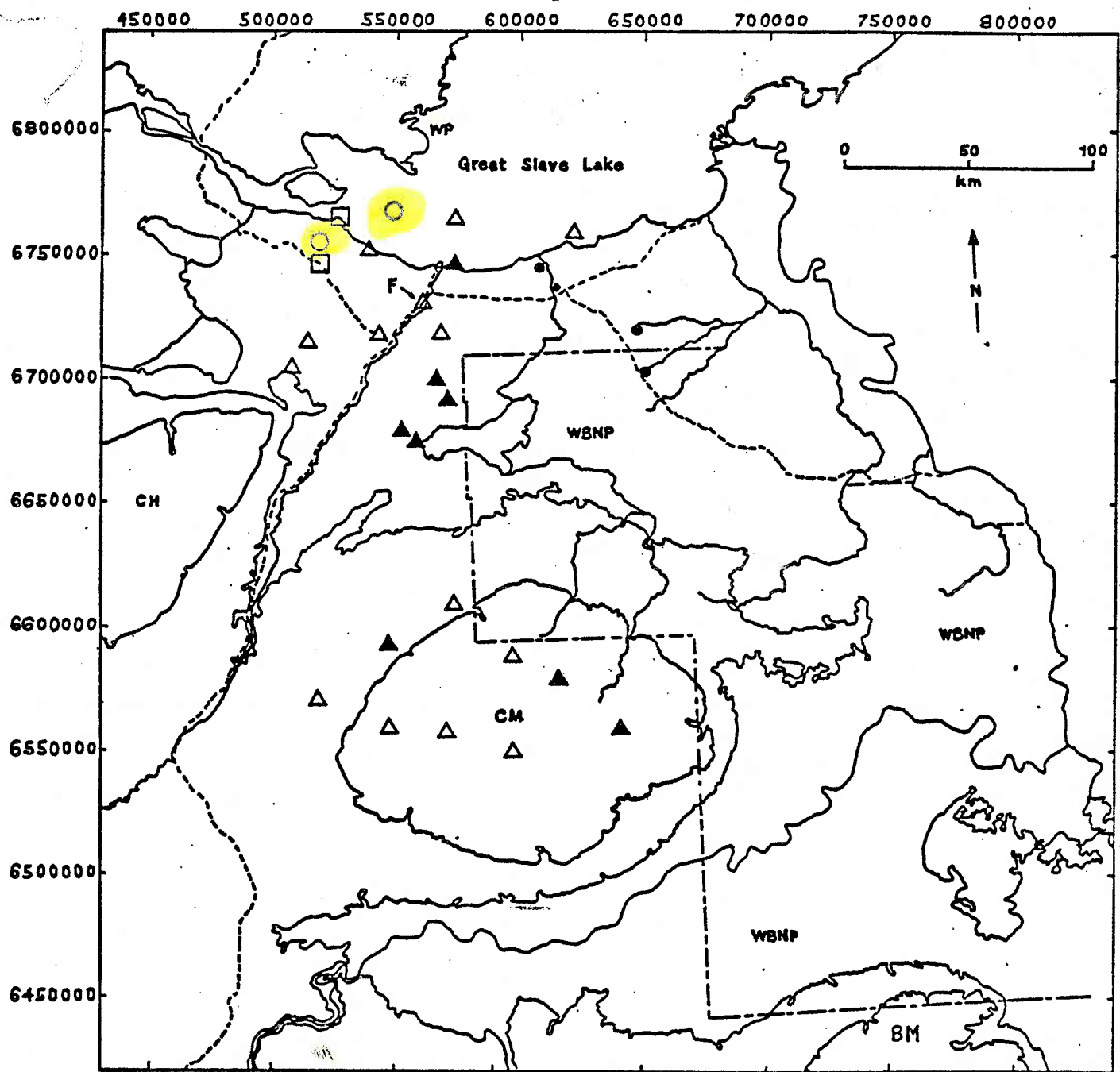


FIG. 4-13



CL \square 100-999
 \triangle 1000-9999
 \blacktriangle > 10 000

FIG. 4-14



SO_4

- \circ 10-99
- \square 100-999
- \triangle 1000-2999
- \blacktriangle > 3000

FIG. 4-15

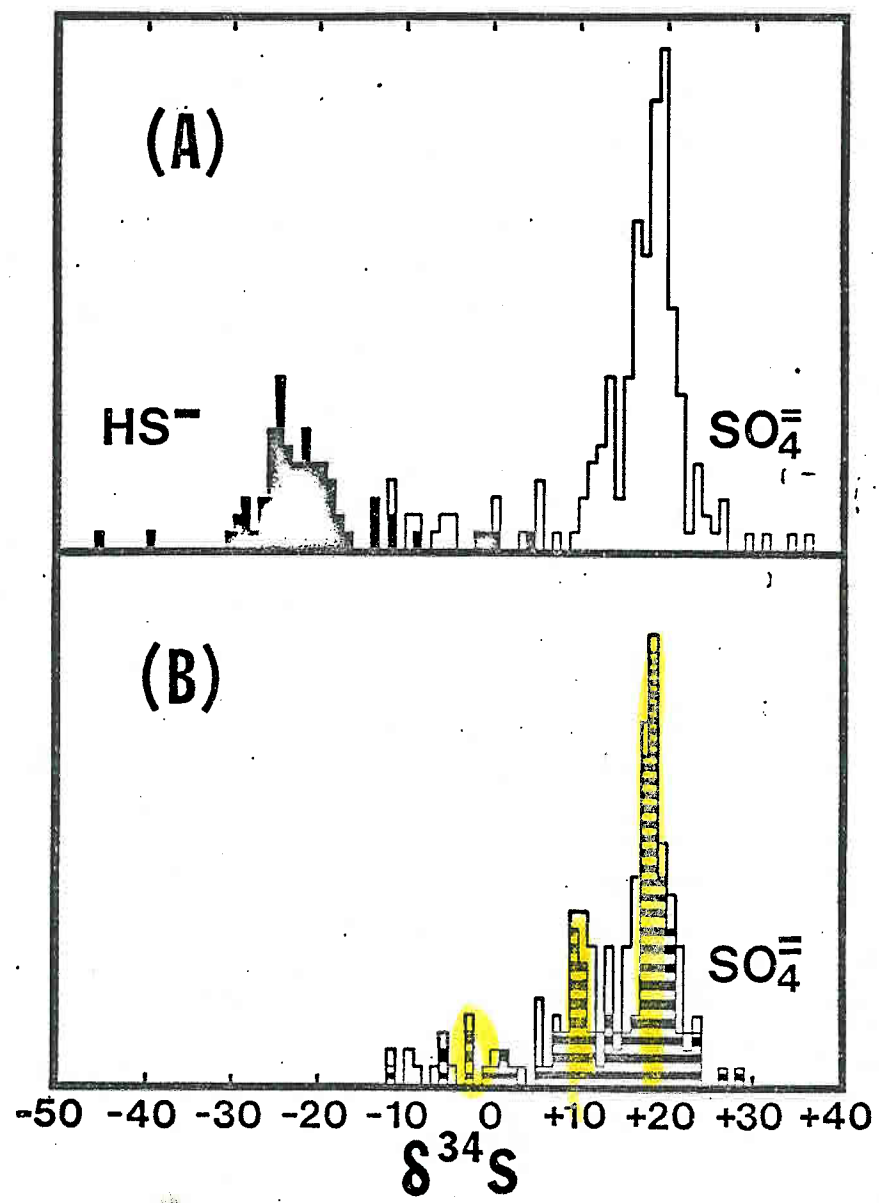


FIG. 4-16

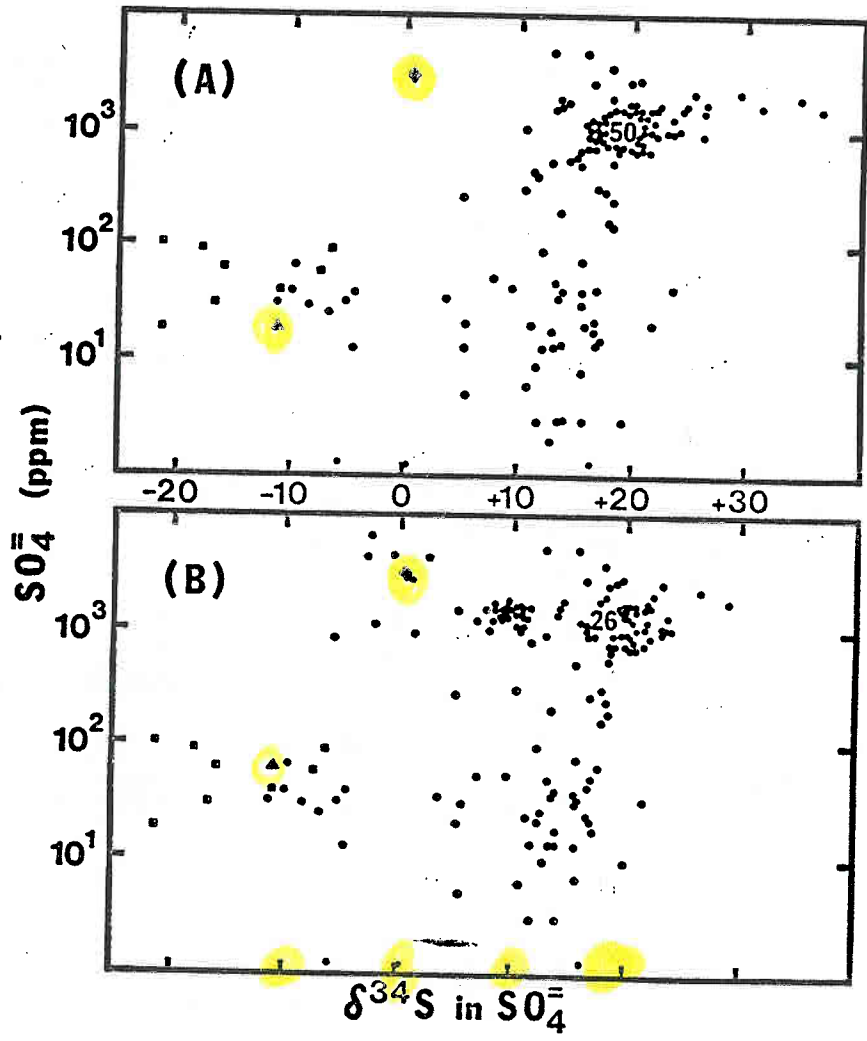


FIG. 4-17

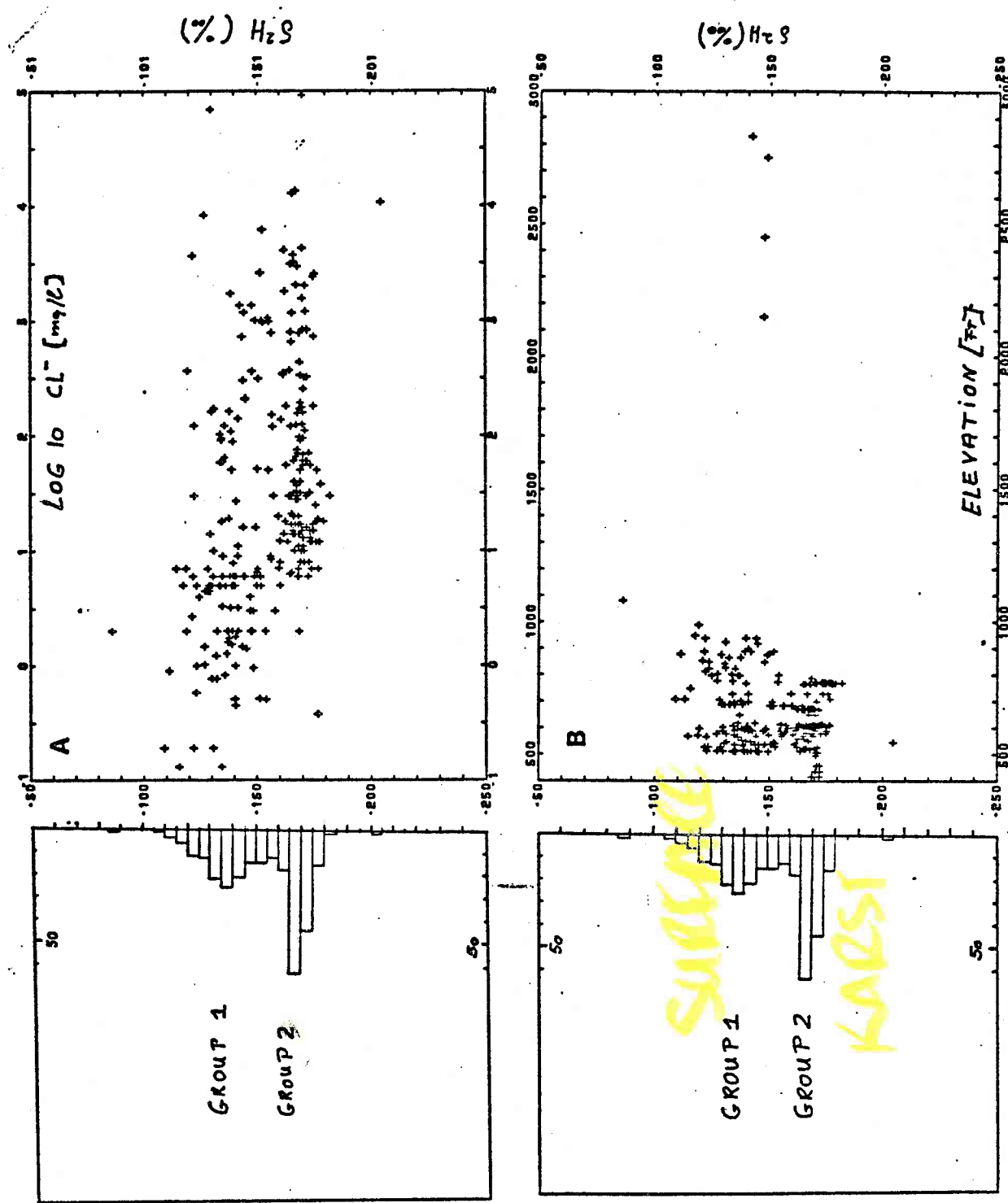
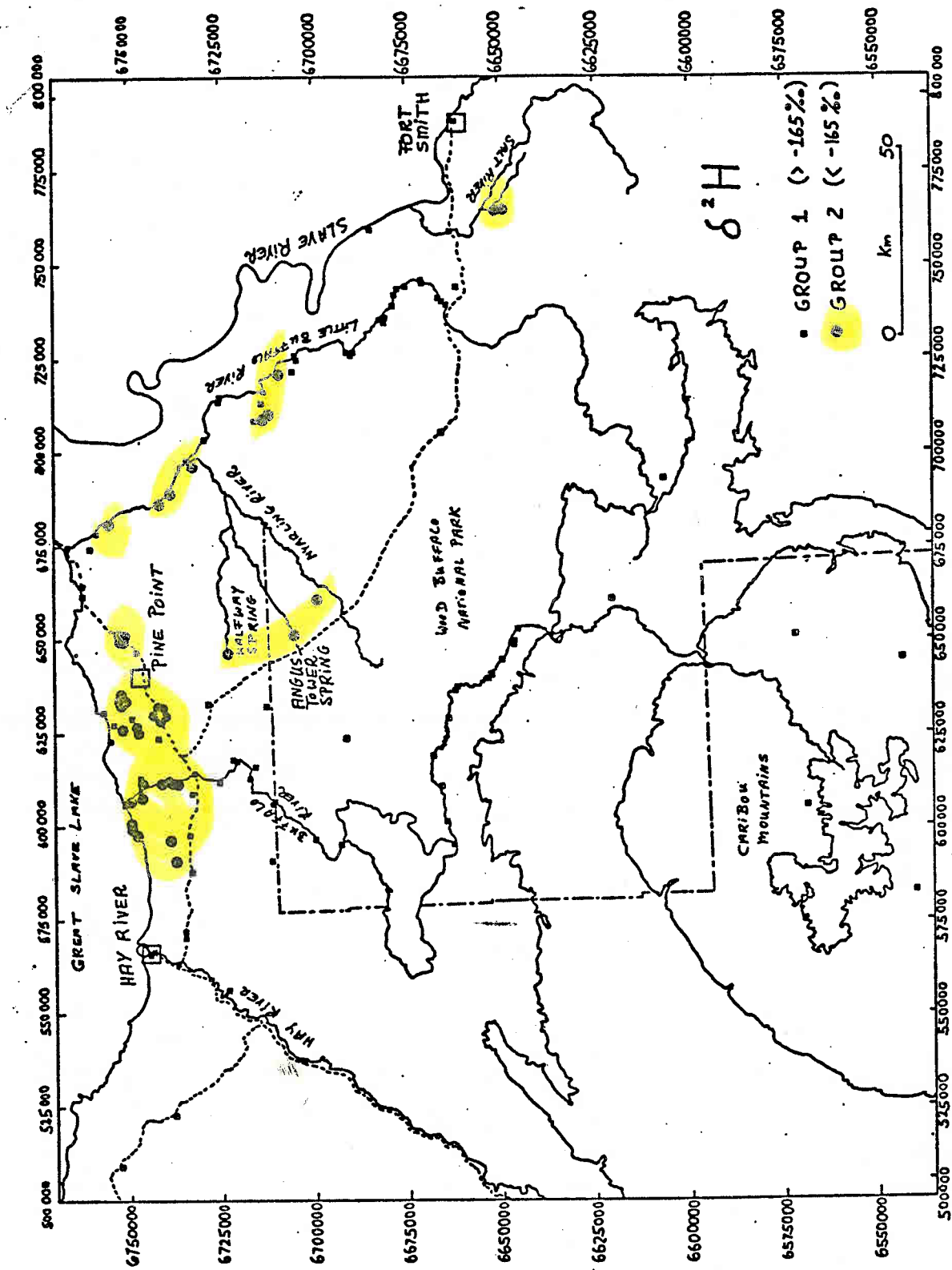
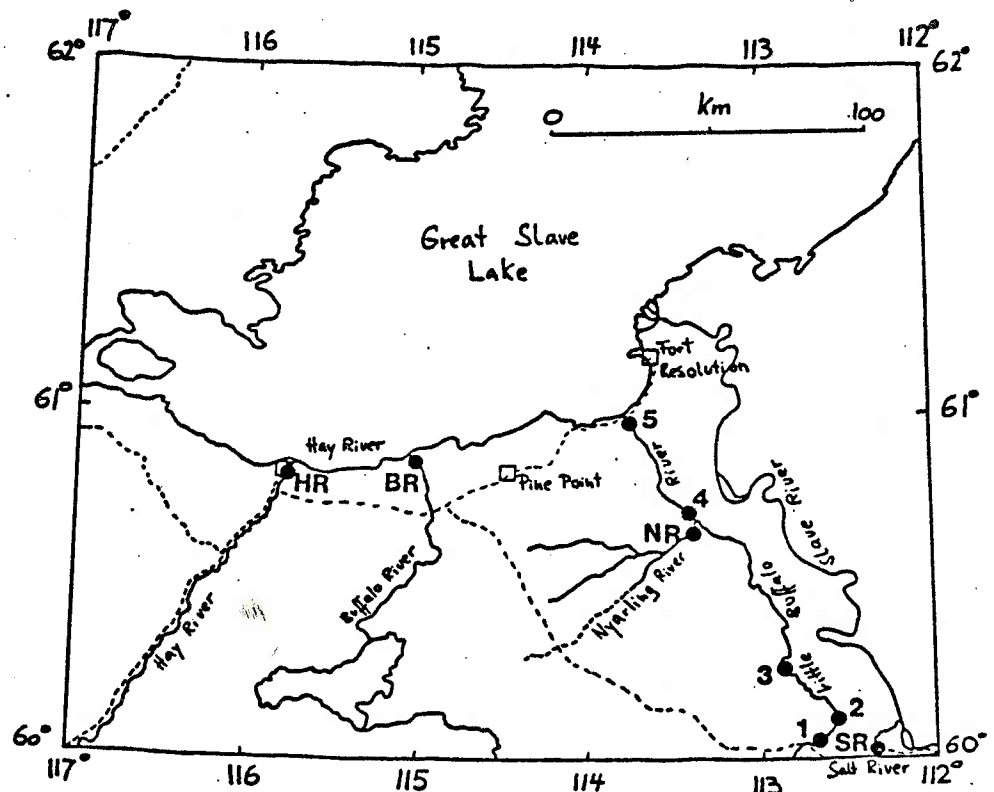
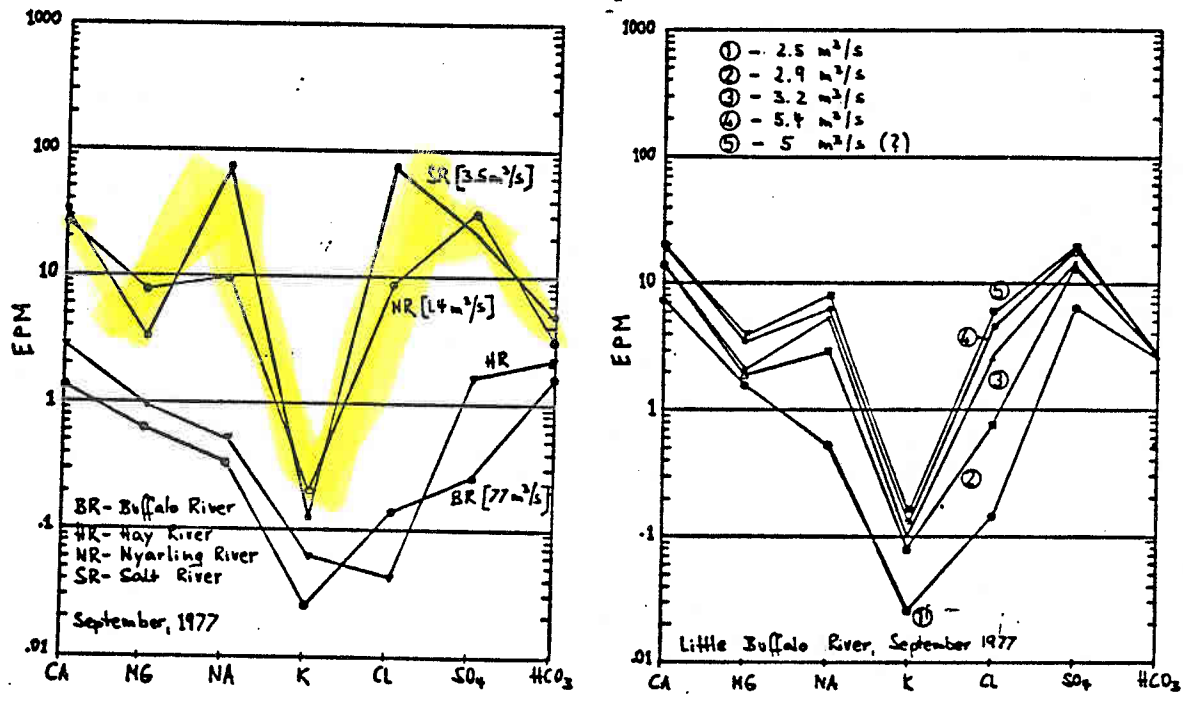


FIG. 4-18

FIG. 4-19





CHEMISTRY AND FLOW OF RIVERS, PINE POINT AREA

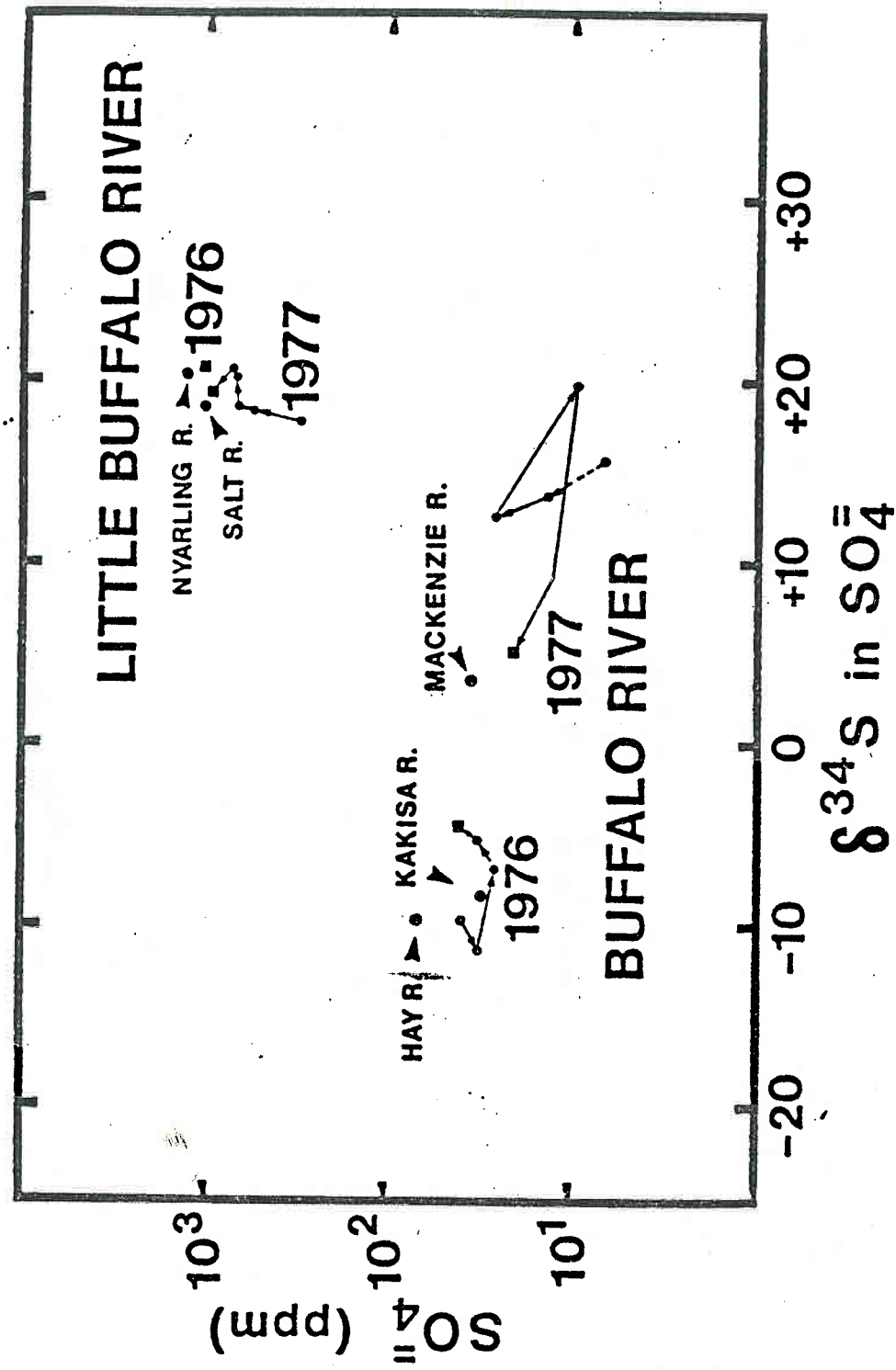


FIG. 4-21

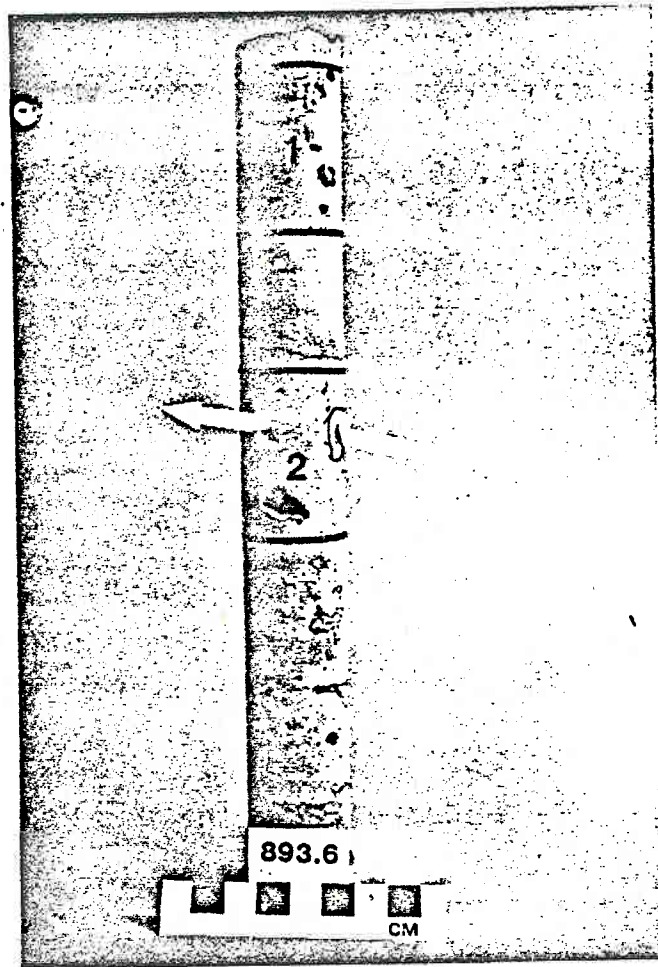


FIG. 4-22 A

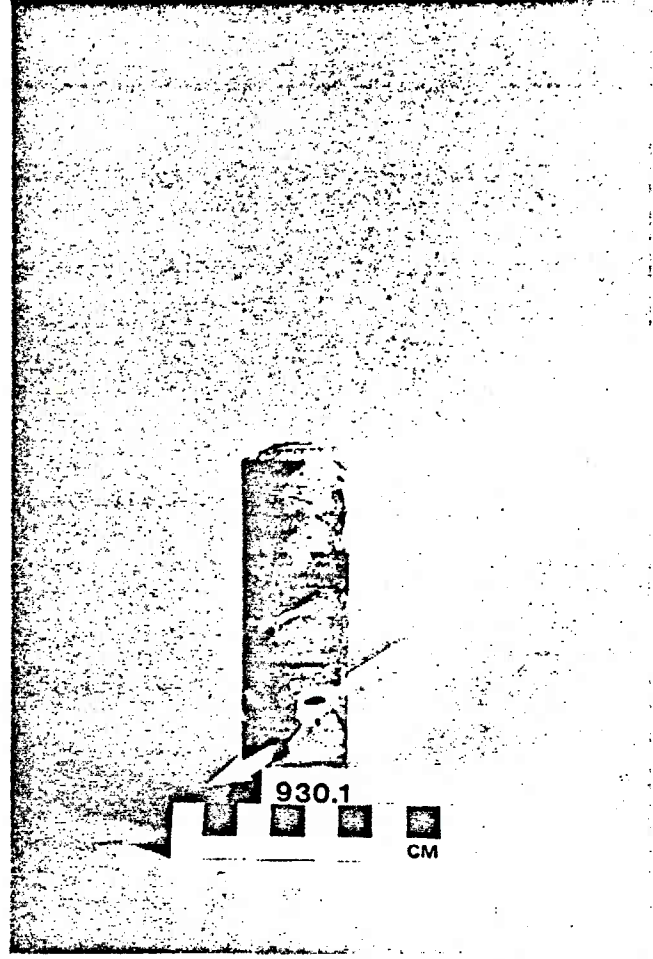


FIG. 4-22 B

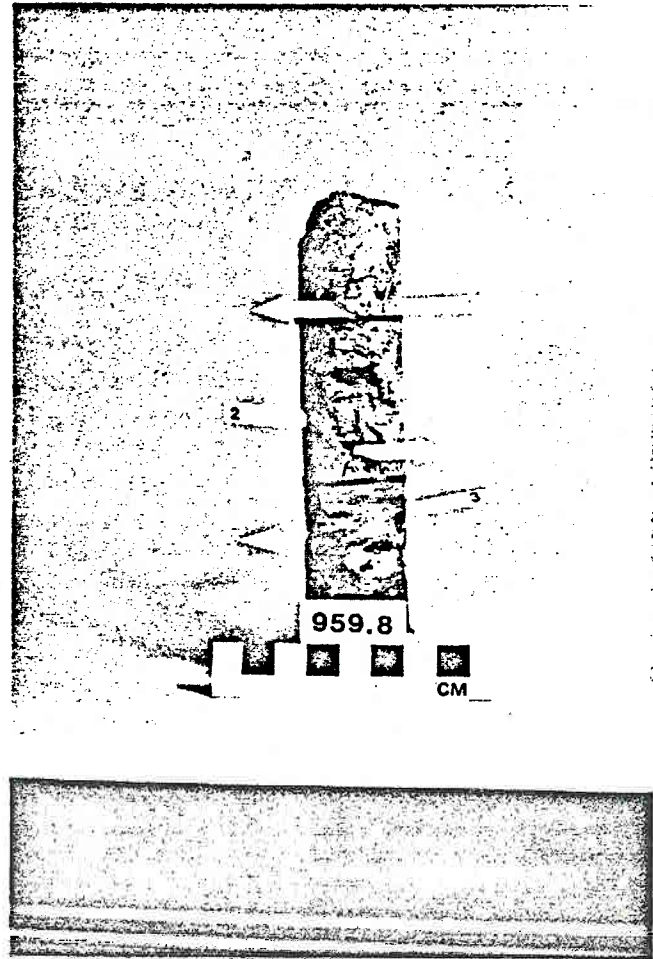


FIG. 4-22 C

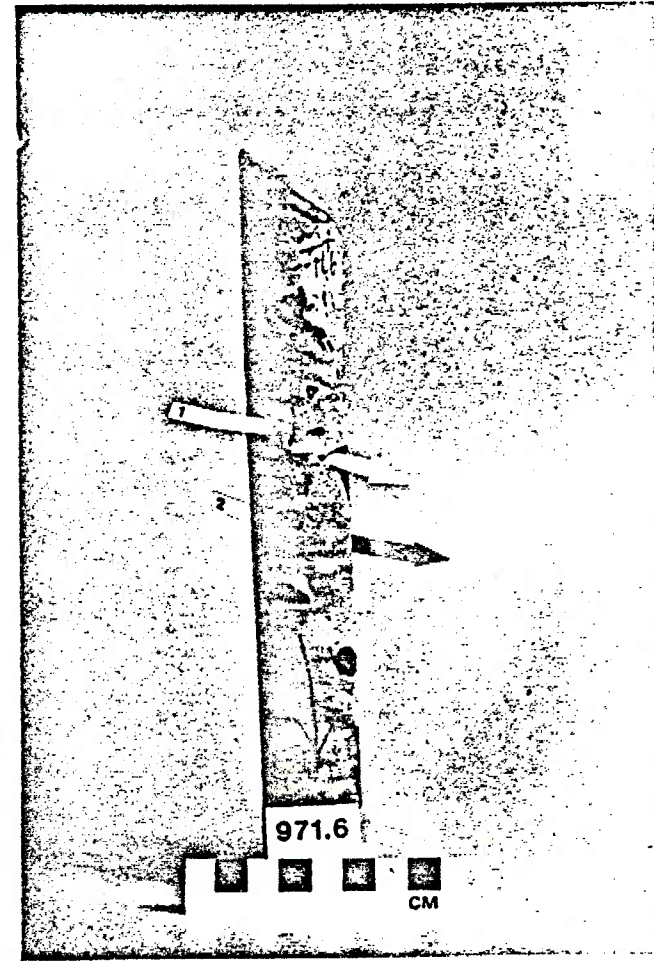
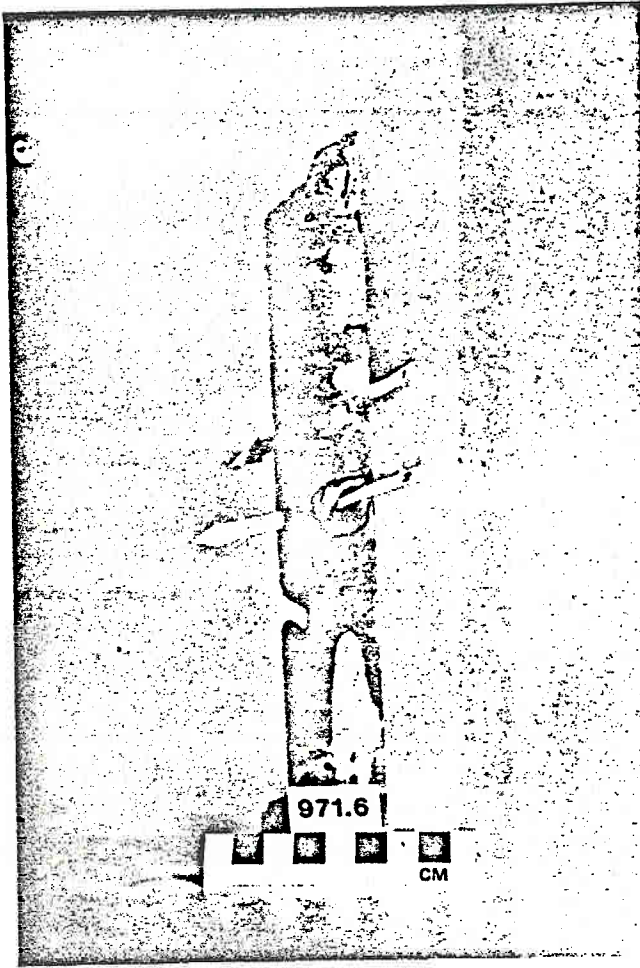


FIG. 4-22 D

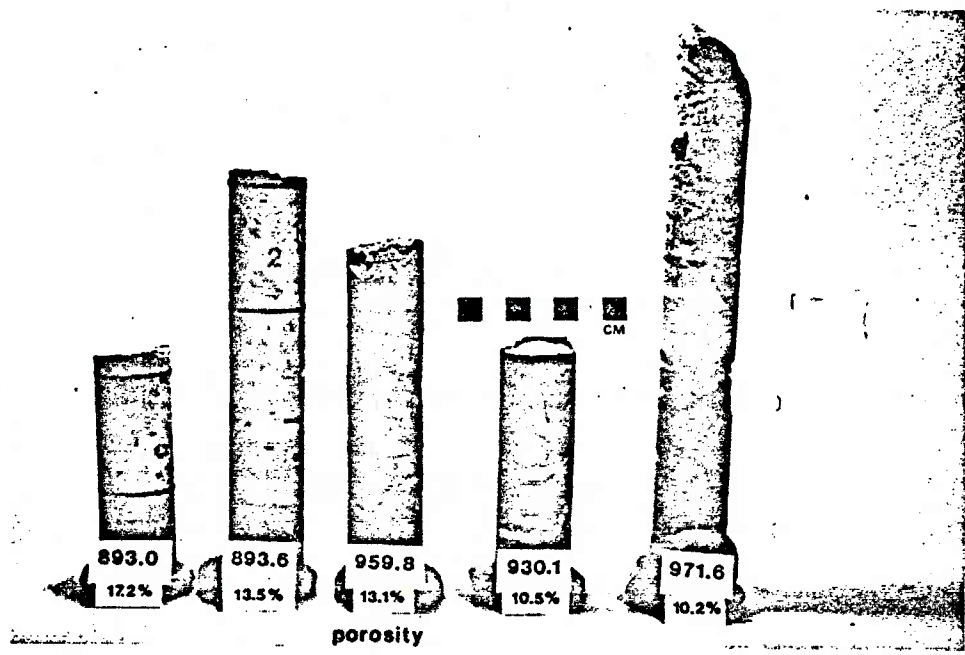
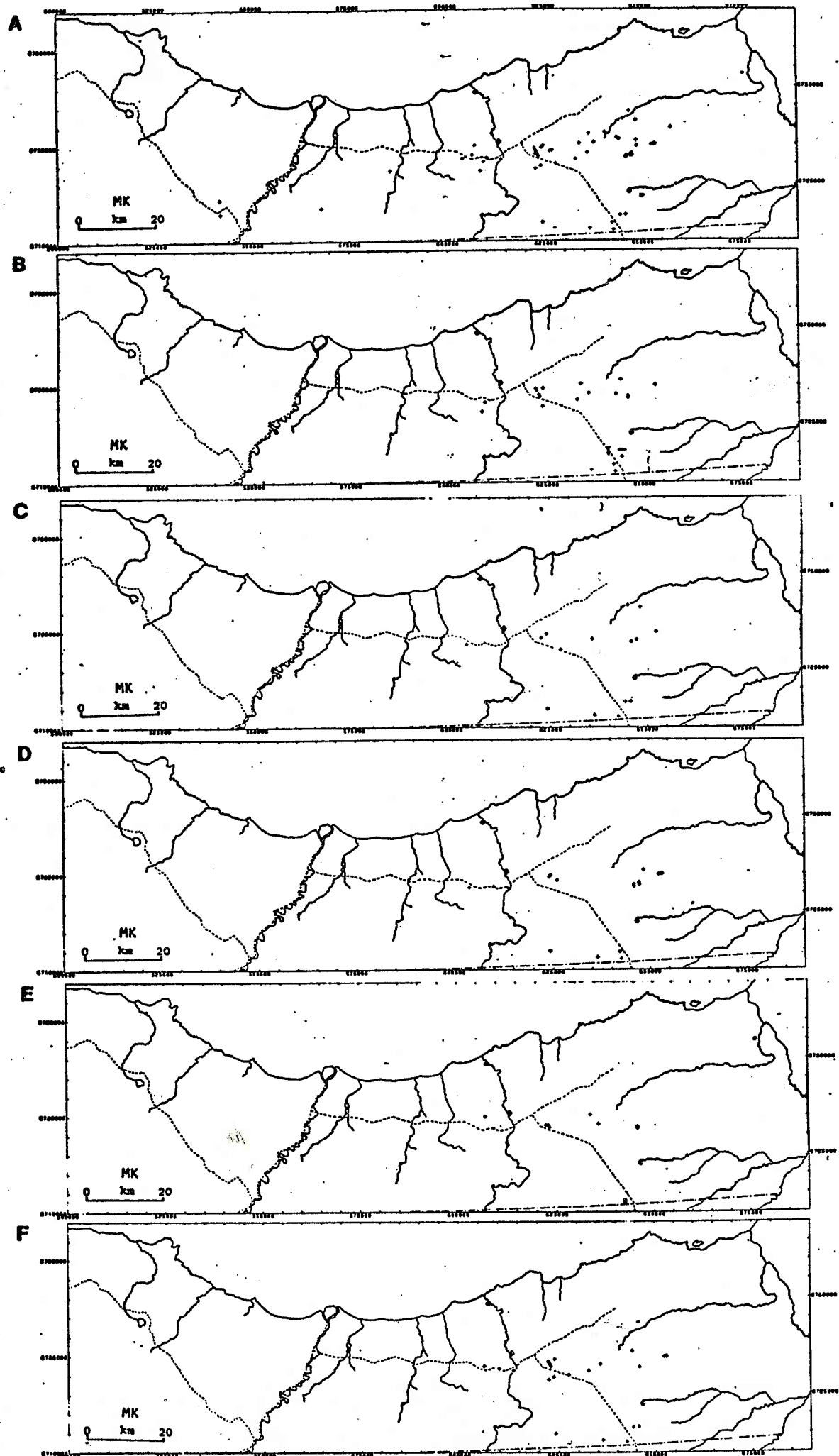


FIG. 4-23



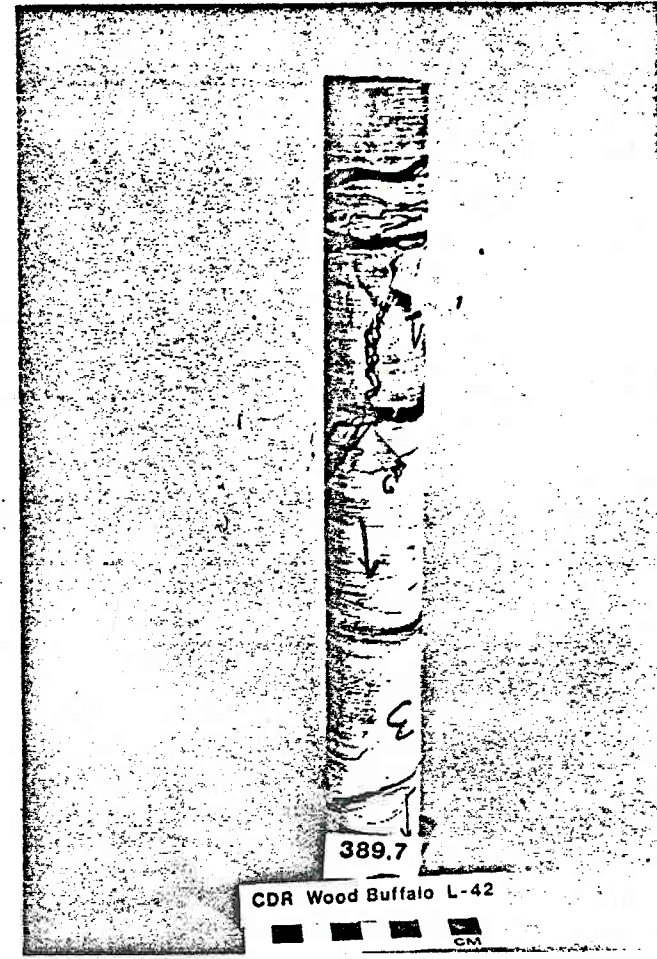
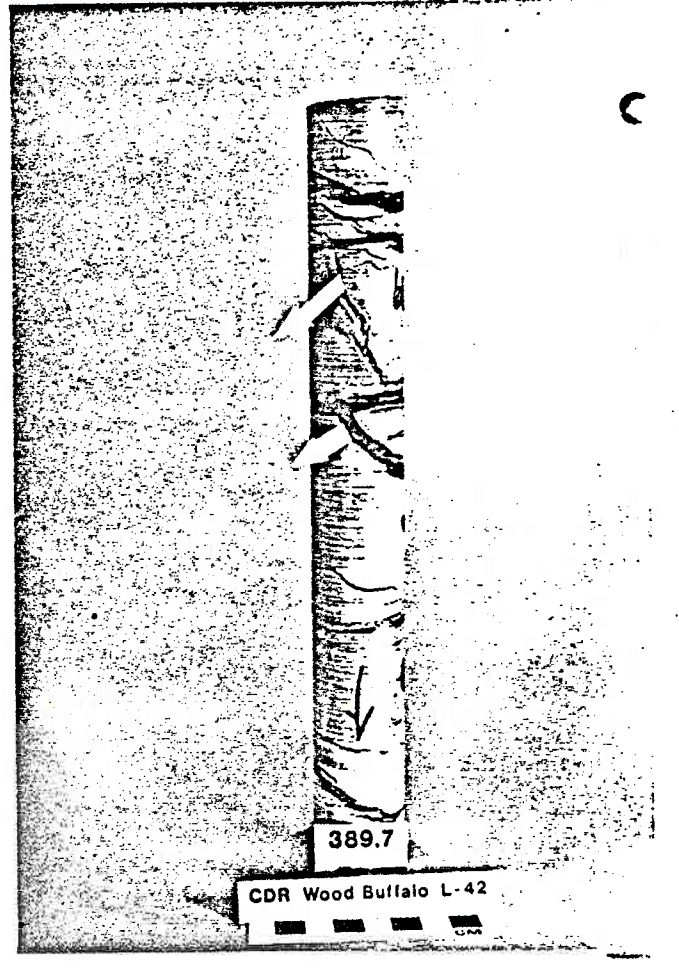


FIG. 4-25

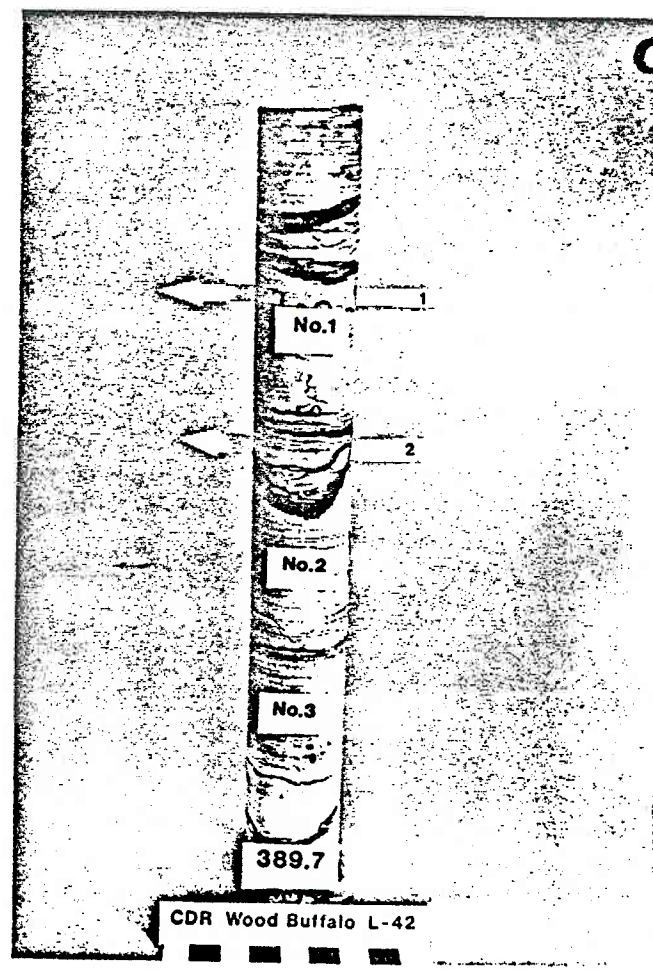
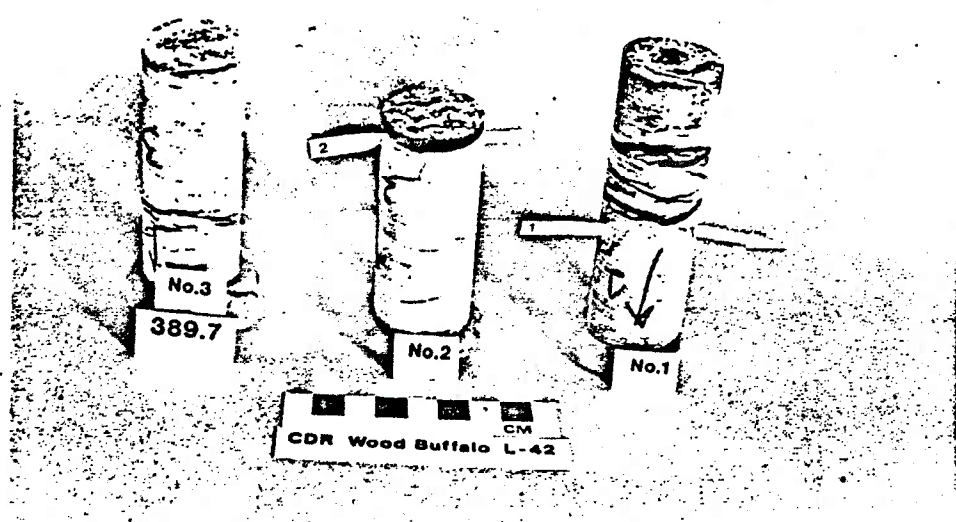


FIG. 4-26

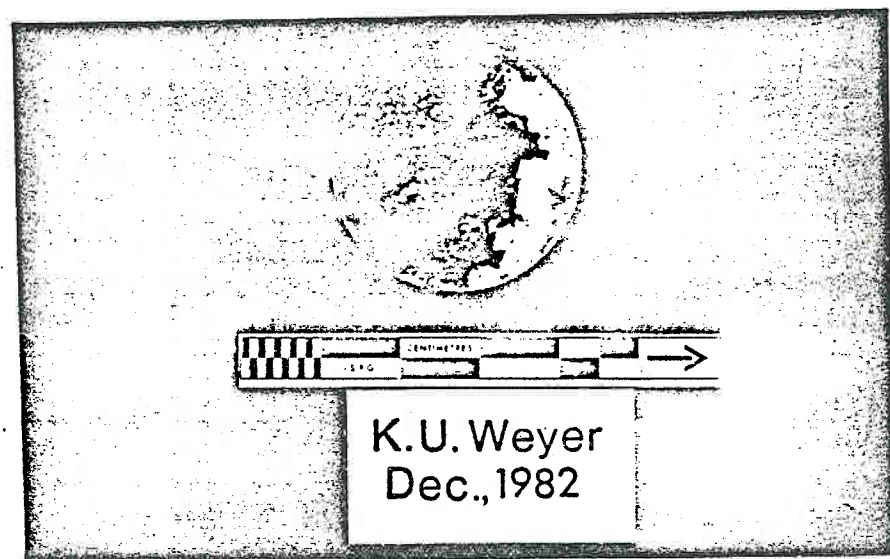


FIG. 4-27

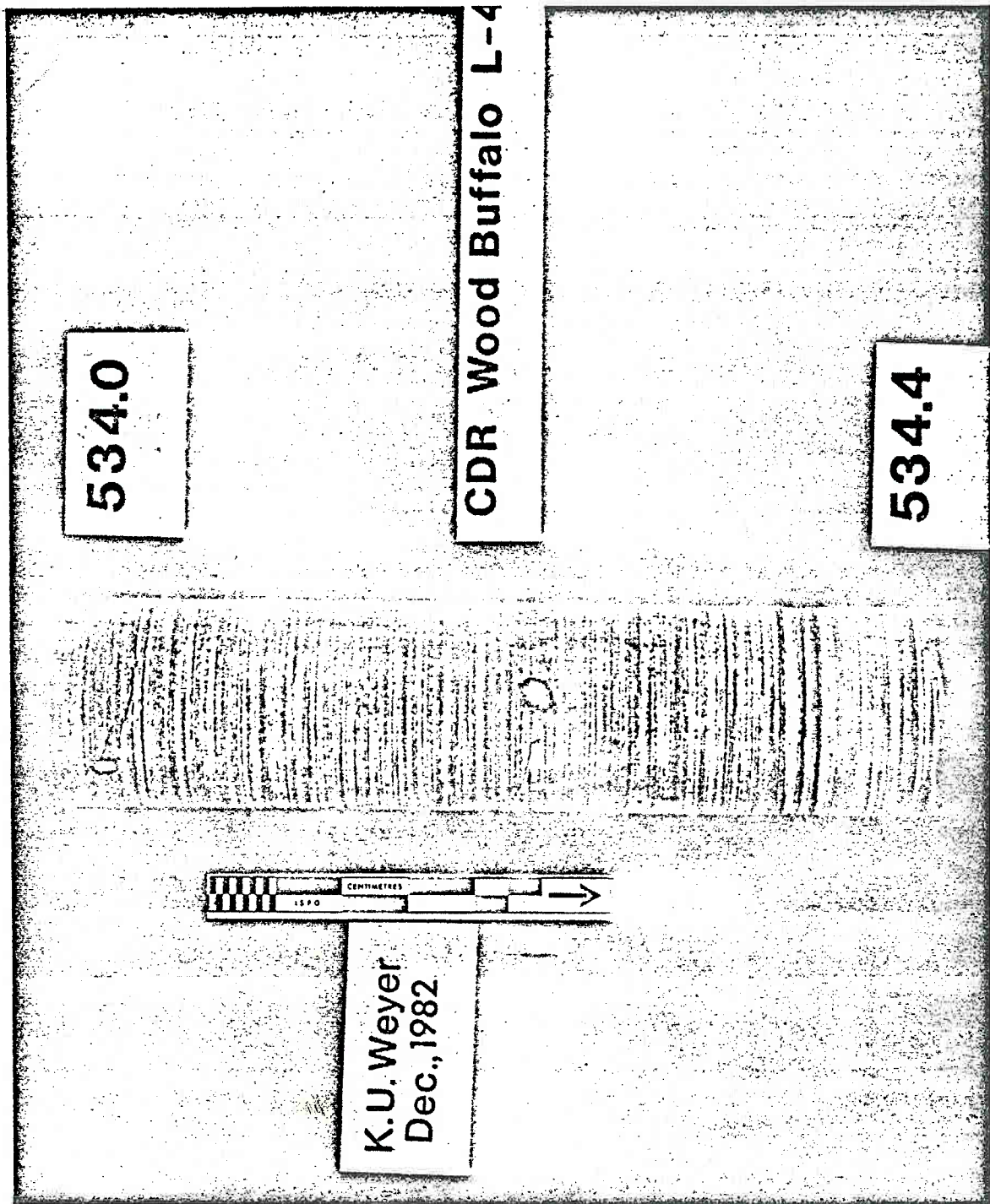


Fig. 4-28

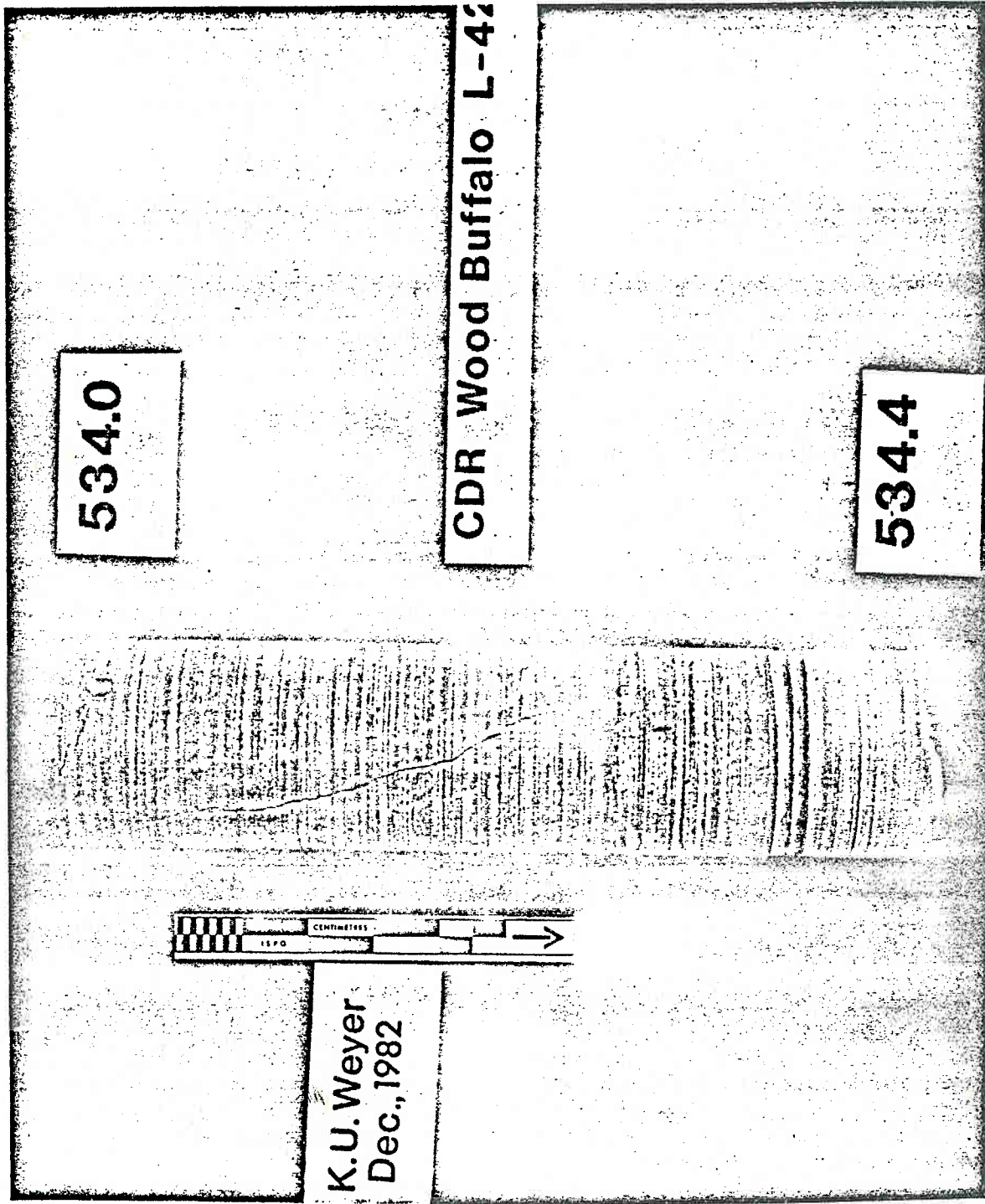


FIG. 4-29

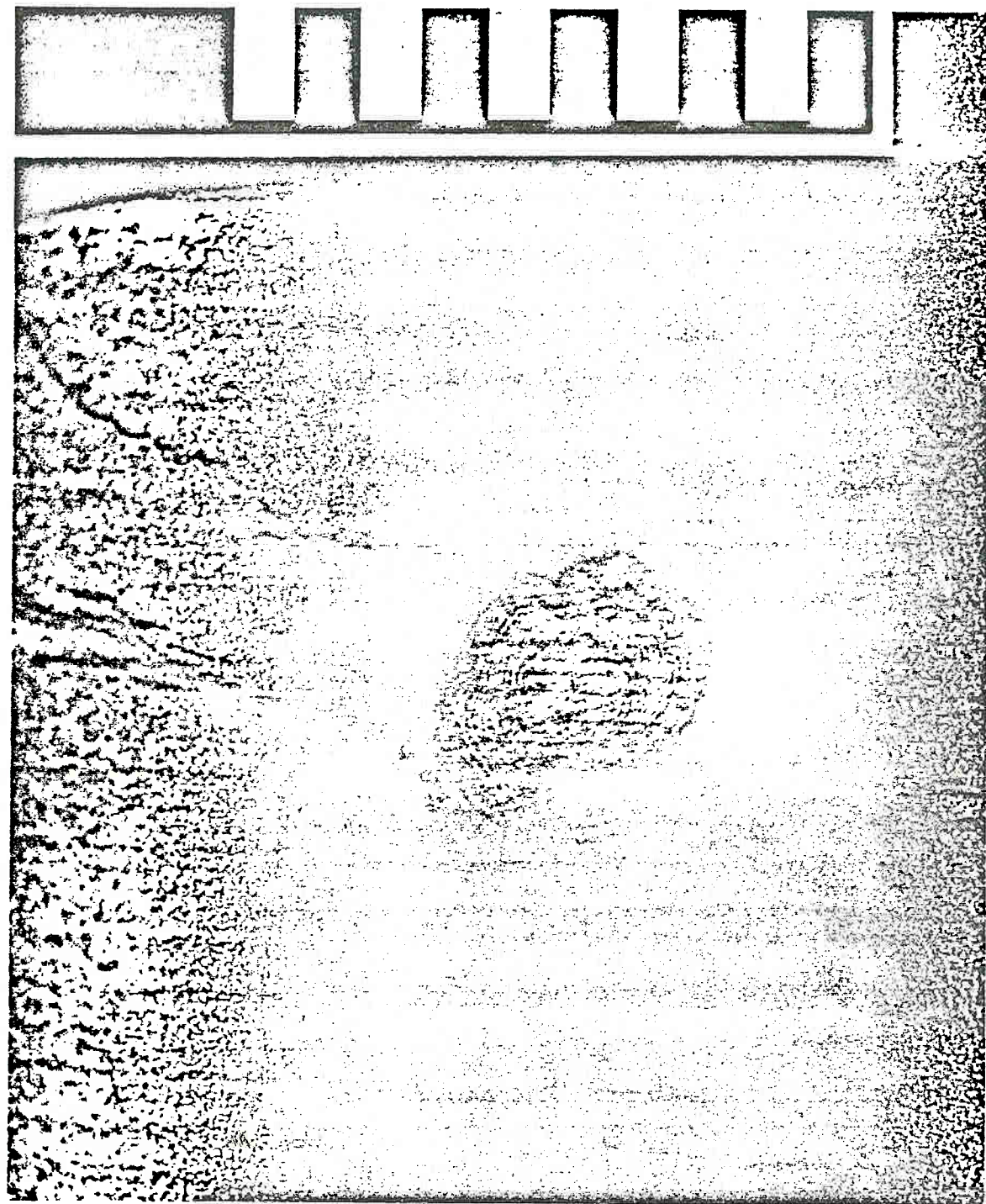


FIG. 4-30

